UNIVERSITÀ DEGLI STUDI DI MILANO

Università degli Studi di Milano

PhD Course in Experimental Medicine

CYCLE XXXV

PhD thesis

Dissecting the clinical and biological relevance of DIS3 gene in multiple myeloma

Candidate: **Dr.ssa Vanessa Katia Favasuli**

Tutor: **Prof. Antonino Neri**
Co-Tutor: **Prof.ssa Raffaella Chiaramonte**

Director: **Prof.ssa Nicoletta Landsberger**

Academic Year 2021-2022

This work is dedicated to my partner and best friend, Sebastiano.

Thank you for encouraging me to believe in myself. This is only the beginning of a wonderful journey together.

Index

1. Abstract

Multiple myeloma (MM) is a B cell malignancy characterized by abnormal proliferation of plasma cells (PCs) within the bone marrow. MM is characterized by a wide clinical spectrum ranging from the presumed asymptomatic pre-malignant condition called monoclonal gammopathy of undetermined significance (MGUS), to extra-medullary plasma cell leukemia (PCL). Notably, MM is characterized by a deep genomic instability involving ploidy, structural rearrangements and a high range of mutations involving both putative oncogenes and tumor suppressor genes that may explain its clinical heterogeneity. Half of MM tumors are hyperdiploid, associated with non-random trisomies of odd chromosomes and low prevalence of chromosomal translocations involving the immunoglobulin heavy chain locus (IGH) on chromosome 14q32, whereas the remaining tumors are non hyperdiploid and characterized by the prevalence of IGH translocations affecting several oncogenic loci. Such a large heterogeneous genomic pattern may represent the basis for the abnormal transcriptional expression profile associated with MM.

Despite the remarkable improvements in treatment and patient care, MM remains an incurable disease.

Over the past years, our and other research groups have provided valuable information on coding and non-coding transcripts aberrantly expressed in MM by expression profiling analyses based on microarray or RNAseq approaches. These studies have been of high relevance to better understand the biology of the disease, to identify of novel prognostic and predictive biomarkers and putative therapeutic targets.

DIS3 (chr.13q22.1 localization) is a conserved exoribonuclease and catalytic subunit of the exosome, a protein complex involved in the 3' to 5' degradation and processing of different species of RNA. Recently, aberrant expression of DIS3 has been found to be implicated in a range of different cancers. Notably, DIS3 is recurrently mutated in multiple myeloma (MM) patients. Most of the identified mutations are predominantly missense variants localized in the ribonucleolytic domain (RNB), mainly abolishing the exoribonucleolytic activity and are often accompanied by loss of heterozygosity (LOH) or biallelic inactivation due to 13q14 deletion. Furthermore, it has been reported in the literature that the inactivity or incorrect activity of DIS3 is also associated with the regulation of non-coding transcripts, as well as long non-coding RNA (lncRNA).

Long non-coding RNAs (lncRNAs) are a large class of non-coding RNAs involved in many physiological cellular and genomic processes as well as in carcinogenesis, cancer metastasis and invasion. The knowledge of the role of lncRNAs in MM is progressively

expanding. Our group provided recent evidence based on microarray and RNA seq analyses of deregulated patterns of lncRNA expression in MM showing that they may be specifically associated with distinct molecular types of the malignancy.

In a paper published during the first years of the project, it has been shown that MM patients carrying Dis3 gene mutations are associated with a distinct transcriptional signature characterized by many non-coding transcripts, mainly lncRNAs.

Firstly, our interest focused on investigating the deregulation of transcripts (including coding and non-coding portion) associated with DIS3 mutations in MM by analyzing RNA-Seq transcriptional profiles in a proprietary publicly available dataset and CoMMpass study, including approximately 1000 MM patients at diagnosis. We demonstrated that DIS3 mutations clinical relevance strictly depended on del(13q) co-occurrence. We observed that the bi-allelic DIS3 lesions significantly affected PFS (Progression Free Survival) and overall survival (OS). As expected, DIS3 mutations affect MM transcriptome involving cellular processes and signaling pathways associated with RNA metabolism. We found the downregulation of gene sets related to oxidative phosphorylation, RNA or amino acid metabolism, translation, and mitotic spindle checkpoint.

Overall, our comprehensive assessment of the clinical and transcriptional consequences of DIS3 mutations or its deletion in MM strongly indicates that they may play an important role in the mechanisms of transformation and progression of MM.

For these reasons, during the last year of my PhD program I focalized the efforts on the functional investigation of DIS3 putative role as potential therapeutic target in MM. To this aim I took advantage of the experimental silencing strategy based on the use of LNA-gapmeR technology and the gymnotic delivery of the in-house designed DIS3-specific antisense oligonucleotide in multiple myeloma cell lines (HMCLs).

The results obtained show that DIS3 silencing decreases cell growth, increases the percentage of apoptosis, reducing the oncogenic potential of MM cell lines. Indeed, interference with DIS3 expression reveals an important perturbation of the cell cycle distribution accompanied by mitotic defects.

I investigated the possibility of translating these results in combination with an available drug currently in clinical trial, such as ARRY-520, an inhibitor that interferes with the correct organization of microtubules. I found that the effect of DIS3 KD sensitizes MM cell lines in combination with ARRY-520, leading to a mitotic catastrophe.

These results suggest that DIS3 could be an important target for the future therapeutic approach in MM disease

Disclosure

I state that this scientific research was conducted following the principles of good research practice of the European Code of Conduct for Research Integrity, based on the principles of reliability, rigor, honesty, respect, and accountability.

Abbreviations

ACU Area under the curve
AML Acute myeloid leukemia
APC/C Anaphase promoting complex/cyclosome
BM Bone Marrow
BP Biological processes
CIN Chromosome instability
CNAs Copy number alterations
CNAs Copy number alterations
CR3 Cysteine residue 3
CSR Class switch recombination
DE Differential expresses
DIS3mts DIS3 mutations
GO Gene ontology
GSEA Gene set enrichment analysis
hDIS3 Homologous DIS3
hDIS3L Homologous DIS3 Like 1
HMCLs Human multiple myeloma cells
IGH Immunoglobulin heavy chain
ISS International staging system
KD Knock-down
LNA-gapmer Locked nucleotide acid gapmer
lncRNA Long non-coding RNA
LOH Loss of heterozygosity
MGUS Monoclonal Gammophaty of Undeterminated significance
MM Multiple Myeloma
MMRF Multiple Myeloma Research Foundation

ncRNA Non-coding RNA
NDMM Newly diagnosticated Multiple Myeloma
NGS Next generation sequencing
OS Overall survival
PC Protein coding
PCA Principal component analysis
PCL Plasma cell leukemia
PCs Plasma cells
PIN PilT N-terminus
PROMPT Promoter upstream transcript
RB1 Retinoblastoma 1
RNB Ribonucleolytic domain
RNR Ribonucleo reductase
RrpX Ribosomal RNA processing protein X
SAC Spindle assembly checkpoint
SHM Somatic hypermutation
siDIS3 siRNA DIS3
SMM Smoldering multiple myeloma
snoRNA Small nucleolar RNA
snRNA Small nuclear RNA
sPCL Secondary plasma cell leukemia
ssRNA Single strand RNA
VAF Variant allele frequency
WES Whole-exome sequencing
WGS Whole-genome sequencing
WT Wilde-type

2. Introduction

2.1. Multiple Myeloma

Multiple Myeloma (MM) is an incurable hematologic cancer characterized by malignant plasma cells (PCs) accumulation in the bone marrow (BM) (1). MM is typically characterized by clonal proliferation of PCs in the bone marrow, presence of monoclonal protein in the blood or urine, and bone lesions (1).

It accounts for 13% of all hematological malignancies with incidence in Western countries of about 6.3 new cases per 100,000 persons (2).

Survival of MM has improved significantly in the last 15 years. Recently, the possibility of autologous stem-cell transplantation and the availability of active drugs to treat MM in addition to those used up to a few years ago, have changed the overall survival (OS) (3,4).

Anyway, despite recent remarkable improvements in the treatment of the disease and the advances in drugs discovery, MM still remains an incurable disease with a median OS of 10 years (4).

2.1.1. Multiple Myeloma: overview on the biology

MM is a hematologic neoplasm of B lymphocytes residing in the terminally differentiated bone marrow known as PCs that produce antigen-specific immunoglobulins detected in the blood. PCs residing in the bone marrow include a distinct population of long-lived plasma cells (LLPCs) that can live for very long periods of time (5).

The myeloma cell is a post-germinal center plasma cell which has undergone immunoglobulin (Ig) gene recombination, class switching and somatic hypermutation (6).

MM is a multi-stage process beginning from a premalignant stage termed monoclonal gammopathy of undetermined significance (MGUS) (7,8). MGUS is characterized by minimum plasmacytosis in the bone marrow and the presence of serum monoclonal protein (M-protein or paraprotein) without any other observed impairment.

MGUS does not necessarily develop into MM, further progression of MGUS into the active MM occurs with a rate of ~1% per year (9).

MM is preceded by an intermediate stage referred to as smoldering multiple myeloma (SMM) which can progress in time-dependent manner.

MGUS and SMM are usually asymptomatic stages characterized by different levels of M-protein presence and different ratios of clonal plasma cells in bone marrow. The progression curve from SMM to symptomatic MM is about 10% risk per year for the first 5 years following

diagnosis, 3% risk per year for the following 5 years, and a subsequent 1% risk per year (10) (Figure 1).

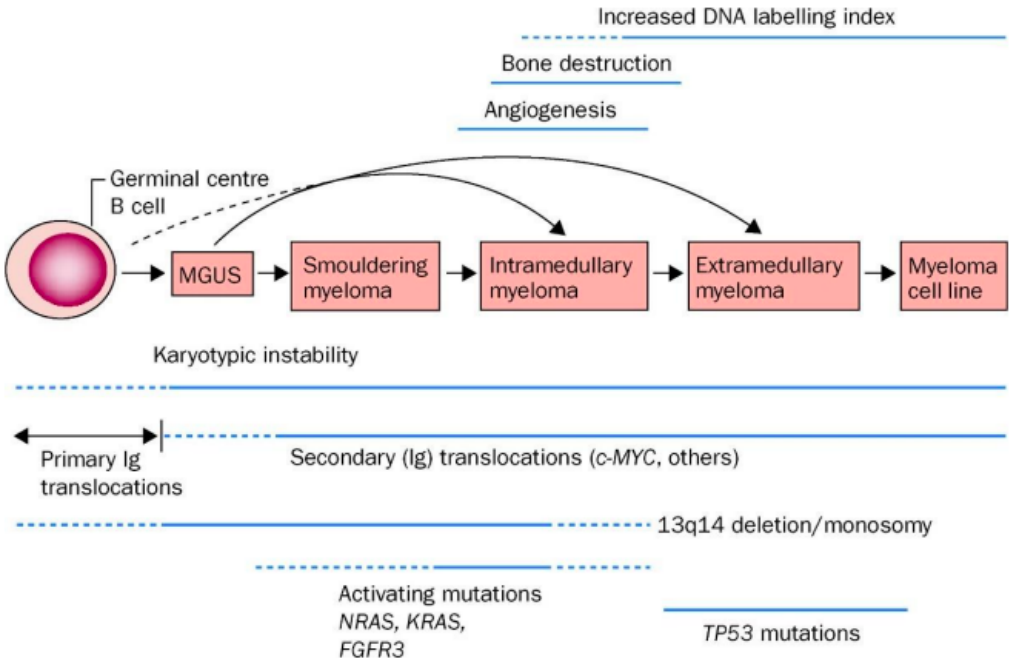

Figure 1. MM development and their characteristics. MM starts from the asymptomatic MGUS to active MM (11).

In addition, MM patients could develop a more aggressive clinical condition known as plasma cell leukemia (PCL) that can be divided in primary PCL (PCL) and secondary PCL (sPCL) associated to late or advanced stage of MM.

PCL is characterized by peripheral blood plasmacytosis, with splenomegaly and hepatomegaly related to the accumulation of plasma cells in these organs accompanied by severe anemia and thrombocytopenia; the prognosis of PCL is poor and worse than that of high-risk multiple myeloma witch include old age, poor performance status and comorbidities, plus presence of two or more adverse cytogenetic characteristics (12).

MM development follows the rules of branched evolution. In branched evolution, the subclonal architecture of the tumor is shaped by clonal competition for the limited resources of the microenvironment. Some of the subclones are subject to positive selection and further expansion, while other poorly adapted subclones are eliminated from the tumor cell pool.

In this way, genetic heterogeneity in branched evolution undergoes constant fluctuations; independent subclones often undergo parallel evolution by acquiring mutations in the same pilot genes that produce equivalent phenotypes.

Recent advances in studies of MM and its precursors have centered the pattern of dotted evolution as best characterizing the early stages of MM development. For example, significant heterogeneity is present before disease manifestation in the MGUS and SMM stages while further progression from MGUS/SMM to MM is characterized by clonal stability in some tumors (13–15).

In recent years, the use of next generation sequencing technologies (NGS) provided a large amount of genomic data that are of fundamental importance for diagnosis, the most appropriate therapeutic choices, the evaluation of drug response and understanding of the evolution of the disease (16–18).

Whole-exome (WES) or whole-genome (WGS) sequencing of MM genomes allows for the detection of point mutations, insertions or deletions, and structural variations.

Of fundamental importance is the presence of many NGS data available by the CoMMpass study (19), designed to provide as much information as possible about myeloma, studying more than a 1000 patients during the course of their myeloma, starting with the new diagnosis and collecting all their data.

2.1.2. Complexity of Multiple Myeloma genetics

MM is characterized by a profound genomic instability that involves chromosomal gains or losses, structural variation and known driver genes mutation (16).

For these reasons, could be considered a collection of condition that drives the complex genomic landscape of MM; cells with genomic instability have an increased probability of genome alterations during cell division (20,21).

MM can be divided into hyperdiploid and non-hyperdiploid subtypes, in fact total chromosome number in myeloma cells raging between 38 and 92 (22).

Hyperdiploid patients show trisomies of chromosomes 9, 15, 19, 5, 3, 11, 7, or 21 (in order of occurrence), and co-occurrence of up to five trisomies in the same karyotype.

Non-hyperdploid is mainly composed of cases harboring IgH translocations, generally associated with more aggressive clinical features and shorter survival. The main IgH translocations in myeloma are t(11;14)(q13;q32), t(4;14)(p16;q32), t(14;16)(q32;q23) and t(14;20)(q32;q11) (1).

In detail, t(4;14)(p16;q32) witch take place in 13-15% of patients leads to the upregulation of fibroblast growth factor receptor 3 (FGFR3) and the myeloma SET domain (MMSET) proteins. MMSET can be responsible for epigenetic and DNA repair alterations, whereas

the role of FGFR3 is not clear because in 30% of patients it is not expressed upon translocation.

Translocations t(11;14)(q13;q32) result in dysregulated expression of the cyclin D1 (CCND1) gene and occurs in approximately 17% of myeloma cases with the consequent cell cycle overactivation.

Other chromosomal rearrangements highlighted in the 5-10% of cases are t(14;16)(q32;q23) and t(14;20)(q32;q11). These events force the expression of MAF family oncogenes, which are related to myeloma cell proliferation through cyclin D2 expression and augmented adhesion to bone marrow stromal cells. MM patients carrying the t(14;16) and t(4;14) translocations are associated with worst outcome compared to the others translocations (23).

Another indicator of poor prognosis is the overexpression of MYC protein as a consequence of t(8;14); because MYC is a master transcription factor gene in B-cells its dysregulation is reflected by alterations in a large pool of downstream effectors involved in cellular events such as metabolism and proliferation (23).

Other different genetic progression factors have been identified in MM, including chromosome 13 and 17 deletions, chromosome 1 abnormalities (1p deletion and 1q amplification); considered adverse risk factors and indicative of high-risk MM (24,25).

About 50% of MM cases show deletions of chromosome 13 (del13q), with the downregulation of the tumor suppressor gene Rb1.

Another important gene involved in the progression of MM is located on chromosome 13: DIS3 encodes the highly conserved RNA exonuclease, which is the catalytic part of the exosome complex, involved in the regulation of the degradation and abundance of all RNA.

Less frequent chromosomal loss is on chromosome 17p, where the TP53 gene is located. In this case, the expression of TP53 in patients is reduced and which is related, together with MYC translocations in late pathology, to refractory disease and negative outcomes.

Also tumor suppressor genes are recurrently mutated in many diagnosed cases, leading to deep alterations in downstream pathways.

Some examples of altered signaling systems are the RAS/MAPK pathway, mutated in above 40% of patients with alterations on NRAS, KRAS and BRAF.

Other examples of altered genes are TP53, FAM46C, DIS3, HIST1H1E, IRF4, and MAX. Among the mutation present in MM patients, mutations identified in DIS3 thus far lead to loss of function (26).

Further evidence for translational control in the pathogenesis of MM comes from the mutation of FAM46C. The expression of FAM46C is highly correlated with the expression of ribosomal proteins; however, its exact function remains unclear (27).

Other genetic abnormalities involve epigenetic dysregulation, such as alteration of lncRNA and microRNA expression and modifications of gene methylation.

As described, MM exhibits an extremely complex pattern of genetic alterations (Figure 2). This complexity is related to disease progression and prognosis and patient characterization is important in defining the best and most effective therapeutic approach.

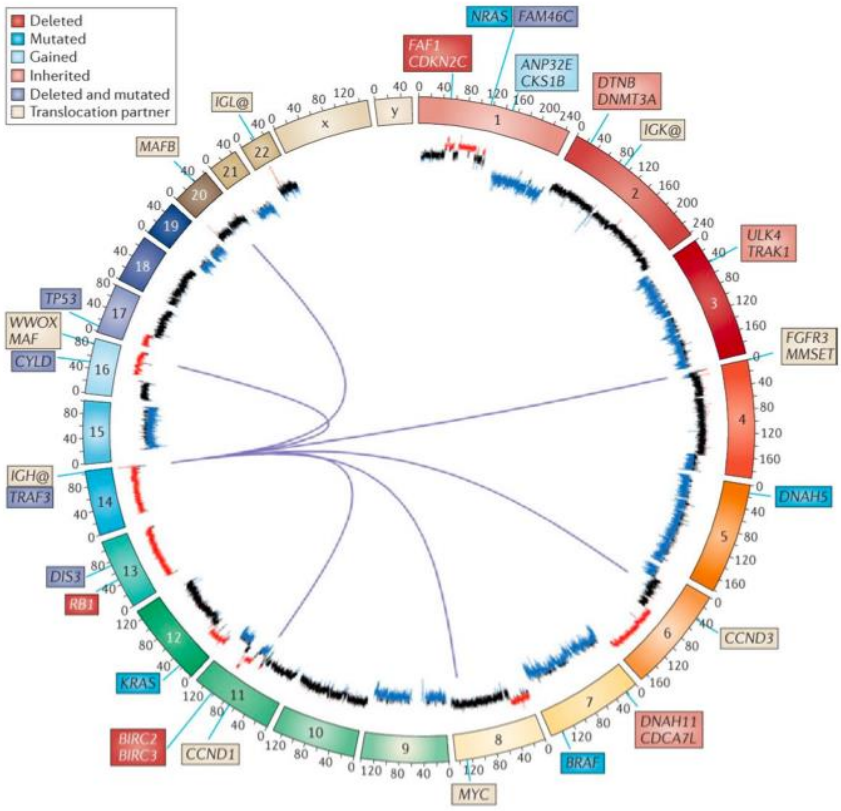

Figure 2. The genomic complexity in multiple myeloma. In the Circos plot translocations, copy number abnormalities and mutations in myeloma are reported. The chromosomes are arranged around the circle. IGH translocations are shown as lines emerging from chromosome 14 to the partner chromosomes. Copy number data are reported inside of the circle, showing deletions (red) and gains (blue) as well as normal copy number (black). Genes targeted by deletions and/or mutations are labelled outside the circle and colored according to the abnormality (28).

2.2. DIS3: a fundamental component of the exosome complex

The multi-subunit RNA exosome complex is composed of eleven structural and catalytic subunits and can be divided in two parts: the cap located above the exosome core and DIS3, a fundamental ribonuclease protein of the exosome complex.

DIS3 is a highly conserved ribonuclease which serves as the catalytic component of the exosome complex involved in processing, quality control and degradation of all RNA species in Eukaryote (29).

Dis3 gene map on chromosome 13q22.1 and it is composed by 22 exons; it is involved in the regulation of cell cycle progression and mRNA surveillance.

2.2.1. The exosome structure

RNA exosome is a ubiquitously expressed $3' \rightarrow 5'$ endo-exoribonuclease in eukaryotic cells that must collaborate with multiple cofactors to process all classes of RNA, including regulation of RNA abundance, elimination of dysfunctional RNA or misfolded and the processing of precursor RNAs to their mature form.

The eukaryotic exosome can be divided into two main groups based on their structural and functional contributions.

The first group includes nine proteins that form the exosomal nucleus; they are all rather small proteins with molecular masses of 20-50 kDa. Three of these are constructed entirely from RNA binding domains and motifs, while the remaining six are single domain proteins homologous to RNase PH.

The second group of components of the exosome includes the proteins DIS3 and Rrp6, which bind to the nucleus in different combinations giving rise to the isoforms of the complex. DIS3 and Rrp6 are both large multidomain polypeptides with molecular masses around 100 kDa, they are quite different from each other and carry out all the catalytic activity of a typical eukaryotic exosome; the schematic structure of the eukaryotic RNA exosome is shown in Figure 3 (29,30).

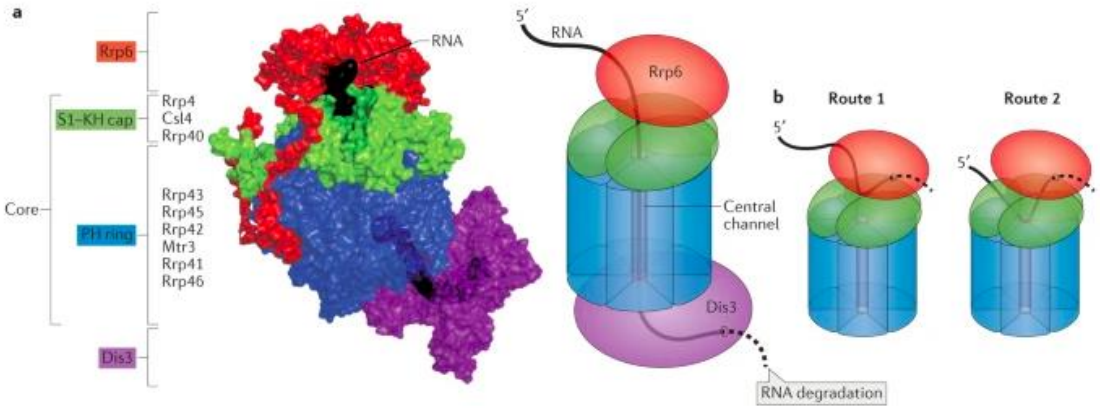

Figure 3. **RNA exosome structures.** Side view of the eukaryotic RNA exosome with the hexamer in blue, Rrp6 in red and the cap complex in green. the associated ribonucleolytic subunits in purple (DIS3) and RNA in black (31).

The structure of the global architecture of the exosome nucleus is well established, thanks to the crystalline structure obtained for the Homo sapiens complex (29). Its nine subunits are arranged in a two-layered ring, the lower layer is formed by six subunits homologous to the bacterial RNase PH: Rrp41, Rrp42, Rrp43, Rrp45, Rrp46 and Mtr3 and referred to as 'hexamer', while the upper layer is consisting of the three RNA binding subunits, Rrp4, Rrp40 and Csl4, and is called 'cap'. The cap subunits do not form contact with each other but instead each is firmly attached to two subunits of the hexamer (29). The central channel running through the ring is large enough to contain the single-stranded RNA (ssRNA) that will be processed.

The architecture of the exosome core is ancient and perhaps even precedes the exosome itself as two complexes of prokaryotic origin have exactly the same domain composition and spatial arrangement. One is the exosome found in most Archaea, sometimes called the "exosome-like complex" and the other is the polynucleotide phosphorylase (PNPase) found in eubacteria as well as in the mitochondria of plants and vertebrates. RNA exosome is present in all eukaryotic cells; however, today it has been studied more thoroughly in budding yeast and thus the yeast nomenclature has been indicated for eukaryotic RNA exosomes where RrpX stands for "Ribosomal RNA processing protein X" (32)

2.2.2. The exosome ribonucleases: DIS3 and Rrp6

DIS3 protein is homologous to RNase II and RNase R of E. coli, which makes them members of the ribonucleotide reductase (RNR) superfamily (29).

The RNR homology region of DIS3 proteins has the typical domain layout: two cold-shock domains (CSDs), a ribonucleoprotein domain (RNB) and an S1 domain.

CSD and S1 are region that non-specifically bind RNA, while RNB is a catalytic domain with processive exoribonuclease activity. In the N-terminal region, on the other hand, there is a Cys residue 3 (CR3) motif and a PIN domain (33), of which the CR3 motif is named for its three conserved cysteine residues.

The PIN active site consists of four acidic amino acid residues but, unlike in RNB, they are dispersed throughout the otherwise weakly conserved sequence of the domain (29,34). Although details are not clear, the motif also plays a role in the core-DIS3 interaction and is required for some of the cellular functions of the exosome (30).

DIS3 is an endoribonuclease and a 3'–5' exoribonuclease. The enzyme is not able to cleave double-strand RNA (dsRNA) but only circular and linear ssRNA are eligible substrates; preferring substrates with phosphorylated 5' termini (34). The exonuclease activity of DIS3 depends on four conserved aspartate residues localized in the PIN domain that coordinate two magnesium cations to hydrolytically cleave the RNA backbone; mutation of any one of these residues completely abolishes its activity (31). The active site is in the RNB domain, deep in the bottom of a narrow channel and can only be reached by ssRNA not exceeding 7 nucleotides (nt) in length (35). DIS3 exonucleases are highly processive, attack from 3' ends of the ssRNA and once bound they degrade substrate completely, releasing nucleoside 5'-monophosphates (36).

The human genome encodes three DIS3 homologs, of which only hDIS3 and hDIS3L are associated with the exosome. Both have processive 3'-5' hydrolytic exonuclease activities, while only hDIS3 maintained in addition to the exonuclease activity also the endonuclease one in its PIN domain.

In vivo localization studies and analyses of substrate specificities revealed that hDIS3L is restricted to the cytoplasmic exosome, whereas hDIS3 is mainly a nucleoplasm protein, with a small fraction present in the cytoplasm (36,37).

The third human homolog of DIS3, hDIS3L2, does not interact with the exosome nucleus, due to the lack of the PIN domain and has been shown to be responsible for an alternative pathway of 3'-5' RNA decay in the cytoplasm (38). An important role of hDIS3L2 in maintaining proper cellular metabolism is supported by the fact that mutations in this gene have been associated with the Perlman syndrome of overgrowth and predisposition to Wilms tumor development (39,40)

Rrp6 proteins belong to the superfamily of nucleases, which includes enzymes with various functions, e.g. oligoribonuclease and proofreading domains of DNA polymerases (41,42). Rrp6 proteins are 3'–5' exoribonucleases that cleave RNA hydrolytically and release nucleoside 5'-monophosphates (41). The enzymatic activity derives from the active site which is exposed to the solvent and consists of four conserved amino acid residues that coordinate two magnesium cations. The mode of action is selectivity for ssRNA and should preclude digestion of structured substrates; however, Rrp6 proteins can break down structured substrates containing a single stranded region upstream of the structure.
The mechanistic background of its activity is not yet fully known (42–44).

2.2.3. RNA exosome functions

Exosome plays an essential role in most RNA metabolic pathways, acting in both the nucleus and the cytoplasm (Figure 4) (29,45), processing numerous non-coding RNAs (ncRNAs) in the nucleus and degrading many defective processed RNAs improperly in nuclear and cytoplasmic surveillance pathways (46,47).
In particular, the RNA exosome processes rRNA, snRNA and snoRNA and degrades unstable ncRNAs, including unstable cryptic transcripts (CUT), in budding yeast has been shown an involvement in PROMPT processing and site associated antisense RNAs (TSS - RNA) (48,49).
Finally, the RNA exosome degrades aberrant, improperly processed RNAs, including pre-mRNAs and hypomodified tRNA (49).
Furthermore, exosome plays a crucial role in RNA quality control, demonstrated by its activity in the degradation of unwanted molecules in the nucleus and cytoplasm, including incorrectly processed pre-mRNA, rRNA and tRNA, as well as translationally incompetent mRNA.
In current models, RNA exosome specificity for distinct RNA substrates is conferred by several exosome cofactors that target the exosome to specific RNAs for processing/degradation (45,47,50–52).

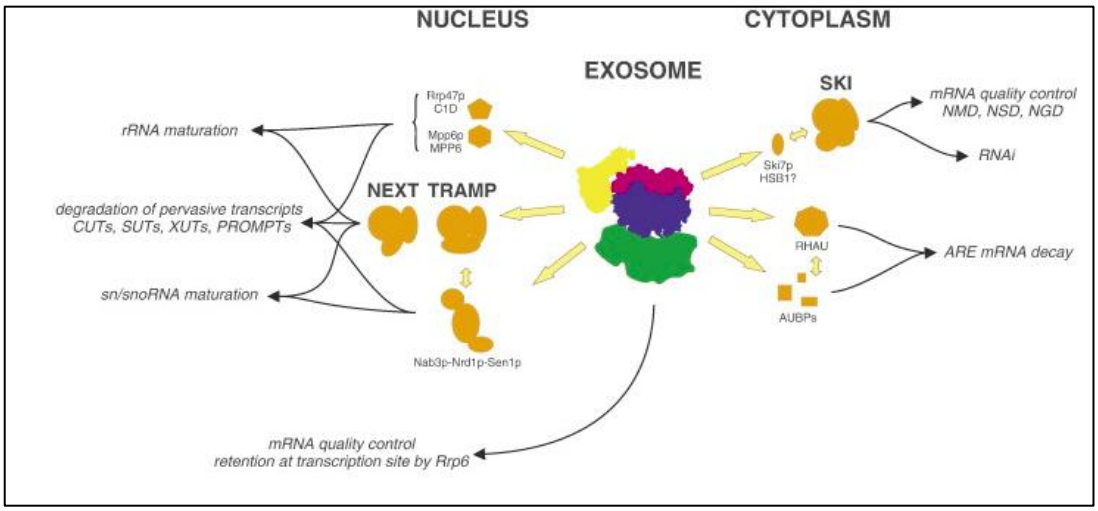

Figure 4. Map of the exosome's cellular functions and cofactors. DIS3 acts mainly in the nucleus but also in cytoplasm, interacting with different cofactors **(29).**

2.2.4. Mutations in DIS3 gene are linked to MM disease

Recurrent somatic mutations in DIS3 have been linked to multiple myeloma disease. Genome-wide targeted sequencing of multiple myeloma patients, performed by multiple studies, revealed approximately 11% of individuals with heterozygous DIS3 mutations (53). In most cases, myeloma cells display the monoallelic deletion of the chromosome 13q and a DIS3 missense mutation on the remaining allele. These cells carrying DIS3 mutations are specifically non-hyperdiploid and can harbor chromosomal translocations (14,53,54). DIS3 is currently the only subunit of the RNA exosome complex found to be associated with cancer. The variants identified are predominantly missense mutations located in the RNB domain of the exoribonuclease and are often detected at low allelic frequency (55). Notably, hotspot amino acid substitutions in DIS3 occur at residues D488 and R780 in the RNB domain, most frequently DIS3-D488N and DIS3-R780K. Many of the frequently altered residues in the disease are spatially close within the RNB and PIN domains and are concentrated around the RNB D487 and PIN D146 catalytic residues (Figure 5). The numerous amino acid changes identified in DIS3 in individuals with multiple myeloma are therefore expected to impair the catalytic activity of DIS3 and the degradation of RNA by the RNA exosome.

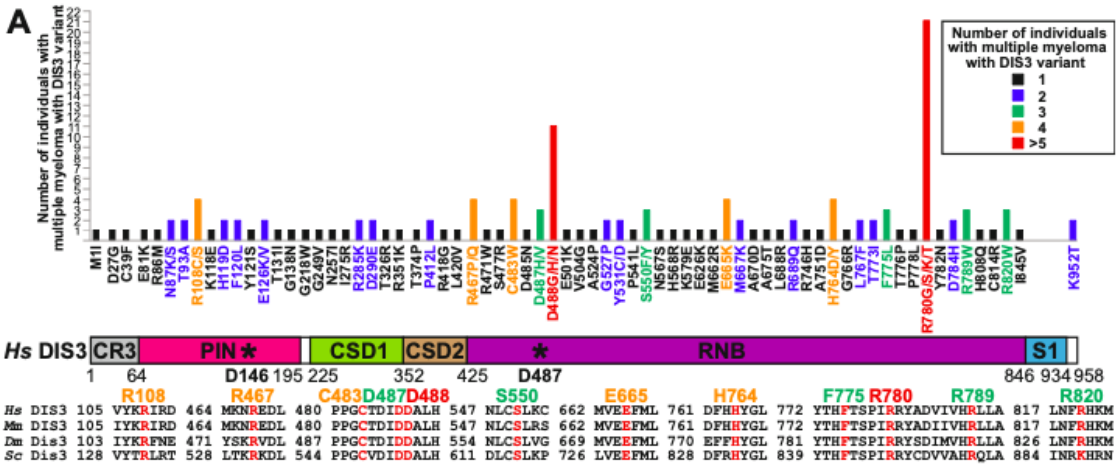

Figure 5. Amino acid substitutions identified in the DIS3 catalytic subunit in individuals with multiple myeloma. Domain structure of human DIS3 protein highlighting the amino acid changes identified in individuals with multiple myeloma. The amino acid substitutions are shown in the domains of DIS3 in which they are located. Most of DIS3 mutations in individuals with multiple myeloma are in the RNB domain (purple) and PIN domain (pink), but additional amino acids altered in disease are in other domains such as CR3 (gray), CSD1 (green), and CSD2 (brown). A graph shows the number of individuals with multiple myeloma that have been identified with each DIS3 variant. The color code of the amino acid substitutions indicates the number of affected individuals with each DIS3 variant: 1 (black), 2 (blue), 3 (green), 4 (orange), 5+ (red) (32).

An yeast-based study addressed the functional consequences of some of the DIS3 amino acid changes associated with multiple myeloma (56). In particular, the exonucleolytic activity of the common variant DIS3-R780K is almost completely compromised, while variants DIS3-S477R and DIS3-G766R variant show functional alterations that have a milder impact in exonucleolytic activity. Furthermore, yeast cells expressing the DIS3-R847K variant exhibit impaired growth and aberrant accumulation of exosomal substrates (56). Finally, human HEK293 cells expressing the DIS3-R780K variant and silenced for DIS3 show slower growth rate and also in this case accumulation of exosomal substrates, e.g. PROMPT and rRNA precursors (56). Moreover, reported data strongly support the idea that impairment of DIS3 function causes mitotic cell cycle defects and impairs cell growth in yeast, drosophila, and human cells (56–60).

To date, the literature has attempted to explain how DIS3 mutations lead to proliferation in multiple myeloma. One possibility is that inactivating mutations in DIS3 may disrupt proper kinetochore formation, potentially through effects on heterochromatin, leading to defects in sister chromatid separation and aneuploidy, as observed for the dis3-54 RNB mutant in S. pombe (60). A second possibility is that inactivating mutations in DIS3 may work

synergistically with mutations in other genes in myeloma cells to enhance cell proliferation. A third possibility is that inactivating mutations in DIS3 could increase non-coding regulatory RNA levels in myeloma cells, leading to enhanced genomic instability and increased proliferation (56). Indeed, the RNA exosome regulates xTSS-RNA (transcription start site associated antisense transcripts that can be 500 base pairs in length), xTSS-RNA levels that target the DNA mutating protein AID (activation-induced cytidine deaminase) at immunoglobulin (Ig) heavy chain (Igh) loci for recombination class change and Ig variable regions for somatic hypermutation in B cells (61). Since impaired RNA exosome function elevates xTSS-RNAs and increases RNA-DNA hybrids at Igh loci, the reduction in DIS3 activity could also increase double-strand breaks and translocations, leading to increased proliferation (61).

2.3. Multiple Myeloma Treatment

Today it is increasingly necessary to develop the best clinical approach considering the initial condition of the patient and his genetic characteristics.

In the case of MGUS and SMM, patients are typically closely monitored over time with recurrent assessments of the clinical status.

Diagnosis of MM requires the presence of one or more myeloma-causing events (MDE) in addition to evidence of 10% or more of clonal plasma cells on bone marrow examination or a biopsy-tested plasmacytoma. MDE consists of established CRAB features (hypercalcemia (C), renal failure (R), anemia (A), and lytic bone lesions (B)) and three specific biomarkers: bone marrow clonal plasma cells of 60%, serum free light chain (FLC) ratio of 100 or greater (a provided that the level of FLC involved is ≥100 mg / L) and more than one focal lesion on magnetic resonance imaging (MRI) (62).

The primary goal of treatment for patients with multiple myeloma is to increase survival and quality of life by reducing disease-related complications through long-term tumor suppression.

The most significant advances in multiple myeloma therapy have been the introduction of proteasome inhibitors (bortezomib, ixazomib and carfilzomib), immunomodulatory agents (thalidomide, lenalidomide and pomalidomide), monoclonal antibodies directed against myeloma cell surface antigens (daratumumab, isatuzumab and elotuzumab) and autologous hematopoietic stem cell transplantation (if eligible) (63).

Therapeutic strategies should include the use of induction regimens associated with high complete response rates, followed by maintenance treatment. This approach consists of

maximal tumor shrinkage achieved with continuous treatment, which is essential to delay tumor regrowth. The level of response, and in particular the achievement of a complete response, is associated with a better long-term outcome. A complete response is defined as the elimination of disease detectable on routine testing (64,65).

More rigorous criteria, such as quantification of free immunoglobulin light chains in serum, quantification of bone marrow myeloma cells on multiparameter flow cytometry, and identification of residual tumor cells on polymerase chain reaction assay, were explored to define minimal residual disease, which is one of the most important independent prognostic factors for survival (66,67).

Younger patients who have a complete response after autologous transplantation have a prolonged OS and PFS.

Recent therapeutic trends favor the adaptation of treatment for a specific patient based on that patient's risk factors. Although such risk-adjusted strategies have not been prospectively validated, some investigators have recommended the use of bortezomib-containing regimens for high-risk diseases and regimens containing lenalidomide or thalidomide for standard-risk diseases. These recommendations are based on the evidence that patients with t(4; 14) translocation who received combination therapy with lenalidomide and dexamethasone had shorter OS than those without t(4; 14) (68).

Conversely, induction of bortezomib improved survival for patients with t(4; 14) but not for those with 17p13 deletion (68).

To date, MM remains incurable: most patients develop drug resistance and relapse after treatment.

However, there is still a lack of effective therapies targeting the deregulated biological processes specifically associated with the disease; for these reasons, the discovery of new cellular targets and new therapeutic options are an urgent need and one of the objectives of the research.

2.3.1. ARRY-520 (Filanesib): Kinesin spindle protein inhibitor

Eg5, also known as kinesin spindle protein or Kif11 is a member of the kinesin superfamily of motor proteins (69).

Eg5 is a spindle microtubule associated protein with direct motor activity (70) whose spindle association depends on Cdk1 phosphorylation of its C-terminus (71).

In addition to the functions related to the motor activity of the microtubule, Eg5 includes the transport of secretory proteins from the Golgi complex to the cell surface in non-mitotic cells,

as well as the improvement of translation by acting as a link between ribosomes and microtubules (72,73).

During the transition from G2 to M phase of the cell cycle, Eg5 allows two microtubules to slide over each other, a necessary activity for the establishment of a bipolar spindle (70,74). The lack of Eg5 activity leads to the failure of the separation of duplicated centrosomes and the construction of a monoastral spindle leading to mitotic block (Figure 6) (75).

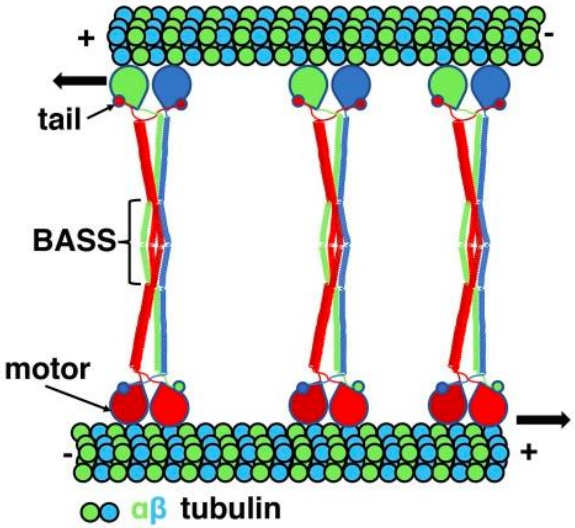

Figure 6. Representation of antiparallel microtubule sliding by Eg5. At each end of the Eg5 tetramer interact with microtubules moving towards the + ends of microtubules. The central helical bundle (BASS domain) formed by two antiparallel alpha helical coiled-coils is responsible for the tetramerization of Eg5 (75).

Eg5 is expressed in CD34 ± cells, testis, heart muscle cells and some other normally proliferating human tissues; however, it is important to underline that the level of expression is significantly lower than that of malignant tissues.

Eg5 overexpression leads to significant genome instability in mouse models and carcinogenesis.

The studies evaluated Eg5 expression and its correlation with clinicopathological features in various malignant tumors. For example, the activation of Eg5 expression contributes to the onset of B-cell leukemia and other solid tumors, its overexpression is linked to a poor prognosis (76,77).

However, it is unclear whether Eg5 overexpression reflects a higher proliferation rate of a cell population or a true excess of protein in the cell population (75).

For these reasons, Eg5 is a valid target for the development of inhibitors for antimitotic drug therapy.

In recent years, ARRY-520 has demonstrated clinical efficacy in patients with multiple myeloma and could enter Phase III clinical trials (78,79); in particular for patients diagnosed with refractory/relapsed multiple myeloma (80).

In acute myeloid leukemia patients (AML), ARRY-520 as a single agent achieved only a partial response in 1 of 34 patients and no significant clinical responses were observed with patients with solid tumors.

Contrary, in MM ARRY-520 as a single agent showed an overall response rate of 16% and 15% when the anti-inflammatory dexamethasone was added at low doses in patients with heavily pretreated multiple myeloma (78,81).

An even greater result, in terms of OS, was obtained when ARRY-520 was used in combination with dexamethasone and proteasome inhibitors such as bortezomib and carfilzomib (82,83).

3. Aim of the study

Multiple Myeloma (MM) is a still uncurable malignant hematological disease characterized by clonal expansion of malignant plasma cells (PCs) in the bone marrow (BM) and heterogeneous genomic landscape (1,84).

DIS3 is a conserved exoribonuclease and catalytic subunit of the exosome, a protein complex involved in the 3' to 5' degradation and processing of both nuclear and cytoplasmic RNA species. Most striking is the finding that DIS3 is recurrently mutated in multiple myeloma (MM) patients.

Somatic variants are predominantly missense variants localized in the RNB domain mainly abolish the exoribonucleolytic activity (53,55), and are often accompanied by loss of heterozygosity (LOH) or biallelic inactivation due to 13q14 deletion (54,85). Much work has been done to elucidate the structural and biochemical characteristics of DIS3, including the mechanistic details of its role as an effector of RNA degradation.

Unfortunately, the role of DIS3mts (DIS3 mutations) in the pathobiology of MM remains largely unknown.

Starting from this evidence, the first part of this thesis is focalized to understand the clinical impact of DIS3 mutations in MM patients.

To do this, we leveraged the large public CoMMpass dataset to study DIS3mts in MM and their impact on transcriptional signature and clinical outcome. The clinical relevance of DIS3mts is strictly dependent on the co-occurrence of del(13q) and for this reason we have studied not only the mutation but also the effect of the biallelic condition in terms of PFS and OS.

The second part of this thesis is focused on the molecular and functional characterization of DIS3 in MM; to date there are no data in the literature regarding DIS3 KD in MM.

To determine if DIS3 silencing could have a biological impact on HMCLs, we thought of silencing DIS3 using LNA-gapmeR ASO technology by gymnosis.

Furthermore, we investigated the transcriptional profile associated with DIS3 KD in NCI-H929 cells. It has already been reported, at least in the yeast and Drosophila models, that the RNase activity of DIS3 is required for proper mitotic cell division and correct chromosomal condensation; for this reason, we analyzed by immunofluorescence the morphological changes in the spindle organization of DIS3 silenced cells.

At the and we try to combine the silencing of DIS3 in association with ARRy-520 that act on spindle organization, in order to evaluate if DIS3 KD could enhance the efficacy of spindle inhibitor.

4. Materials and Methods

4.1. Computational Task

4.1.1. Multi-Omics Data in CoMMpass Study

Non-synonymous (NS) somatic mutation variants and counts data were derived in 930 BM_1 MM samples from whole exome sequencing (WES) analyses (MMRF_CoMMpass_IA12a_All_Canonical_NS_Variants,MMRF_CoMMpass_IA12a_All_Canoni cal_NS_Variants_ENSG_Mutation_Counts). Main IgH translocations were inferred from RNA-sequencing (RNA-seq) spike expression estimates of known target genes and were available in 724 common MM cases that were analyzed by RNA-seq (MMRF_CoMMpass_IA12a_RNAseq_Canonical_Ig_Translocations). Copy number alteration (CNA) data were obtained by means of Next generation Sequencing (NGS)-based fluorescence in situ hybridization (FISH) analyses (MMRF_CoMMpass_IA12a_CNA_Exome_FISH_CN_All_Specimens) in 847 common MM cases. The presence of a specific CNA was considered when occurring in at least one of the investigated cytoband at a 20 percent cut-off for each considered chromosomal aberration. Transcript per Million (TPM) reads values were obtained by Salmon gene expression quantification (MMRF_CoMMpass_IA12a_E74GTF_Salmon_V7.2_Filtered_Gene_TPM) for 655 MM patients for which DIS3 RNA mutation frequency was accessible. Clinical data regarding Overall Survival (OS) and Progression free Survival (PFS), International Staging System (ISS) and treatment classes were available for the entire cohort of 930 MM cases profiled for DIS3 mutation occurrence (CoMMpass_IA12a_FlatFiles). Four main groups of therapy were identified as first line of treatment, i.e. combined bortezomib/IMIDs-based, bortezomib-based, IMIDs-based, or therapy based on carfilzomib (i.e. combined IMIDs/carfilzomib-based, combined bortezomib/IMIDs/carfilzomib-based, or carfilzomib-based).

4.1.2. Statistical and survival analyses

Kaplan-Meier analysis was applied on OS and PFS data in differently characterized MM patients cohorts. Log-Rank test p-value was calculated to measure the global and pairwise difference between survival curves, Benjamini-Hochberg (BH) correction was applied in pairwise comparisons. The number of samples at risk in each group across time was calculated. Cox proportional hazards model was applied as univariate analysis on single molecular variables and International Staging System (ISS) groups in relation to OS and

PFS data, in 630 MM cases for which all information were accessible. Cox regression multivariate analysis was applied on all significant features after BH correction. Forest plot was used to summarize Cox Proportional Hazard Models.

4.1.3. Differential expression analysis on CoMMpass MM cohort

Global dataset of 655 MM cases was stratified on the base of DIS3 RNA frequency mutation and 56 DIS3 mutated cases with at least 20% RNA mutational load were considered in differential expression analysis. Principal Component Analysis (PCA) was applied on differentially expressed (DE) annotated transcripts by means of prcomp function in R. Volcano plot was used in R to represent significantly up- or down-regulated transcripts. The heatmap of the expression levels of the top 100 DE annotated transcripts, according to limma B statistics value, was obtained by means of dChip software.

4.1.4. Functional enrichment analysis on DE protein coding genes

Global DE protein coding gene list (3464 genes) and 490 DE protein coding genes common to at least one molecular subgroup or in all comparisons were ranked based on fold change value and analyzed by Gene Set Enrichment Analysis (GSEA), respectively. Cluster Profiler analysis was performed in R environment on DE global protein coding gene list and the top 100 (BH adjusted pvalue) GSEA gene sets, based on Gene-Ontology (GO) Biological Process (BP) terms, were represented by the Enrichment map. In the GSEA analyses, gene set dimensions were set to 15-500 genes using Hallmark, KEGG, Reactome and C2-Gene Perturbations collections (version 7.1). The last ones were filtered according to "Multiple Myeloma" involvement. Significant gene sets were selected on nominal p-value.

4.1.5. LncRNAs expression validation

We investigated lncRNAs expression in a proprietary dataset that includes 43 MM patients. All the samples were characterized for the presence of DIS3 mutations as previously described and for the main chromosomal aberrations. CD138+ cells were isolated from the BM aspirates by Ficoll-Hypaque (Lonza Group, Basel, Switzerland) density gradient sedimentation, followed by antibody-mediated positive selection using anti-CD138 magnetic activated cell separation microbeads (Miltenyi Biotech, Gladbach, Germany). RNA extraction, cDNA and qRT-PCR were developed as described in **paragraph 4.2.7**. To determine RNA levels by qPCR, the following primers were used:

Primer Name	Sequence (5'-3')
GAPDH FW	5' - ACAGTCAGCCGCATCTTCTT - 3'
GAPDH RW	5' - AATGAAGGGGTCATTGATGG - 3'
AC093510.1 FW	5'- CAAGGTCTGCGAAAATTGGC - 3'
AC093510.1 RW	5' - AATCACGGCCTCCAAGAAAT - 3'
AC015982.2 FW	5' - AAGAACGTGGAGCCCTTTCT - 3'
AC015982.2 RW	5' - GTGCTTTACAATCGCCAGCT - 3'
AC099778.1 FW	5' - CGTATTGTCAAGAGCCGTGG - 3'
AC099778.1 RW	5' - CCAGTCTCCGGTCAGTGATT - 3'
AL138976.2 FW	5' - TTGTGAGTACCAGGGTTCCC - 3'
AL138976.2 RW	5' - GGCCTCTCACCTCAGACTAG - 3'

4.2. Functional Biology Task

4.2.1. MM cell lines

Human cell lines NCI-H929 were purchased from DSMZ, which certified authentication performed by short tandem repeat DNA typing. AMO-1 were kindly provided by Dr. C. Driessen (University of Tubingen, Germany). All these cell lines were immediately frozen and used from the original stock within 6 months. Human myeloma cell lines were cultured in RPMI-1640 medium (Gibco®, Life Technologies, Carlsbad, CA, USA) supplemented with 10% fetal bovine serum, 100 U/ml penicillin, and 100 mg/ml streptomycin (Gibco®) at 37°C in 5% CO2 atmosphere and tested for mycoplasma contamination.

4.2.2. Primary Patient cells

Following informed consent approved by Fondazione IRCCS Ca' Granda Ospedale Maggiore Policlinico (Ethical Committee approval N°575, 03/29/2018), CD138+ cells were isolated from the BM aspirates of MM patients by Ficoll-Hypaque (Lonza Group, Basel, Switzerland) density gradient sedimentation, followed by antibody-mediated positive selection using anti-CD138 magnetic activated cell separation microbeads (Miltenyi Biotech, Gladbach, Germany). Purity of immunoselected cells was assessed by flow-cytometry analysis using a phycoerythrin-conjugated CD138 monoclonal antibody by standard procedures. CD138+ cells from MM patients were seeded and cultured in RPMI-1640 medium (Gibco®, Life Technologies) supplemented with 20% fetal bovine serum (Lonza Group Ltd.) and 1% penicillin/streptomycin (Gibco®, Life Technologies).

4.2.3. siRNA and in vitro HMCLs transfection

To silence DIS3 we used ON-TARGETplus siRNAs targeting DIS3 and a non-silencing negative control siRNA (CTRL) that were purchased from Dharmacon. NCI-H929 and AMO-1 cells were seeded in a plating density (0.1×10^6 cells/0.5mL). HMCLs were transfected by Neon Transfection System (Invitrogen, CA, US), with the following electroporation conditions: 1100 V, 30 ms, 2 pulse. siRNA was used at 200nM concentration. The transfection efficiency was evaluated by comparative qRT-PCR. Cells were incubated at 37°C and collected at 24-48-72 hr after transfection to assess the downregulation of DIS3 by qRT-PCR and then by Western blot analysis.

4.2.4. Design of GapmeRs and in vitro transfection of HMCLs

LNA gampeR oligonucleotides were provided by Exiqon (QIAGEN). LNA gapmeRs were in house-designed and purified by HPLC followed by Na^+-salt exchange and lyophilization.

NAME	DESIGN ID	SEQUENCE 5'-3'	Mw. calc. (Da)
gDIS3#2	339511-1	ACTTAATGGTAATAGA	5351.29
gDIS3#13	339511-2	GAGTCGAGACACCATG	5268.21
gDIS3#15	339511-3	TTCTATGCGACAAGGG	5302.21

HMCLs were transfected through the use of Neon Transfection System, with the following electroporation conditions: 1100 V, 30 ms, 2 pulse. LNA gapmeRs were used at 100nM. The transfection efficiency was evaluated by comparative qRT-PCR.

4.2.5. Cell viability and growth assessment

Cell viability was evaluated by counting the number of viable cells after trypan blue staining. Cells were suspended in well and mixed with trypan blue solution (ratio 1:1). 10 µl of this cell solution were seeded in a Bürker chamber and the cells were counted. At the end of the counting, the percentage of viability of each sample was evaluated.

4.2.6. Colony-forming assay

For colony-forming assay, CTRL and gDIS3 silenced cells were suspended in RPMI-1640 medium with 10% fetal bovine serum (FBS) and plated on methylcellulose-based media (MethoCult TM STEMCELL Technologies) containing 1% methylcellulose in RPMI-1640 medium, 10% FBS. Each condition was evaluated twice in triplicates. Colonies were scored

by an inverted microscope after a 21-day incubation at 37 °C in a fully humidified atmosphere at 5% CO2.

4.2.7. Cell cycle analysis and apoptosis

Cell cycle distribution of DIS3 silenced and relative control HMCLs was assessed using BD FACSVerse™ flow cytometer (BD Bioscience, Italy). Samples for cell cycle analysis were fixed in 70% ethanol at 4 °C for at least 2 h and incubated with FxCycle™ PI/RNase Staining Solution (Life Technologies) for 30 min in the dark, according to the manufacturer's instructions. Fluorescent emissions were collected through a 575 nm band-pass filter. To detect apoptosis, control and silenced cells were harvested, washed twice, and suspended in binding buffer. Then, the cells were stained using a PE Annexin V Apoptosis Detection Kit (BD Biosciences), following which they were subjected to BD FACSVerse™ flow cytometry (BD Biosciences) to analyze apoptotic distribution.

4.2.8. RNA extraction, RT-PCR and qPCR

Total RNA was extracted using TRIzol® Reagent (Invitrogen) according to manufacturer's instructions. The purity and concentration of total RNA was determined by the NanoDrop 1000 spectrophotometer (Thermo Fisher Scientific). The ratios of absorption (260 nm/280 nm) of all samples were between 1.8 and 2.0. cDNA was synthesized from 500 ng of total RNA with random primers using the High-Capacity cDNA Reverse Transcriptase Kit (Invitrogen, Life Technologies) according to the manufacturer`s instructions. mRNA expression was performed by real-time quantitative PCR reaction using SYBR green PCR Master Mix (Applied Biosystems) after optimization of the primer conditions. 10 ng of reverse-transcribed RNAs were mixed with 300 nM of specific forward and reverse primers in a final volume of 10 µl. RT-PCR was performed on an Applied Biosystems StepOnePlus Real-Time PCR system for 40 cycles. The relative expression level was calculated with the $2^{[\Delta\Delta Ct]}$ method and expressed as a fold change: normalization of data was performed on house-keeping gene (GAPDH) expression. To determine RNA levels by qPCR, the following primers were used:

Primer Name	Sequence (5’-3’)
GAPDH FW	5’-ACAGTCAGCCGCATCTTCTT-3’
GAPDH RW	5’-AATGAAGGGGTCATTGATGG-3’
DIS3 FW	5’-GCGATTCGAGTAGCAGCAAA-3’
DIS3 RW	5’-TGAGTTCGGGGTTAGCAGTT-3’
RAD51B FW	5'-CATGTTAGGAGCGCTGGAAC-3’
RAD51B RW	5'-TGGCCCTGGTCTTCTTTTCT-3'
ARID5B FW	5’-GGCAGAAATAGCGACCATGG -3’
ARID5B RW	5’-CCCAAGGCCTCAGTTTTCAC -3’
CCNB1 FW	5’-TTTCTGCTGGGTGTAGGTCC-3’
CCNB1 RW	5’-GCCATGTTGATCTTCGCCTT-3’
CDC20 FW	5’-CGTTCGAGAGTGACCTGCA-3’
CDC20 RW	5’-CCAGGTTTGCTAGGAGTGGT-3’
KIF14 RW	5’-TGCCATGGGATTGATTAGATCTC -3’
KIF14 RW	5’-TGGAGCACGATTAACCATCCT-3’
TOP2A FW	5’-ACATATTTTGCTCCGCCCAG-3’
TOP2A RW	5’-CTTTGTTTGTTGTCCGCAGC-3’
POLR2H FW	5’-CTCGACTGCATTGTGAGAGTG-3’
POLR2H RW	5’-AAGGCCTATCATCAGTGGGG-3’

4.2.9. Protein detection by Western blots

For protein analyses cells were homogenized in lysis buffer M-PER® Mammalian Protein Extraction Reagent (Thermo Scientific) and Halt Protease and Phosphatase inhibitor cocktail, EDTA-free, 100X, (Thermo Scientific). Protein lysates were centrifuged at 13000 rcf for 10 min. Whole cell lysates (40 µg per cell line) were separated using Bolt™ 4-12% Bis-Tris Plus Acriliamide Gels (Invitrogen), electro-transferred onto nitrocellulose membranes (Bio-Rad, Hercules, CA, USA), and immunoblotted over night at 4°C with primary antibody (Table 1). Membranes were washed three times in PBST solution and then incubated with a secondary antibody conjugated with horseradish peroxidase (HRP) in BSA 2% - PBST for 2 hours at RT. Chemiluminescence was developed using Clarity ECL Western Blot Substrate Kit (BIO-RAD) and signal intensity was detected using ChemiDoc MP System (Bio-Rad). The experiments were repeated at least three times.

Ab	Company	Code	Dilution	Secondary Ab
Anti-CCNE1	Cell Signaling Technology	20808	1:1000 BSA 5%-PBS TW 0,1%	Rabbit: 1:2000 BSA 2%-PBS TW 0,1%
Anti-CCNA2	Cell Signaling Technology	4656	1:1000 BSA 5%-PBS TW 0,1%	Mouse: 1:2000 BSA 2%-PBS TW 0,1%
Anti-pCCNB1 Ser133	Cell Signaling Technology	4133	1:1000 BSA 5%-PBS TW 0,1%	Rabbit: 1:2000 BSA 2%-PBS TW 0,1%
Anti-CCNB1 Ser133	Cell Signaling Technology	4138	1:1000 BSA 5%-PBS TW 0,1%	Rabbit: 1:2000 BSA 2%-PBS TW 0,1%
Anti-pCDK1 Thr161	Cell Signaling Technology	9114	1:1000 BSA 5%-PBS TW 0,1%	Rabbit: 1:2000 BSA 2%-PBS TW 0,1%
Anti-CDK1	Cell Signaling Technology	77055	1:1000 BSA 5%-PBS TW 0,1%	Rabbit: 1:2000 BSA 2%-PBS TW 0,1%
Anti-pCDC20 Ser51	Cell Signaling Technology	8038	1:1000 BSA 5%-PBS TW 0,1%	Rabbit: 1:2000 BSA 2%-PBS TW 0,1%
Anti-CDC20	Cell Signaling Technology	4823	1:1000 BSA 5%-PBS TW 0,1%	Rabbit: 1:2000 BSA 2%-PBS TW 0,1%
Anti-GAPDH	Santa Cruz	Sc-7899	1:2000 BSA 5%-PBS TW 0,1%	Mouse: 1:2000 BSA 2%-PBS TW 0,1%
Anti-DIS3	Proteintech	14689-1-AP	1:1000 BSA 5%-PBS TW 0,1%	Rabbit: 1:2000 BSA 2%-PBS TW 0,1%

Table 1. List of the antibody used for western blot analysis.

4.2.10. Drug treatment

AMO-1 and NCI-H929 cells were treated with ARRY-520 in combination with gapmeR against DIS3. ARRY-520 was obtained from Cayman Chemical and used at working concentration of 1nM.

4.2.11. Cellular synchronization

For cellular synchronization was used Synchroset kit from EuroClone. Cells were seeded at a concentration of $0.050x10^6$/ml and DIS3 was added the same time of the seeding. After 4 days of culture were added 20 µl/ml of solution A (min 14-max 20 hours) was added per ml to block cells at G0/G1 phases of the cell cycle. After 16 hours were added 20µl/ml of solution B and cells were incubated for 5 hours to release cells. At the end of the release cells were collected following a time course (T0-2hrs-4hrs-6hrs after release).

Another method to synchronize cells were used: cells were seeded at a concentration of $0.050x10^6$/ml and DIS3 was added the same time of seeding. After 4 days of culture cells were synchronized with 7,5µM/ml RO-3306 (Selleckchem) for 24hr at 37°C. The day after

cells were treated with MG-132 25μM/ml (Selleckchem) for 90min at 37°C. At the end cells were fixed and processed for immunofluorescence.

4.2.12. Immunofluorescence

0.050 x 10^6 cells were harvested, centrifuged onto glass slides (Cytospin 4, Thermo Scientific), then fixed in 4% paraformaldehyde in PBS1X for 6 min at 22°C, followed by three 5-min washes in PBS. Cells were permeabilized (0.1% Triton X-100 in PBS, 15-min), washed in PBS (3X, 5 min each), blocked 1 h at 22°C with 2% BSA in PBS, and then incubated 1 hour at 4°C with DIS3 antibody (#14689-1-AP; Proteintech; 1:100) or y-Tubulin (#5886; Cell Signaling Thecnology; 1:100) to detect centriole. Thereafter, slides were washed in PBS (3X, 5 min each) and incubated 1 h at 22°C in the dark, with Alexa Fluor 555 Anti-Rabbit IgG secondary Antibody (Cell Signaling Technology, 1:500).
Anti-alpha-Tubulin alexa fluor 488 (Abcam; 1:100) was used to detect microtubule. After three PBS washes, cells were mounted under coverslips with DAPI-containing Vectashield (Vector Laboratories). Images were acquired by Leica TCS SP8 confocal laser scanning microscope (DMi8); acquisitions were performed with 40X and 63X immersion oil objectives. Conversion of imaged z-stacks into average intensity projections was processed by Leica Microsystem software (Leica Application Suite X - LAS X).

4.2.13. Global transcriptome profiling

Total RNA samples were processed using WT PLUS Reagent Kit in accordance with the manufacturer's protocols (Thermo Fisher Scientific, Waltham, MA, USA). Global gene expression profiles were obtained using Clariom D array (Thermo Fisher Scientific, Waltham, MA, USA) in NCI-H929 triplicates that were subjected to gymnotic DIS3 silencing in comparison to NCI-H929 control triplicates. Robust Multichip Average (RMA) normalization was applied on raw data and a custom annotation pipeline was applied using the Chip Definition File (CDF) version 25 for GENECODE transcript annotations, freely available: at http://brainarray.mbni.med.umich.edu/Brainarray/Database/CustomCDF/25.0.0/gencodet.asp. Therefore, the expression levels of Ensembl genes specific for 19241 protein coding genes and 15485 lncRNAs were obtained.

4.2.14. Differential expression analysis

Differential expression in gymnotic DIS3 silenced compared to control NCI-H929 triplicates was performed by means of Significance analysis of Microarrays (SAM) analysis (86) applying 500 permutations and default analysis conditions. Specific transcriptional patterns were defined using a 10% cut-off on FDR q-value. Global differentially expressed gene lists were selected on FDR < 10% cut-off.

4.2.15. Functional enrichment analysis

Enrichment analysis was carried out using clusterProfiler package (version 3.18.1) (Guangchuang Y et al., A Journal of Integrative Biology. 2012) in R 4.0.0 environment, on Gene Ontology (GO) Biological Process (BP) and Molecular Function (MF) terms. Barplot charts of the top 20 most significant annotation category terms were depicted using the global differentially expressed (DE) gene list ranked by Fold Change (FC) and setting p-value < 0.05 and q-value < 0.10 cut-off. Network interactions between the top five GO-BP or GO-MF annotation terms were visualized by using the cnetplot function. Gene Set Enrichment Analysis (GSEA) was achieved on global expression profiles of 19048 Ensembl annotated protein coding genes in DIS3-silenced compared to control NCI-H929 triplicates, by applying 1000 gene set permutations and default analysis conditions. Significant Hallmark, KEGG and Reactome gene sets (version 7.4) were selected on the base of nominal p-value <0.05 and FDR q-value < 5%.

4.2.16. Statistical analysis

Statistical analysis was performed using Student *t* test for comparing two groups and by ANOVA for multiple group comparisons. All experiments were performed in two or more replicates.

5. Results, part 1: Transcriptional signature and clinical out came of DIS3 mutations in Multiple Myeloma

5.1. Evaluation of DIS3 mutations in myeloma patients

We focused on a CoMMpass cohort of 930 bone marrow PC samples from newly diagnosed MM (NDMM) patients for whom non-synonymous somatic mutation data by whole exome sequencing (WES) were available, identifying 103 DIS3 mutations (DIS3mts) in 94/930 cases. The variant allelic frequency (VAF) ranged between 5.3 and 100% (mean: 48%; median: 43%). Most of the mutations were in the coding region (100/103) and were missense variants (95/103) or within the splice site region (2/103), while in a minority of cases they consisted of start-loss (3/103). Three mutations have been classified as splice or donor acceptor variants involving intronic sequences (3/103), all by means of SnpEff and SnpSift tools (//snpeff.sourceforge.net/). DIS3mts occurred mainly in the active domains of the protein: in detail, 70/103 mutations were in the RNB domain and 10 in the PIN domain. Regarding the major mutational hotspots reported occurring within the RNB domain, R780 was involved in 12 cases of MM, while residues D488 and D479 were affected in samples of 11 MM each (Figure 7A).

Then, we also evaluated the association of DIS3mts with the presence of the main IGH chromosomal translocations in 724 patients.

We observed a significant co-occurrence both with t(4;14) and MAF (MAF, MAFB or MAFA) translocations (p=0.0035). Furthermore, a trend towards translocation t(11; 14) was highlighted in the cases mutated in DIS3 even though it did not reach statistical significance (27.3% vs 18.4% in the non-mutated cases), while no relevant association was found with t(6; 14) or MYC translocations.

The association of DIS3mts with CNAs commonly found in MM disease was evaluated in 847 MM cases, for which specific data by WES were available. As expected, a very significant association (p=0.0003) was observed between DIS3mts and del(13q): specifically, 62 out of 86 patients harboring DIS3mts and for which CNAs data were available, showed a 13q deletion. Next, we considered the distribution of del(13q) across the different types of DIS3mts and only 9 out of 29 MM affected by the mutational hotspots also carried del(13q). Notably D479 hotspot was involved in 5 of these 9 cases.

On the contrary, 50 out of the 54 cases harboring not-hotspots DIS3mts were associated with del(13q) (Fisher exact test P-value<0.0001). Concerning the other main CNAs, was observed a very significant association (p=0.0020) with 1q21 gain/amplification (1q

gain/amp), occurring in 45 out of 86 DIS3-mutated patients, 38 of which also carrying the (13q).

On the contrary, was found a highly significant inverse correlation with the hyperdiploid condition (p=0.0003) and the occurrence of 1p22/CDKN2C loss (p=0.0205).

Moreover, were present 17p13/*TP53* deletions only in 4 out of 86 cases harboring DIS3mts.

We also examined the co-occurrence of DIS3mts with the most frequently mutated genes in MM, namely KRAS, N-RAS, BRAF, FAM46C, TP53 and TRAF3. A statistically significant association with DIS3mts was observed only for BRAF mutations (p = 0.0126).

Notably, the kinase-dead BRAF D594 mutation was observed more frequently in DIS3 mutated (5/12) compared to wild-type cases (10/56), albeit not reaching a statistical significance. This is probably related to the higher prevalence of BRAF D594 mutations in MAF-translocated cases (85). Figure 7B displays the global landscape of co-occurrence of DIS3mts with other main molecular lesions.

A

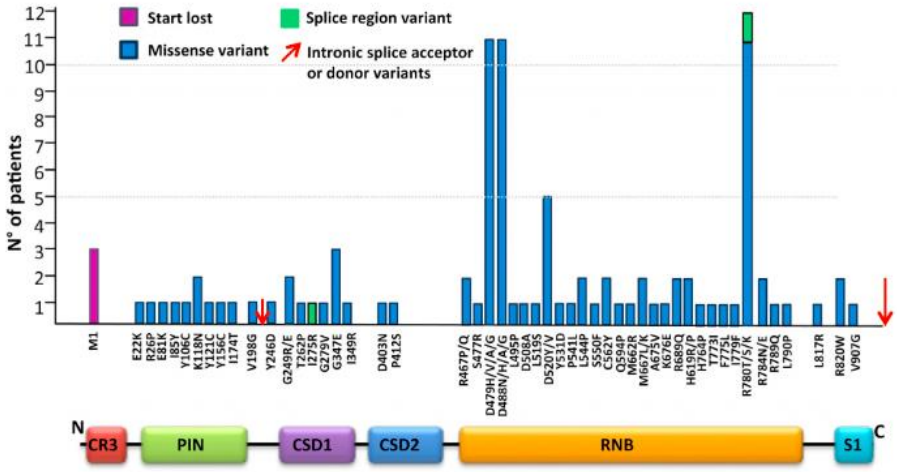

B

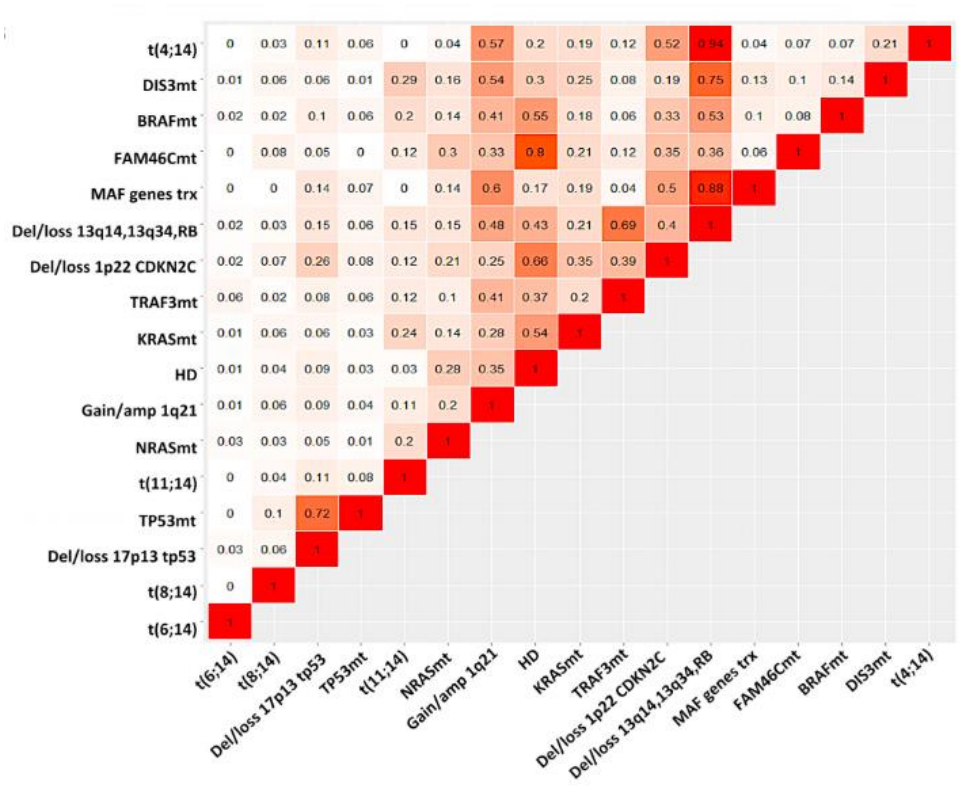

Figure 7. DIS3 distribution of non-synonymous somatic variants of patients derived from CoMMpass cohort and their correlation with other genetic alterations. (A) Incidence of the 100 missense SNVs in DIS3 protein domains are represented in the histogram below; red arrows indicate the splice acceptor or donor variants. **(B)** Plot of co-occurrence of main CNAs, Igh translocations and non-synonymous somatic mutations in 651 MM of CoMMpass dataset entirely profiled by WES and RNA-seq.

5.2. Correlation of the DIS3 mutations with clinical parameters

We examined the clinical impact of DIS3mts in 930 MM cases with available PFS and OS data. With a median follow-up of 889 and 868 days for PFS and OS, respectively, was observed a significant lower survival rate for both OS (Log-rank p=0.039) and PFS (Log-rank p=0.021) in 94 DIS3 mutated cases versus 836 DIS3 WT MMs.

In detail, the median PFS was 800 days in DIS3mut vs 1176 days in WT MM cases (Figure 8A-B), whereas the OS evaluated in DIS3 mutated cases vs WT group was 65% at 3 years. As described above, DIS3mts co-occur significantly with del(13q) and therefore with the loss of the second allele, affecting other several genes in MM.

For this reason, we stratified the cases of the CoMMpass series into four groups based on: absence of both DIS3mts and del(13q) (381 cases), the presence of only DIS3mts (24 cases), the del(13q) alone (380 cases) or the occurrence of both DIS3mts and del(13q) (62 cases).

As illustrated in Figure 8C-D, the presence of the bi-allelic alterations was associated with a poor prognosis compared to WT condition, respectively reaching a 3-years OS of 62% vs 82%, and a median PFS of 772 days vs 1215 days.

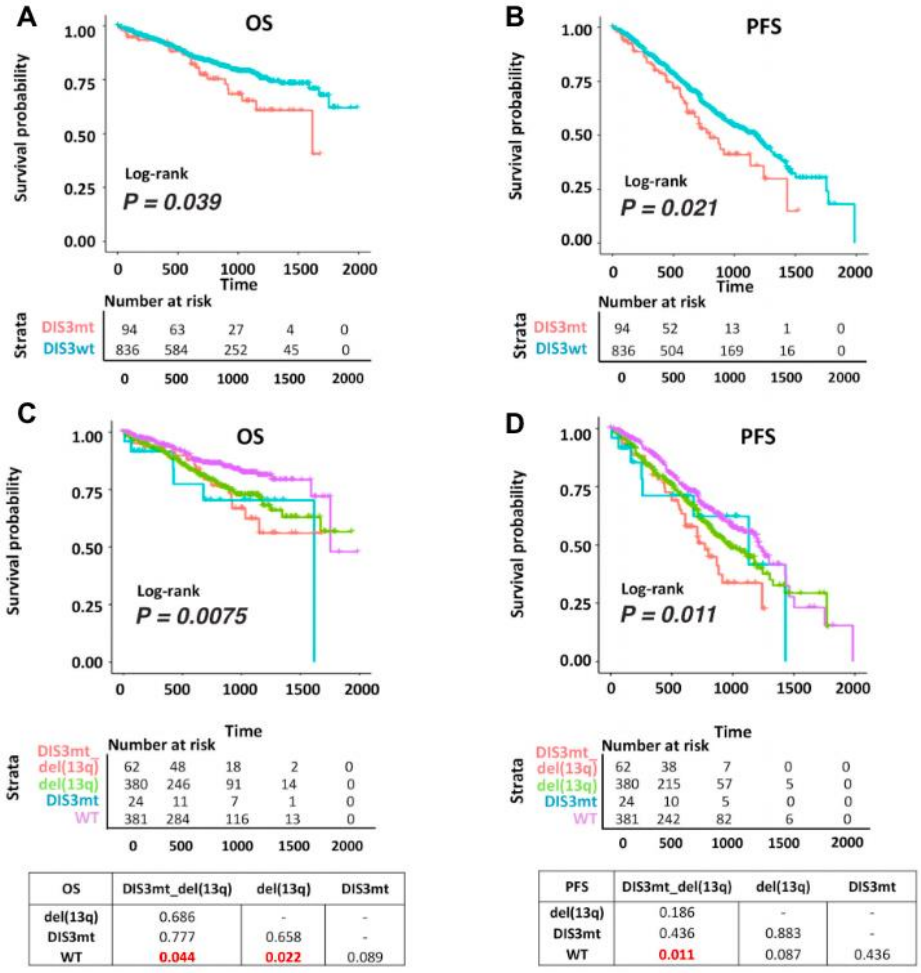

OS	DIS3mt_del(13q)	del(13q)	DIS3mt
del(13q)	0.686	-	-
DIS3mt	0.777	0.658	-
WT	**0.044**	**0.022**	0.089

PFS	DIS3mt_del(13q)	del(13q)	DIS3mt
del(13q)	0.186	-	-
DIS3mt	0.436	0.883	-
WT	**0.011**	0.087	0.436

Figure 8. **Kaplan-Meier survival curves**. Kaplan-Meire curves on 930 MM cases stratified agreeing to DIS3 mutation occurrence with respect to OS **(A)** and PFS **(B).** Kaplan-Meier survival curves in 847 cases stratified in four molecular groups: the presence of DIS3 mutation and del(13q) as single or bi-allelic alterations, with respect to OS **(C)** and PFS **(D).** Log-rank test p-value measuring the global difference between survival curves and number of samples at risk in each group across time are reported. Log-rank test p-values of pairwise comparisons are also reported in **C-D**. Significant adjusted p-values by BH correction (< 0.05) are in bold red. OS median follow up time: 862 days, IQR: [594 days; 1092 days]; PFS median follow up time: 828 days, IQR: [535 days;1094 days].

In addition, we tested the clinical impact of DIS3mts and del(13q), as single or bi-allelic condition, along with other parameters, such as the International Staging System subgroups (ISS I-III) and the other most important molecular lesions, by Cox regression univariate analysis for both OS and PFS outcome, in 630 MM patients for which all the information were available. A significant higher risk, both in PFS and OS, was associated with ISS stage

III and the occurrence of 1q gain/amp in association with TP53 alterations. A higher risk in OS was also associated with the presence of DIS3mts or del(13q) as monoallelic condition, whereas the bi-allelic alteration was associated to a shorter PFS.

On the contrary, a significant lower risk, both in PFS and OS, was associated to ISS I stage. All these features retained their clinical impact both in OS and PFS, when tested in Cox regression multivariate analysis (Figure 9).

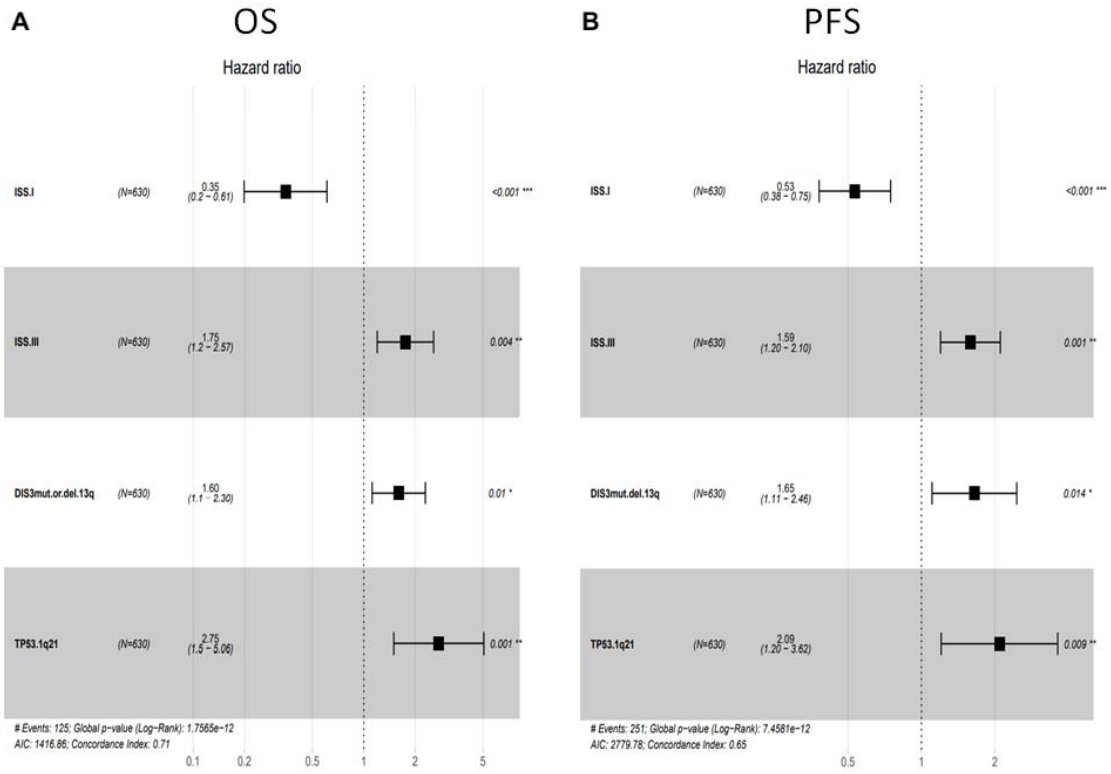

Figure 9. DIS3 mutations impact and other clinical/molecular variables on survival of multiple myeloma patients. Forest plots of cox regression multivariate analyses considering all features with adjusted p-value<0.05 in univariate analysis with regards to OS **(A)** and PFS **(B)**, in 630 MM cases of CoMMpass cohort for which were available all considered data. Hazard Ratio, 95% Confidence Interval and p-value are reported for each variable. Global Log-rank p-value is reported for each analysis.

Based on these results of the differential effects of mono-allelic or bi-allelic DIS3 lesions, we reanalyzed the association of these events with known oncogenic MM lesions.

As regard the main IgH translocations, the t(4;14) was exclusively related to the bi-allelic condition (p=0.0170). Furthermore, was observed a higher prevalence of 1q gain/amp in patients with bi-allelic DIS3 events (61% vs 29%), while a higher fraction of FAM46C mutated cases was evidenced in cases carrying only DIS3mts (5.3% vs 3.1%).

5.3. Transcriptional expression changes associated with DIS3 mutation and del(13q)

To define the molecular pathways and gene expression signatures associated with DIS3mts, we focused on cases with mutation expression at significant levels, in this way using for a stringent cutoff of 20% on the RNA mutational load (RNA_ALT_FREQ), selected based on the analysis of the ROC curve (Area Under the Curve (AUC) 98 %) based on DNA mutation level (VAF).

Further support this cut-off value, we found a global significant correlation (Pearson's correlation r=0.94) between DNA and RNA mutational levels in those 56 MM cases with DIS3 RNA mutational load >20%, compared to the remaining 17 MM cases with lower RNA somatic variant frequencies (r=0.30).

For the analysis, we considered a total of 28346 expressed transcripts and compared the expression profiles in 56 DIS3 mutant cases versus 582 WT DIS3 MM cases. A large list of 7167 differentially expressed transcripts (DE) was obtained, 6564 of which were annotated, with a low stringency cut-off (FDR <10%).

Among them, 3464 protein coding genes and 2062 lncRNAs resulted mostly upregulated (79%) in DIS3 mutated compared to unmutated cases. Principal Component Analysis (PCA) based on the expression levels of 6564 DE annotated transcripts in 56 DIS3 mutated and 582 DIS3 WT samples stratified according to del(13q) alteration, confirmed a robust association between DIS3mt and del(13q) (Figure 10A).

Furthermore, the heat map of the first 100 transcripts most significantly upregulated, involving almost all lncRNA (82%), in stratified MM samples revealed a stronger pattern of positive regulation in the bi-allelic lesion group with respect to MM cases with DIS3mts or del(13q) alone, compared to DIS3 WT MM samples (Figure 10B).

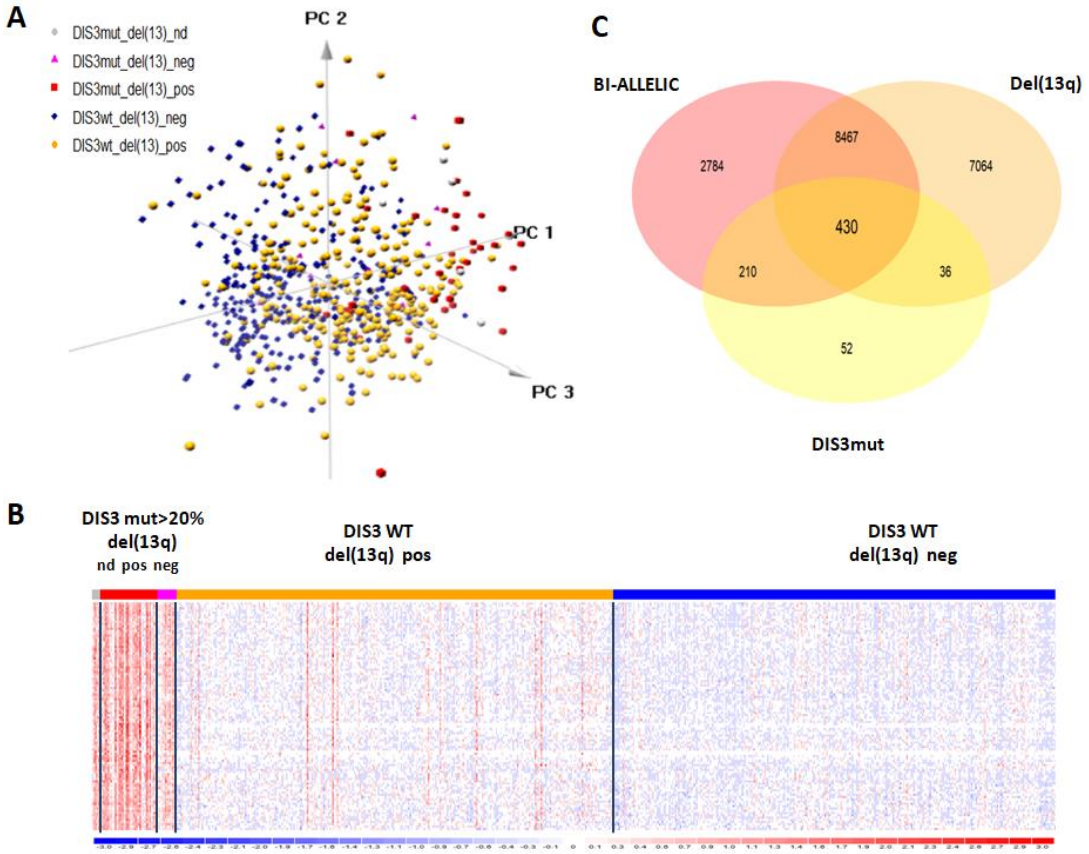

Figure 10. Transcriptional expression chance associated with DIS3 mutations and del(13q). (A) PCA on 6564 DE transcripts in 56 DIS3 >20% mutated vs 582 DIS3 WT MM samples. **(B)** Heatmap of top 100 differentially expressed transcripts in 56 DIS3 >20% mutated versus 582 DIS3 WT MM samples. The colored scaled bar represents standardized rows by subtracting the mean and divided by the standard deviation. Samples in each group are stratified in agreement to the occurrence of del(13q) aberration: 5 DIS3mts and not available (nd) for del(13q) MM samples, 38 MM cases with bi-allelic alteration, 13 MM samples carrying only DIS3 mutation, 289 MM with del(13q) as single lesion and 293 wild type MM samples. **(C)** Venn diagram on differentially expressed transcripts lists resulting from 13 MM cases with DIS3 mutation, 289 MM with del(13q) as single lesions, or 38 MM with bi-allelic alteration compared to 293 WT MM cases.

Based on these findings, we compared the global expression profiles associated with each lesion (DIS3mts, del13q and biallelic condition) to WT; we found a share of 430 DE transcripts in all three comparisons, of which 305 are lncRNA and 56 are protein coding genes (Figure 10C).

5.4. Protein coding transcripts: gene sets and molecular pathways modulated associated to DIS3 mutation

To determine which molecular pathways could be modulated in relation to DIS3mts occurrence in MM, a Gene Set Enrichment Analysis (GSEA) was performed on the list of DE protein coding genes that were ranked based on fold change values.

Specifically, the enrichment map on the top 100 GSEA gene sets based on Gene Ontology (GO) Biological Process (BP) terms showed a complex network of connected functional modules mostly concerning RNA and protein metabolism, nucleosome organization, cell-cycle regulation, cell proliferation and apoptosis, immune response, cell adhesion and tissue development (Figure 11).

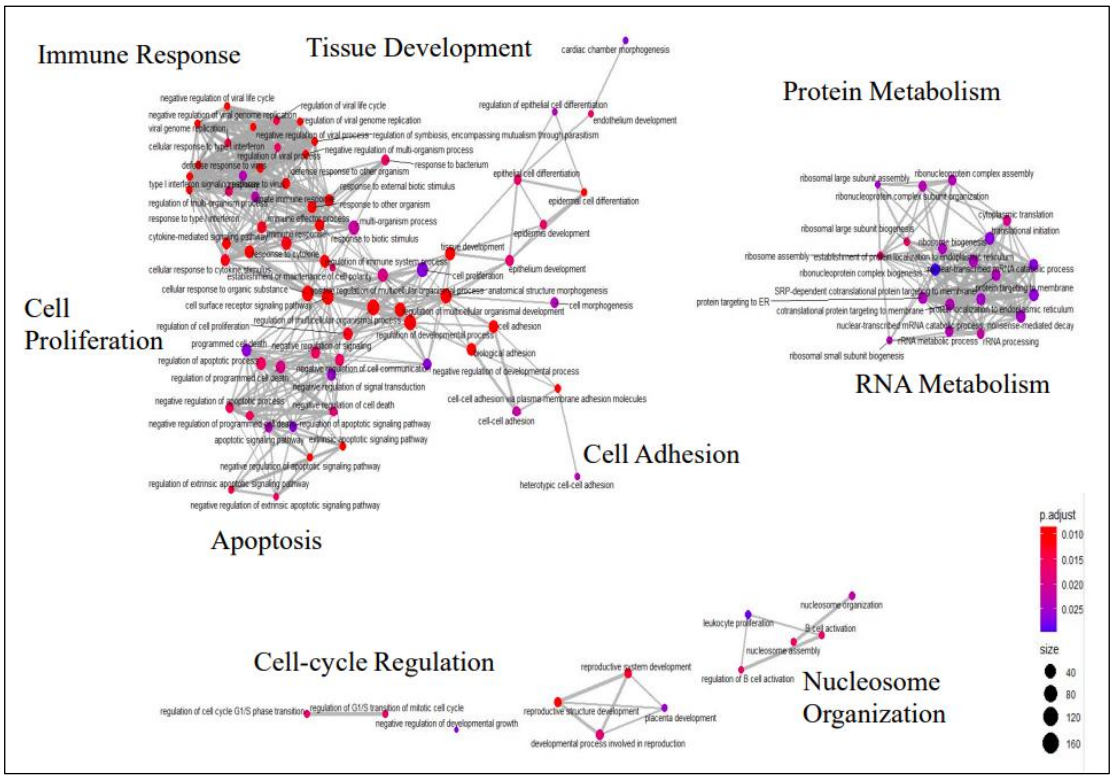

Figure 11. Enrichment map on top 100 GSEA gene sets based on GO-BP terms. Analysis was performed by Cluster Profiler analysis on DE global protein coding transcrip list.

More in details, we evidenced the up-regulation of several cell signaling pathways, among which the interferon response, the TNFα signaling via NFKB, and the B-cell receptor cascade.

Moreover, genes modulated by KRAS activation or involved in TP53 pathway and cell death, cell adhesion and migration, cell-cell communication, chromatin organization and cell cycle check points resulted positively modulated in DIS3 mutated MM samples.

On the contrary, oxidative phosphorylation gene sets were down-regulated, together with genes involved in RNA and protein metabolism, like those codifying for ribosome structural constituents or involved in ubiquitin-mediated proteolysis, amino acid modification and translation. Furthermore, genes implicated in DNA repair process and chromatin modifying enzymes were found downregulated in DIS3 mutated cases (Figure 12).

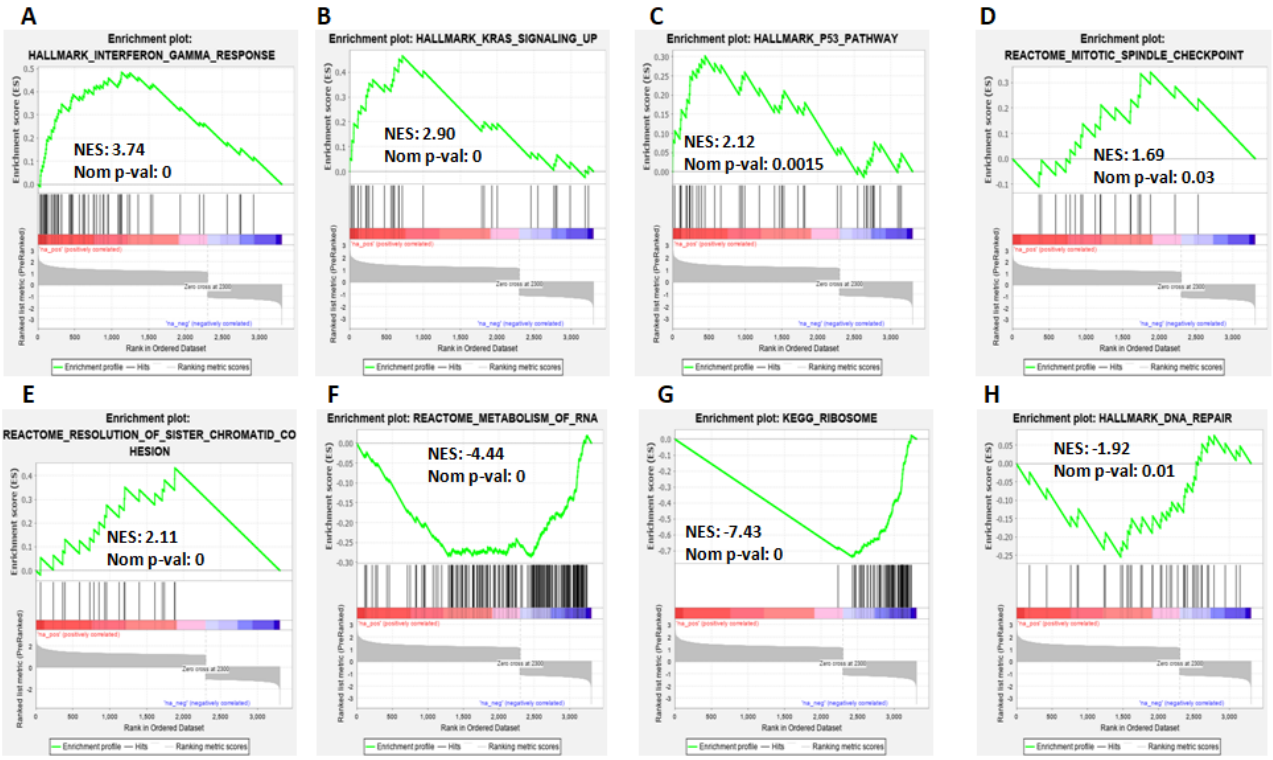

Figure 12. **Gene set enrichment analysis of DIS3 mutations in MM.** Enrichment plots of significantly deregulated gene sets, involving several signaling pathways **(A-C)**, cell cycle **(D-E),** RNA metabolism **(F-G),** and DNA repair **(H),** in DIS3 mutated compared to DIS3 WT MM cases by GSEA. Normalized Enrichment Score (NES) and nominal p-value are reported for each gene set.

Finally, we found a significant enrichment of genes recognized in known transcriptional signatures of MM patients carrying main IGH translocations. These involved translocation target genes like FGFR3, WHSC1 or MAF, concurrently with several genes identified in their specific gene expression patterns (i.e. KLF4, CCND2, SPP1, ITGB7).

On the contrary, an opposite behavior was observed as regard gene sets associated to the hyperdiploid alteration in MM.

Finally, the shared DE transcript list associated with DIS3 mutations was enriched in lncRNA particularly (51% of all DE transcripts), thus further supporting the notion of a significantly stronger impact of DIS3 mutations on the ncRNA transcriptome.

5.5. Differential lncRNAs expression patterns associated with DIS3 mutation

The transcriptional pattern of lncRNAs associated with DIS3 mutations was further investigated.

In detail, based on the large heterogeneity of lncRNAs and their lower expression levels compared to protein coding transcripts, we applied a more stringent analysis on 2062 DE lncRNAs, focusing on the 50 most significant ones at FDR<1% and FC>2.

All lncRNAs were up-regulated in DIS3 mutated cases compared to DIS3 WT and they were mainly represented by lncRNAs which are antisense to the coding genes (80%); the remaining cases involved 3 lncRNAs which are sense to the coding genes, one long intergenic non-protein coding RNA, 2 miRNA host genes and 2 divergent transcripts. To note, the novel transcript Z93930.2 is located less than 100 bp antisense to the XBP1 transcription factor, a consolidated regulator of MM, well-known to be altered during MM initiation and progression (60).

Based on the recurrent evidence that the transcription of mRNAs and lncRNAs appears to be closely regulated, leading to a cis-regulatory relationship between the two transcripts (87,88), we investigated expression levels of nearby or overlapping transcripts localized nearby to the 50 lncRNAs (up to 65 kb window).

Consequently, we considered 81 mRNA-lncRNA pairs and analyzed the correlation between their expression levels over the entire dataset of 767 MM cases that were profiled by RNA-seq in the CoMMpass cohort. Was observed a significant positive Pearson's correlation ($r>0.5$, $p<6.08E-16$) for 9 lncRNA-gene pairs; among them, AL121672.3 and MIRLET7BHG lncRNAs, both mapping at 22q13, showed a relevant correlation within each other ($r=0.65$) and with the PRR34 gene ($r=0.66$, $r=0.73$, respectively) (supplementary information are available on a paper published by our group: Todoerti K et al., Haematologica 2022).

Finally, we found that 26 out of the evaluated overlapping/neighbor transcripts resulted also differentially expressed in association to DIS3 mutated state.

5.6. Clinical relevance of long non-coding RNAs

Next, all 50 lncRNAs were tested with respect to OS or PFS outcome by means of Kaplan-Meier survival analysis taking in consideration 767 MM cases with available RNA-seq and survival data. High versus low expression groups were determined according to the mean cut-off value for the expression level of each lncRNA across the entire dataset.

Interestingly, higher expression levels were associated to a poorer clinical outcome in terms of PFS for 35 out of all the 50 lncRNAs tested. Furthermore, 15 of them resulted as unfavorable prognostic factors also in association to OS (Figure 13).

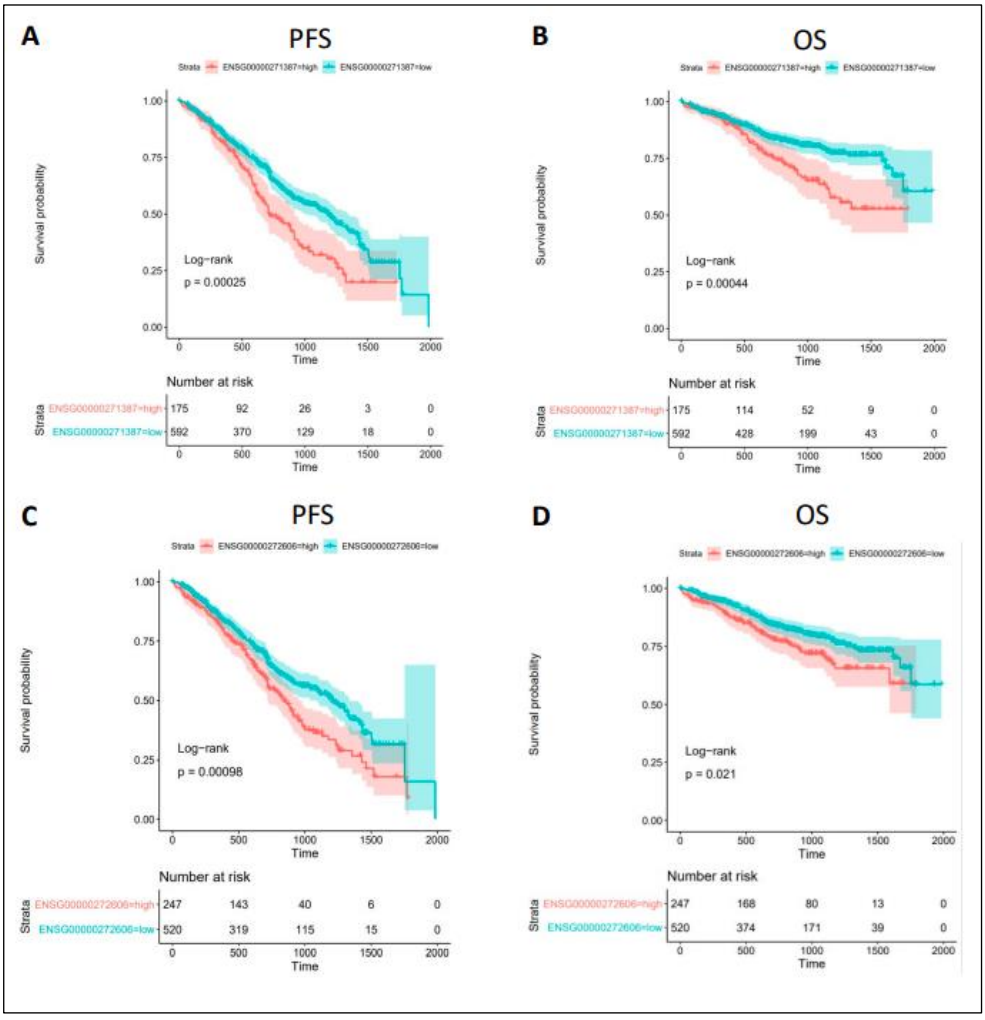

Figure 13. Kaplan-Meier survival curves. Kaplan-Meier survival curves of AL445228.2 and AC015982.2 lncRNAs in 767 MM cases stratified in low and high expression group on the base of mean cut-off, with respect to PFS **(A-C)** and OS **(B-D).** Log-rank test p-value and number of cases at risk in each group across time are reported.

The poorer clinical outcome was further investigated as regard the 35 lncRNAs by Cox regression univariate analysis. The higher expression level for 21 lncRNAs was associated with a significant higher risk in PFS, and for 5 of them (AC015982.2, AL353807.2, AC013400.1, ASH1L-AS1, and AL445228.3) also in OS.

Next, for all these 21 lncRNAs, were tested high and low lncRNA expression levels in 630 cases, taking in consideration the other clinically relevant characteristic, i.e. ISS stage I and III, the occurrence of 1q gain/amp in association to TP53 alterations, the presence of DIS3 mutations or del(13q) as single events for OS, or for PFS the bi-allelic alteration. Notably, all the five lncRNAs associated with a shorter OS retained their clinical impact when tested in Cox regression multivariate analysis together with major poor prognostic molecular features.

Two of them (AC015982.2 and AL445228.3) retained a significance also in PFS; besides these two lncRNAs, other seven (AC099778.1, AP000894.4, AL121658.1, AL356441.1, BX284668.6, AC093510.1, AL138976.2) resulted independent predictors of PFS at multivariate analysis (Figure 14A).

Altogether, from our analysis 12 lncRNAs were predicted to have strong clinical relevance (Figure 14).

In detail, 11 of them code for novel transcripts, and four are antisense to known transcripts whose expression level was highly positively correlated (Figure 14A). Interestingly, we found four couples lncRNA-coding genes that are antisense or nearby, located on chromosome 1q with highly correlated expression (Figure 14); these protein coding transcripts (MGST3, ASH1L, MSTO1, and C1orf21) resulted also significantly upregulated in DIS3 mutated as compared to unmutated samples.

Finally, the expression of four of these lncRNAs was validated by qRT-PCR in 43 newly diagnosed MM samples from our laboratory, characterized for the presence of DIS3 mutations and for which material was available.

From this evaluation, we founded a significant upregulation of AC093510.1, AC015982.2, and AL138976.2 in DIS3 mutated MM without the presence of del (13q) compared to WT DIS3 samples, while AC099778.1 only in the biallelic condition was significantly upregulated (Figure 14B).

A

Gene stable ID	Gene name	Description	Chr.	start (bp)	end (bp)	Strand	Neighbour Gene Name	Pearson's Correlation
ENSG00000232519	AL353807.2	novel transcript, antisense to MSTO1	1q22	155609776	155610380	-1	MSTO1	r = 0.38, p-value < 6.08E-16
ENSG00000235919	ASH1L-AS1	ASH1L antisense RNA 1 [Source:HGNC Symbol;Acc:HGNC:44146]	1q22	155562042	155563944	1	ASH1L; AL353807.4	r= 0.34, p-value < 6.08E-16 r= 0.63, p-value < 6.08E-16
ENSG00000271991	AC013400.1	novel transcript, antisense to TTC32	2p24	19902025	19902569	1	TTC32	r = 0.40, p-value < 6.08E-16
ENSG00000271387	AL445228.2	novel transcript, antisense to C1orf21	1q25	184385753	184386704	-1	C1orf21	r= 0.69, p-value < 6.08E-16
ENSG00000272606	AC015982.2	novel transcript, antisense to PP4R3B	2p16	55617909	55618373	1	PNPT1	r=0.15, p-value = 2.70E-05
ENSG00000236206	AL356441.1	novel transcript, sense to MGST3	1q24	165598356	165624084	1	MGST3	r = 0.28, p-value = 8.93E-15
ENSG00000255647	AC093510.1	novel transcript, antisense to CETN3	5q14	90410000	90410669	1	CETN3	r= 0.13, p-value = 6.39E-04
ENSG00000259775	AL138976.2	novel transcript, antisense to EIF5	14q32	103331674	103332367	-1	EIF5	r= 0.30, p-value < 6.08E-16
ENSG00000260236	AC099778.1	novel transcript, antisense to PTPN23	3p21	47379089	47380999	-1	PTPN23	r= 0.11, p-value = 4.42E-03
ENSG00000272426	BX284668.6	novel transcript, antisense to CROCC	1p36	16904339	16904776	-1	RNU1-2 CROCC	r=0.15, p-value = 3.00E-05 r=0.18, p-value = 1.36E-06
ENSG00000272716	AL121658.1	novel transcript, antisense to SLC30A6	2p22	32165046	32165757	-1	SLC30A6 SPAST	r= 0.07, p-value = 8.94E-02 r=0.15, p-value = 2.71E-05
ENSG00000273355	AP000894.4	novel transcript, antisense to YES1	18p11	813274	813756	1	YES1	r=0.16, p-value = 1.93E-05

Significant in multivariate analysis

OS | OS and PFS | PFS

B

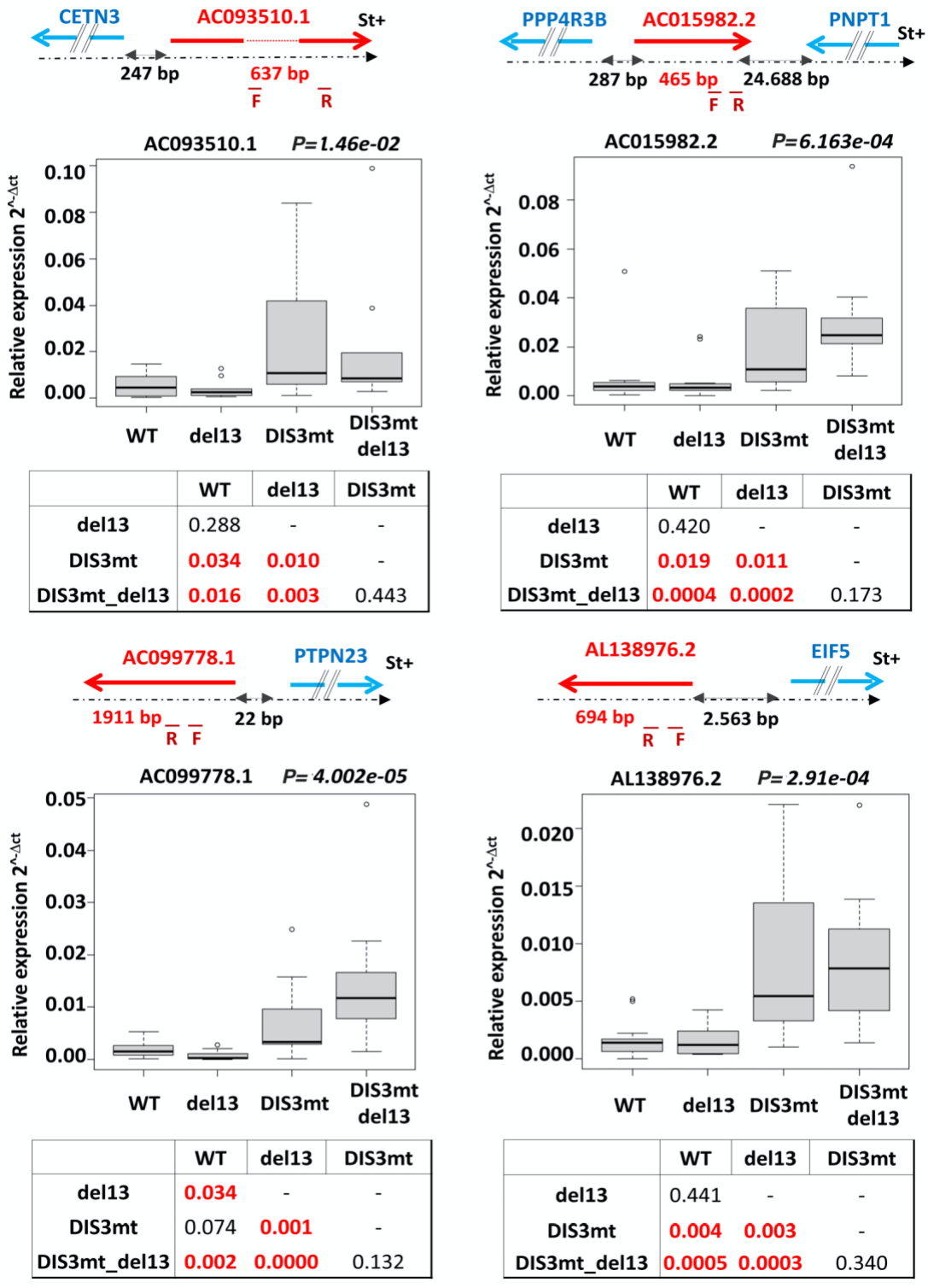

	WT	del13	DIS3mt
del13	0.288	-	-
DIS3mt	0.034	0.010	-
DIS3mt_del13	0.016	0.003	0.443

	WT	del13	DIS3mt
del13	0.420	-	-
DIS3mt	0.019	0.011	-
DIS3mt_del13	0.0004	0.0002	0.173

	WT	del13	DIS3mt
del13	0.034	-	-
DIS3mt	0.074	0.001	-
DIS3mt_del13	0.002	0.0000	0.132

	WT	del13	DIS3mt
del13	0.441	-	-
DIS3mt	0.004	0.003	-
DIS3mt_del13	0.0005	0.0003	0.340

Figure 14. **Summary information on the 12 lncRNAs with clinical relevance and 4 lncRNAs validate in MM patients.** **(A)** Table representing information on the 12 long non-coding RNA significant in multivariate analysis. In the first column, the color indicates the significance in multivariate analysis as specified in the legend. **(B)** Scheme of the genomic region of the four lncRNAs validated by qRT-PCR in 43 patients including 13 with DIS3 wild type, 14 with DIS3 WT and del(13q),

seven with DIS3 mutation, and nine with DIS3mt sand del(13q). In red below are indicated Primer position for each lncRNA. Differential expression was assessed by the Wilcoxon signed-rank test and statistically significant P-values (<0.05) are reported above each boxplot. Dunn test. P-values for pairwise comparisons are reported in tables under each boxplot, with statistically significant P-values in bold red.

6. Results, part 2: Molecular and functional characterization of DIS3 relevance in HMCLs

6.1. DIS3 KD inhibits proliferation of MM cells *in vitro*

To unravel the biological relevance of DIS3 in MM we took advantage of the use of RNA interference strategy to silence DIS3 in NCI-H929 and AMO-1 HMCLs. DIS3 specific siRNA (siDIS3) showed a good silencing efficiency at 24-48hr post electroporation, that is nearly 70% (Figure 15A) also confirmed at protein level (Figure 15B), which decreased after 72hr in both HMCLs tested (almost 30%).

As shown in Figure 15C, DIS3 KD led to a significant reduction of cellular growth as compared to relative control, which resulted to be stronger in NCI-H929 compared to AMO-1 cell line.

A

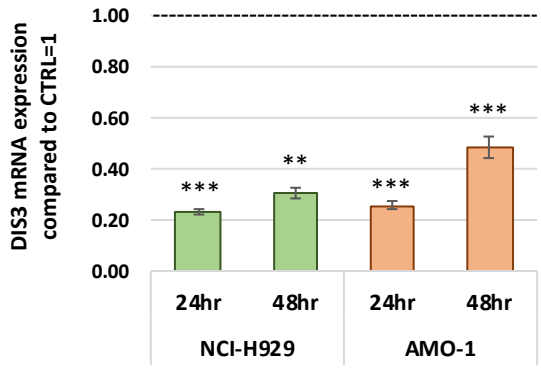

B

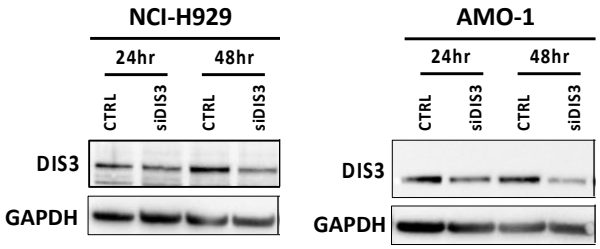

C

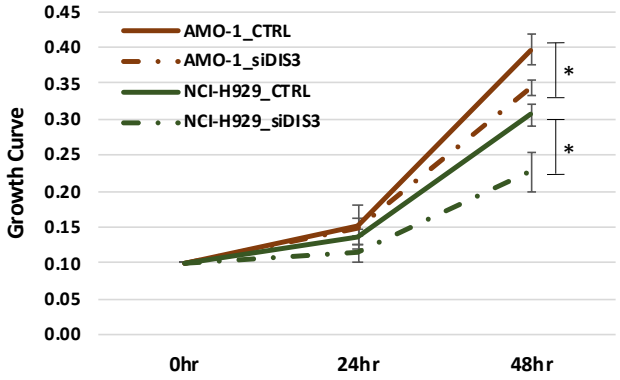

Figure 15. DIS3 silencing using siRNA strategy. A Quantitative real-time PCR (qRT-PCR) of DIS3 in NCI-H929 and AMO-1 cells at the indicated hours using RNA interference strategy; DIS3 expression was expressed as $2^{-\Delta\Delta Ct}$ relative to the scramble siRNA at the same time point. **B** WB of DIS3 in NCI-H929 and AMO-1 cells 24-48hr after siRNA delivery (200nM). **C** Growth curves of AMO-1 and NCI-H929 cells following the transfection of DIS3-specific siRNA. *p < 0.05, **p < 0.01, ***p < 0.001, Student's t test (**A-C**).

To obtain a more pronounced and lasting silencing effect we exploited a second loss of function approach by using the LNA-gapmeR ASO technology.

We designed 3 different LNA-gapmeR sequences (gDIS3#2/13/15) targeting all three DIS3 isoforms (Figure 16A). The silencing efficiency of all three gampeRs was tested in AMO-1 cell line by electroporation. As shown in Figure 16B, gDIS3#13 showed the best silencing efficiency at 24hr (about 50%) also confirmed at protein level (Figure 16C); which decreased 48h after silencing (nearly 80% of remaining DIS3).

To achieve a deeper and prolonged silencing effect, we optimized our experimental condition by using the gymnotic delivery of the selected gDIS3#13 LNA-gapmeR. Based on our previous works (89) we evaluated the time-dependent biological effect of gDIS3#13 delivery using a sub-cytotoxic concentration (5µM) for 9 days in both AMO-1 and NCI-H929 cells.

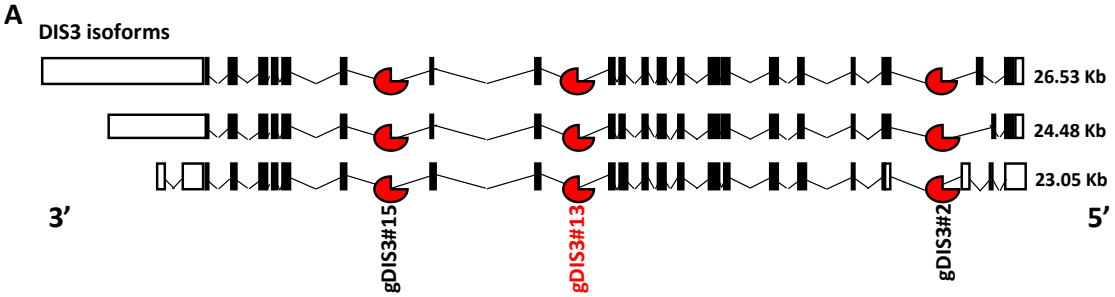

B

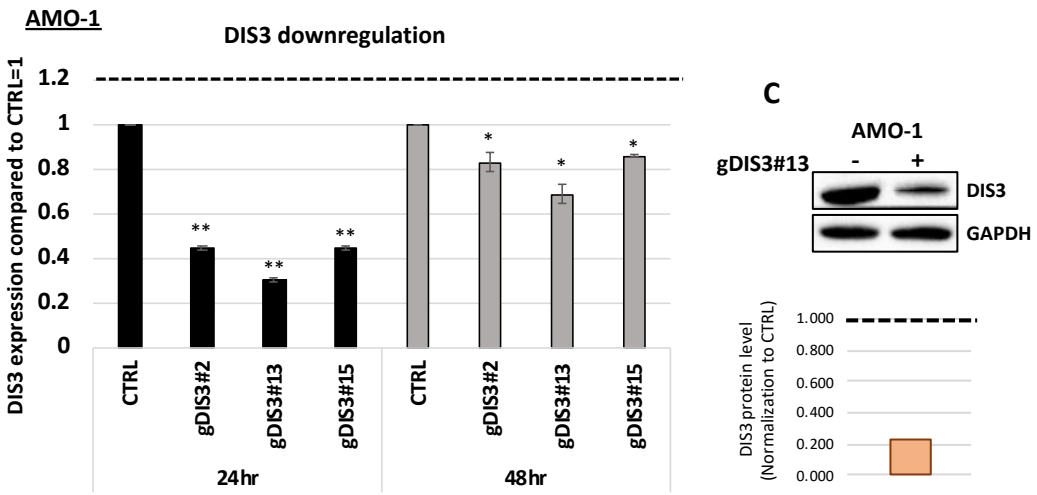

Figure 16. DIS3 silencing using LNA-gapmers in AMO-1 cell line. A Schematic representation of DIS3 protein coding isoforms together with the localization of the three gapmeRs tested. In red DIS3 gapmer selected for following experiments. **B** DIS3 expression in AMO-1 24hr and 48hr after single LNA-gampeR transfection using Neon Transfection System. **C** WB of DIS3 in AMO-1 cells 48hr after gDIS3#13 delivery. *p < 0.05, **p < 0.01, ***p < 0.001, Student's t test.

The gymnotic delivery of gDIS3#13 significantly downregulates DIS3 transcript (Figure 17A) and was associated with a decrease in cellular growth and an increase of the percentage of the apoptotic cells compared to relative control (Figure 17B-C).

Furthermore, DIS3 silencing dramatically suppressed the clonogenic potential of MM cells as evaluated from clonogenic assay (Figure 17D).

Finally, we evaluated anti-MM effects of DIS3 silencing on CD138^{+} cells derived from MM patients. DIS3 downregulation resulted in an important change in CD138^{+} morphology, attributable to vacuolated cytoplasm and non-specific inclusion, indicating an effect also on CD138+ cells (Figure 17E).

A

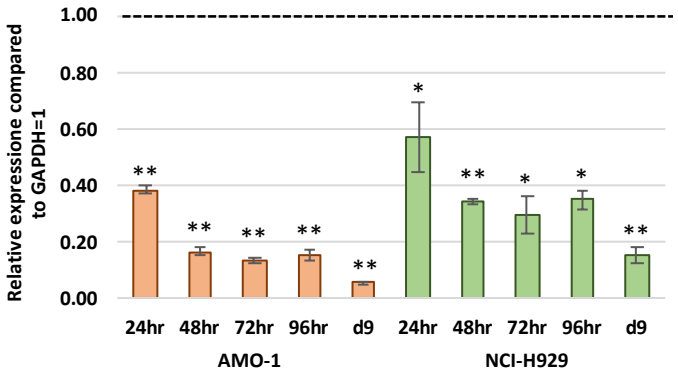

B

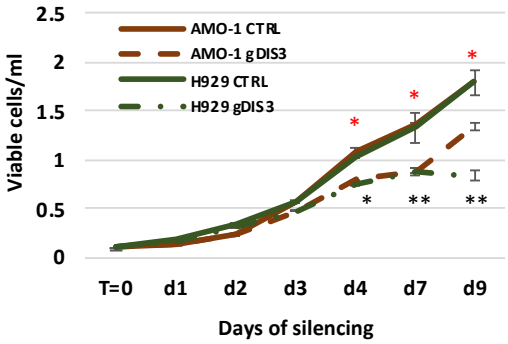

C

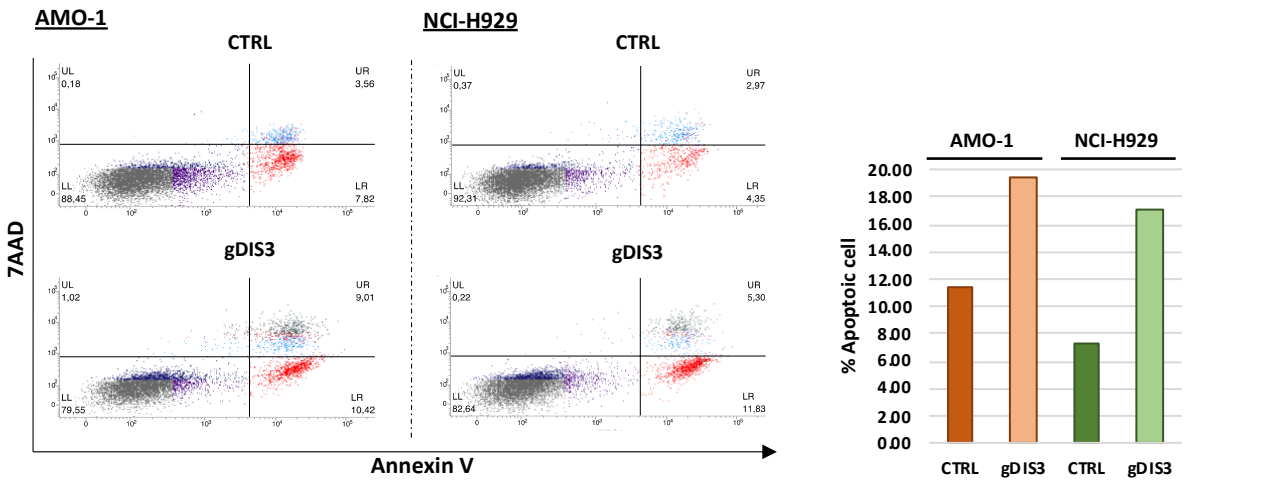

D

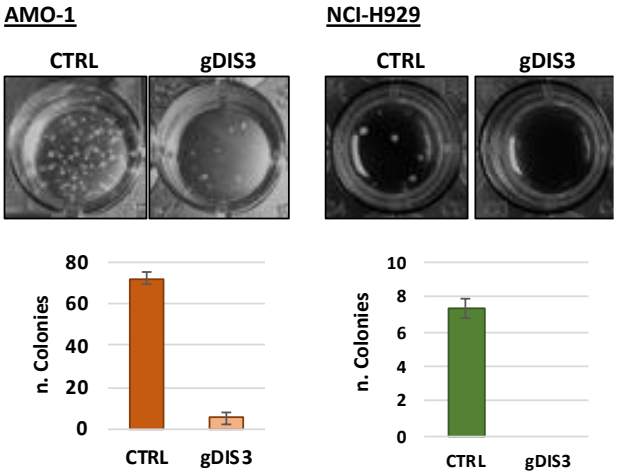

E

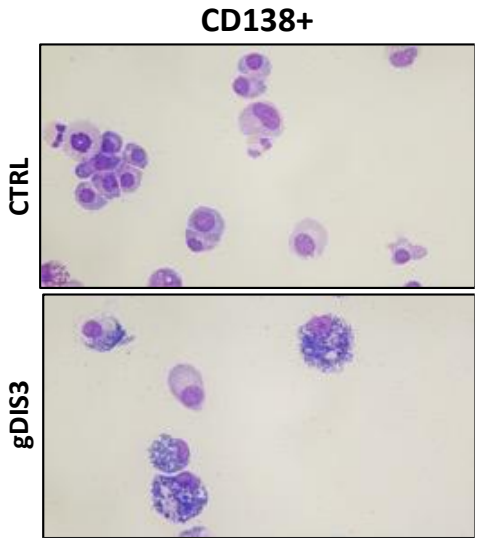

Figure 17. Gymnotic delivery of gDIS3 in MM cell lines and its biological effects on primary CD138+ cells. A Quantitative real-time PCR (qRT-PCR) of DIS3-silenced AMO-1 cells at the indicated days; DIS3 expression was expressed as $2^{-\Delta\Delta Ct}$ relative to the control gapmeR at the same time point. **B** Growth curves of AMO-1 and NCI-H929 cells following DIS3 silencing. **C** Flow cytometry analyses of apoptosis in AMO-1 and NCI-H929 cells 6 days after treatment with gDIS3 gapmeR (5μM). **D** Colony formation assay performed on AMO-1 and NCI-H929 treated for 21 days with gDIS3; representative picture of colonies at day 21 are also shown. **E** Representative image of May-Giemsa staining of CD138+ primary tumors treated for 6 days with gDIS3 gapmeR. Mean and standard deviation on three replicates is reported where

applicable. *p < 0.05, **p < 0.01, ***p < 0.001, Student's t test. *Indicate AMO-1 cell line and *indicate NCI-H929 cell line (**B**).

6.2. Evaluation of DIS3 KD in Synchronous MM cells to better characterize cell cycle perturbation

In the attempt to investigate better the anti-proliferative effects of DIS3 knockdown in HMCLs, we evaluated whether DIS3 silencing affects the cell cycle progression. DIS3-silenced AMO-1 and NCI-H929 cells were collected after 4 days of silencing for flow cytometry analysis. As shown in Figure 18, DIS3 KD in NCI-H929 cells (Figure 18A) caused an increase in the percentage of cells in the G0/G1 phase (52.15% in the CTRL group to 67.87% in NCI-H929 cells and from 55.34% to 61.75% in the AMO-1) of the cell cycle as compared to control samples, with a concomitant significant decrease in the percentage of cells distributed in the S and G2/M phase of the cell cycle (Figure 18A-B). Notably, the effect of DIS3 KD is stronger in NCI-H929 that carry the deletion of chromosome 13 and for which there is only one functional allele, compared to AMO-1 cell line that is WT with two functional allele. These findings suggest that silencing of DIS3 gene is associated with G0/G1 arrest in MM cells.

A

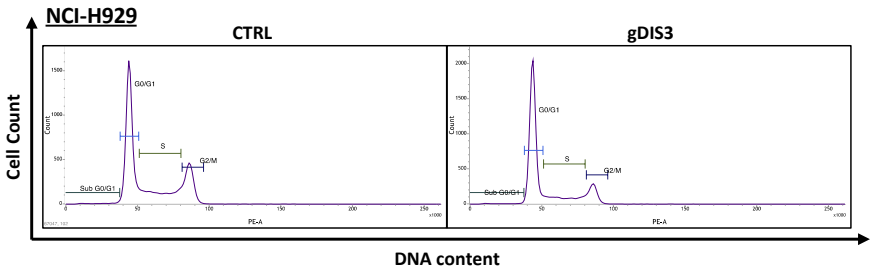

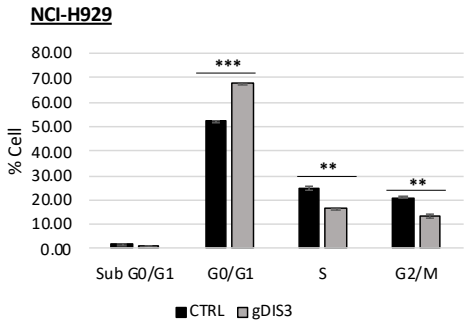

B

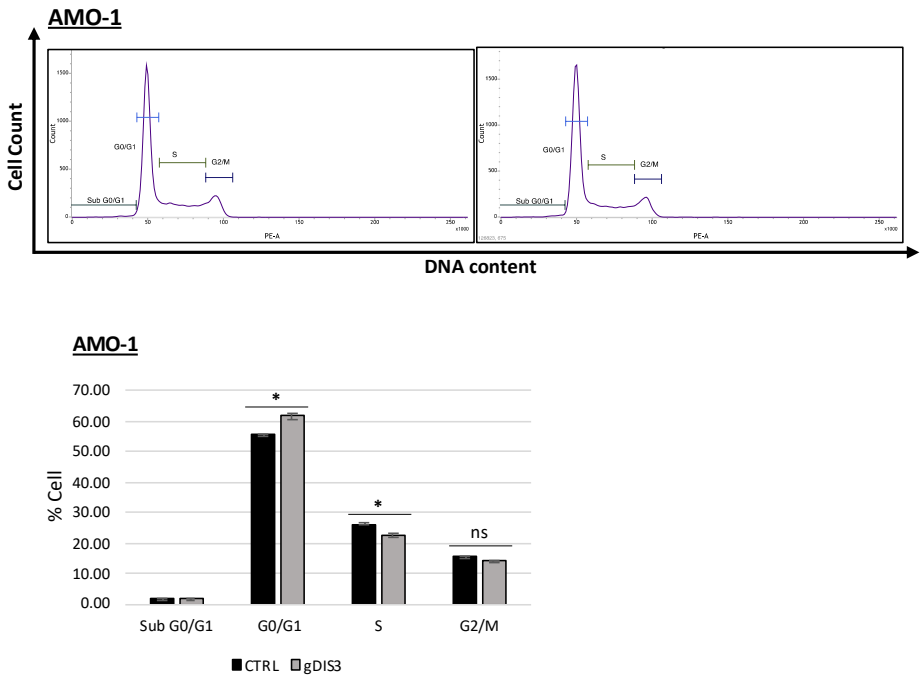

Figure 18. Cell cycle analysis of NCI-H929 and AMO-1 cells (A-B) treated with gDIS3 gampmeR (5μM). Representative histogram data of cell cycle analysis at 4 days after treatment with gDIS3 are also shown. Standard deviation on three replicates are reported, *p < 0.05, **p < 0.01, ***p < 0.001, Student's t test.

Cell synchronization is crucial when studying events that take place at specific points of the cell cycle. The synchronized cells progress through the phases of the cell cycle as a relatively uniform cohort, helping us in the understanding the changes occurring during a particular phase. According to this notion and our results (see above), in which the treatment with gDIS3 affects cell cycle progression, we planned to synchronize MM cell lines to observe more in detail the effect obtained.

Several chemical agents can be used to achieve the cell culture synchronization but not all type of cells respond equally.

In our study we used the SynchroSet (EuroClone) reagent, and we assess the outcome of the cell cycle progression at different time point, collecting sample for RNA, cell cycle and protein analysis 6hr after release, as shown in Figure 19.

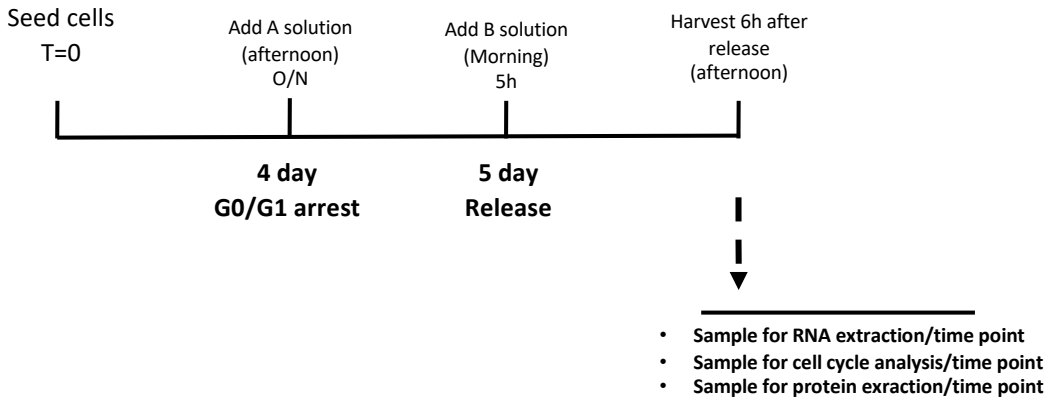

Figure 19. Schematic representation of Synchro-set protocol for cell synchronization. At time 0 cells were seeded and gapmeR against DIS3 was added. At day 4, 20µl/ml of solution A were added to cell suspension that were incubated overnight (min 14 – max 20 hours). This reagent is able to block cells at G0/G1 phases of the cell cycle. At day 5, 20µl/ml of solution B were added to each well and cells were incubated for 5 hrs in order to start cycling again. Samples were collected for RNA, proteins and cell cycle analysis at different time point, respectively 0, 2-4-6 hrs post release.

In detail, we collect samples at selected times, to follow cells distribution during the different phases of the cell cycle, from block, during and after release. AMO-1 and NCI-H929 cells were arrested after 4 days from gDIS3 delivery at G0/G1 phase of the cell cycle and then released the day 5. Cell cycle progression through the different phases of the cell cycle was analyzed by flow cytometry at specific time point: from asynchronous, block, during the release (which has a time of 5hr), time 0 after release, 2-4-6-hr post release (Figure 20A-B).

A

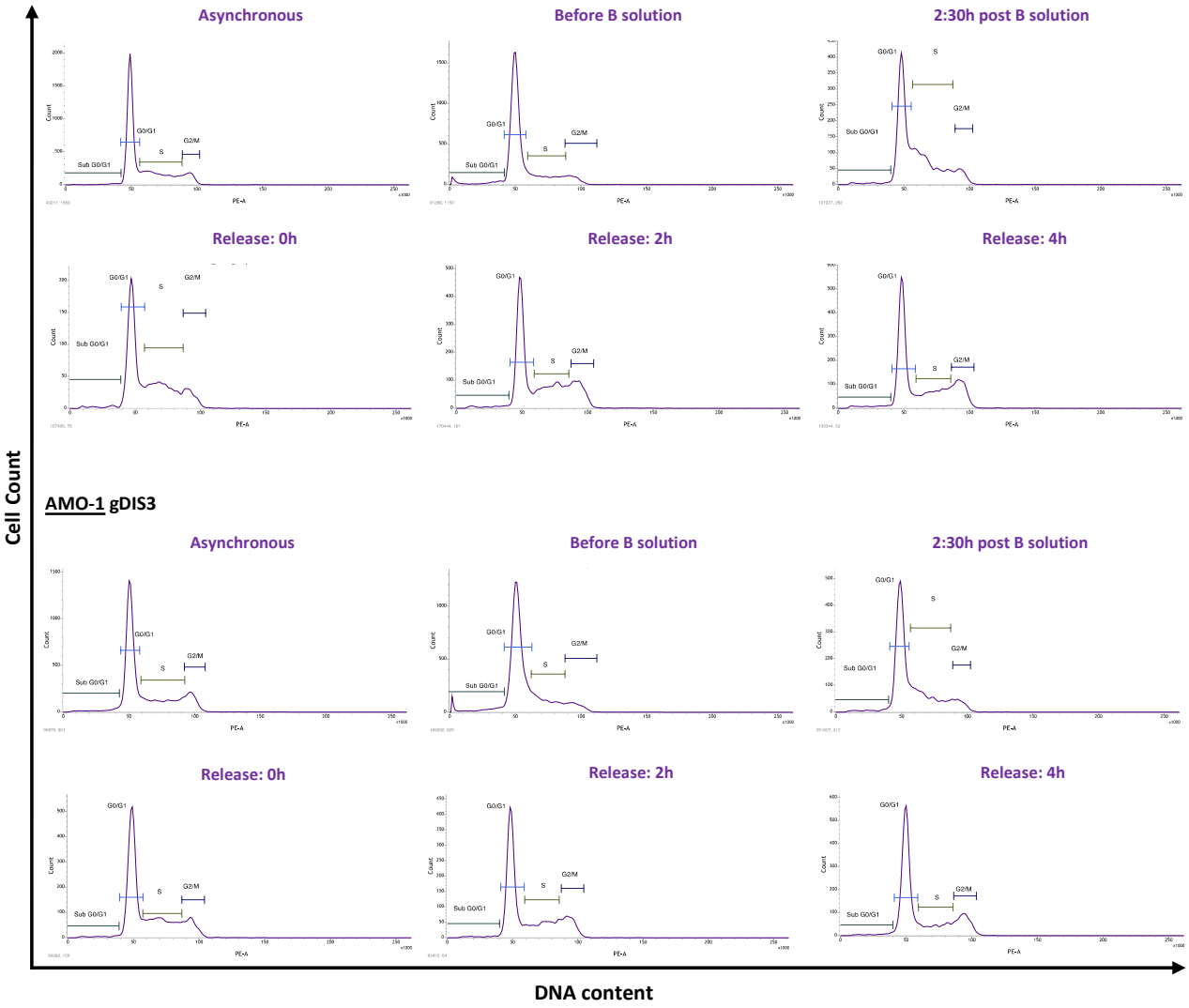
AMO-1 CTRL
Asynchronous
Before B solution
2:30h post B solution
Release: 0h
Release: 2h
Release: 4h
AMO-1 gDIS3
Asynchronous
Before B solution
2:30h post B solution
Release: 0h
Release: 2h
Release: 4h
Cell Count
DNA content

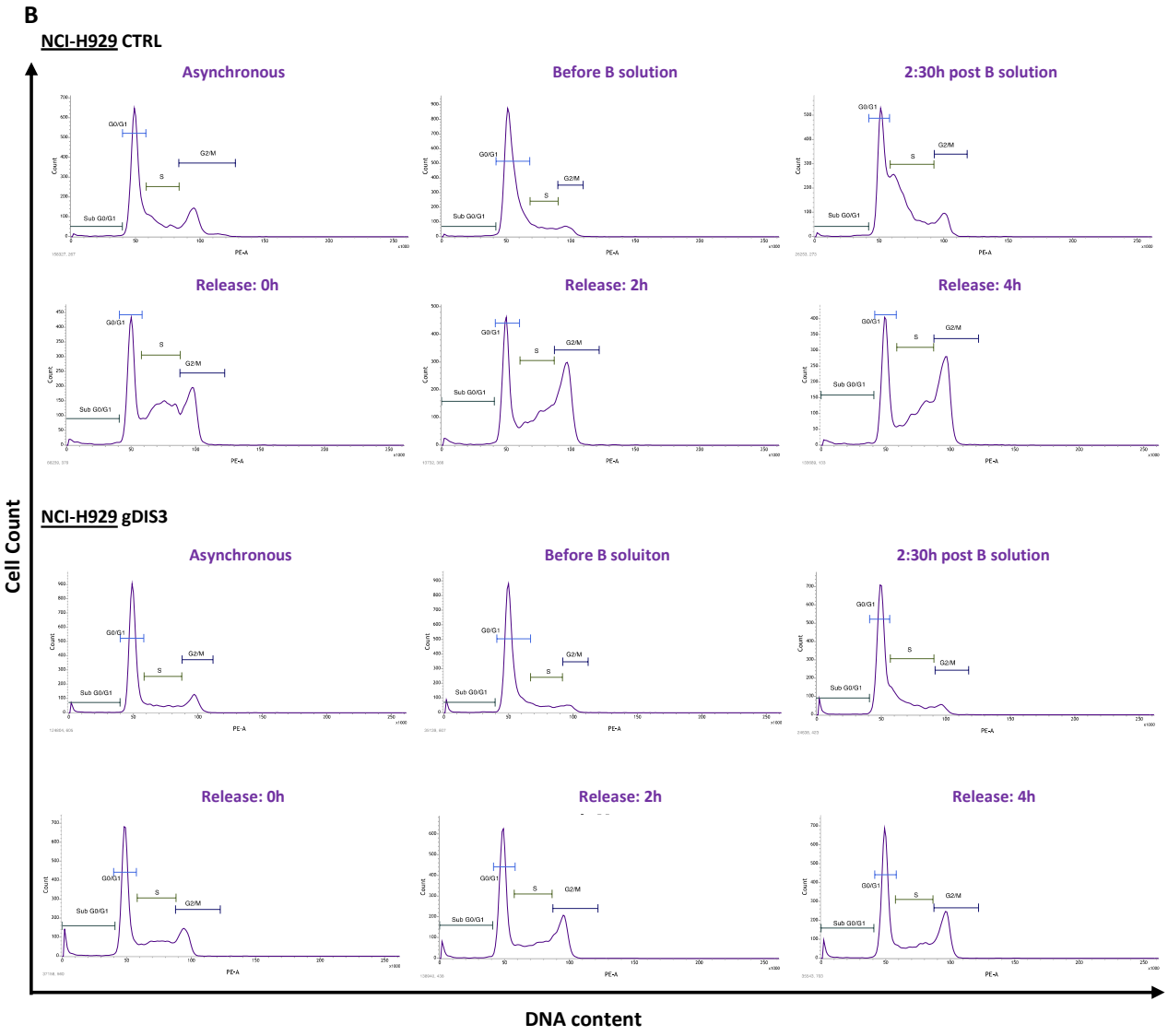

Figure 20. Monitoring of cell cycle progression in DIS3 silenced NCI-H929 and AMO-1 cells. A-B Cycle progression was monitored by PI staining and FACS analysis of the DNA content of cells before synchronization (asynchronous cells), and at different time point after synchronization and after release.

Following experiments in the present work have been performed on samples after 6h release (Figure 21A-B).

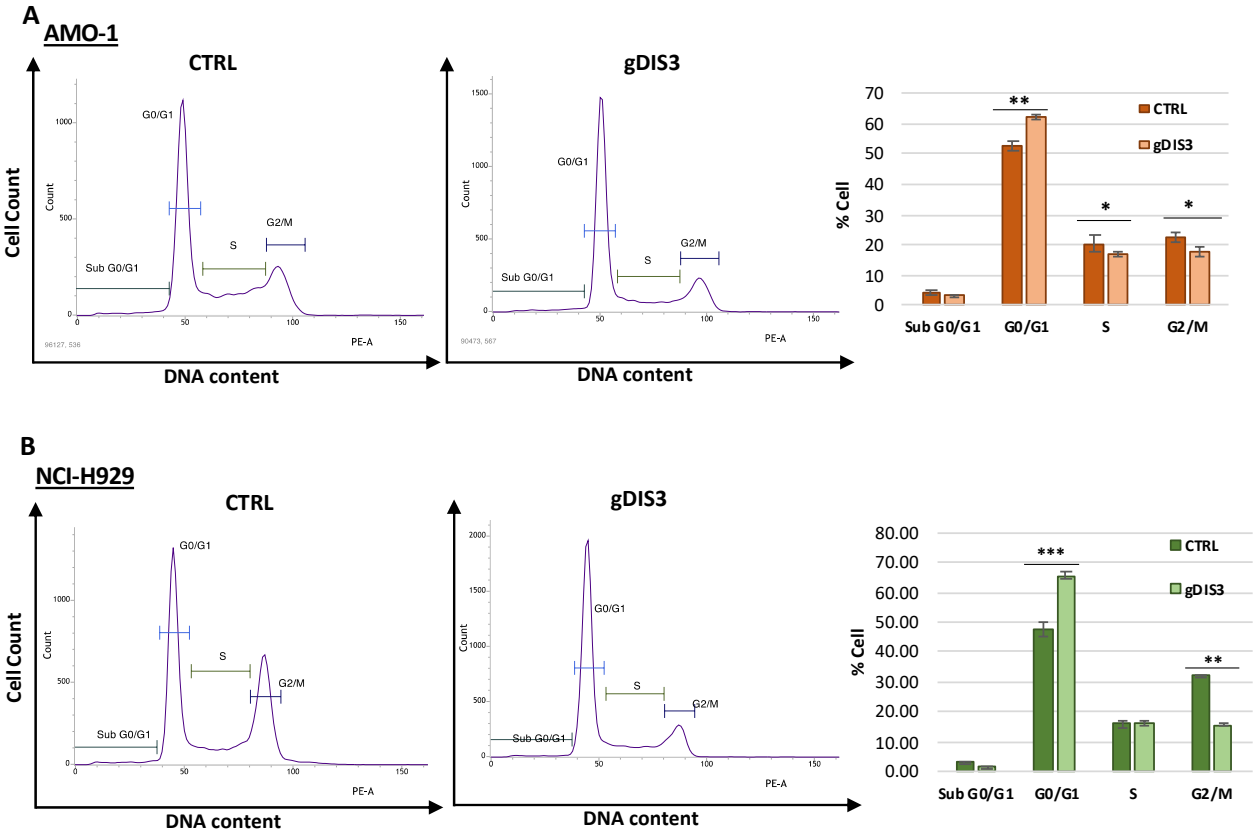

Figure 21. Biological effect obtained in gDIS3 synchronized cell lines. A-B AMO-1 and NCI-H929 cells synchronized. Cell cycle progression was monitored by PI staining and FACS analysis of the DNA content of cells every 6hr after the release. Percentage of cell cycle distribution is represented by the histogram.

6.3. Transcriptional patterns associated with DIS3 silencing in NCI-H929 cell line

Global transcriptome profiles were obtained in three NCI-H929 replicates that were gymnotically silenced for DIS3 in comparison to three control NCI-H929 cells, by means of Clariom D array (ThermoFiSher). Out of 55540 globally analyzed genes, 4032 resulted significantly modulated at FDR q-value less than 10% by SAM analysis. They were almost down-regulated (3995 genes, 99%) in DIS3-silenced cells, principally involving protein coding (PC) genes (2608 genes, 65%) and with a lesser extent long non-coding RNAs (464 lncRNAs, 12%). Chromosome organization, chromatin and histone modification, and cell cycle checkpoint were recognized among the top 20 most significantly enriched GO Biological Process terms for 2595 differentially expressed PC genes with annotated gene symbols (Figure 22A). In addition, genes concerned in protein serine/threonine kinase activity, with helicase function, catalytic activity on RNA, or with tubulin binding function were evidenced in the top 20 remarkably enriched GO Molecular Function terms under DIS3 silencing (Figure 22B).

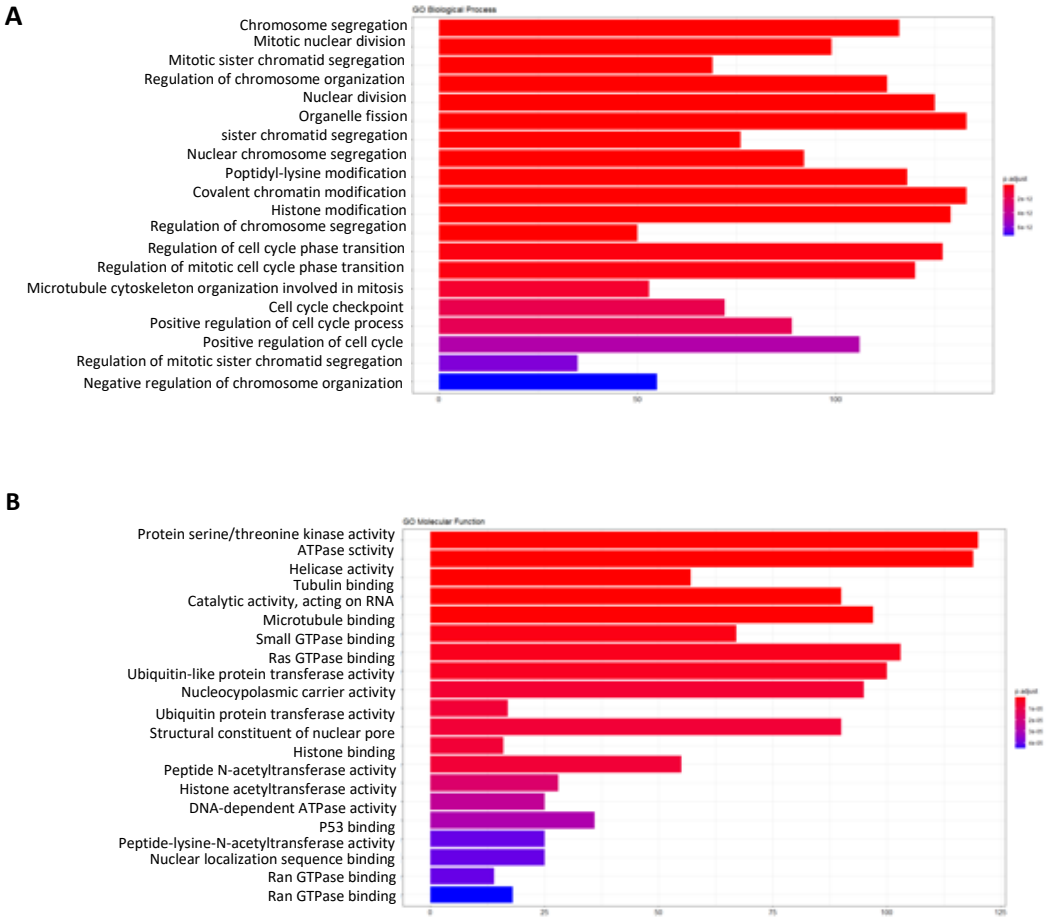

Figure 22. Bar plot. Bar plot of the 20 most significantly enriched GO Biological Process terms **(A)** and GO Molecular Function terms **(B)** under DIS3 silencing.

In particular, numerous protein coding (PC) genes that were significantly enriched in multiple annotation categories linked in complex interactions, regarding chromosome organization and nuclear division, or molecular activities on nucleic acids and tubulin, resulted globally down-regulated in DIS3-silenced cells (Figure 23).

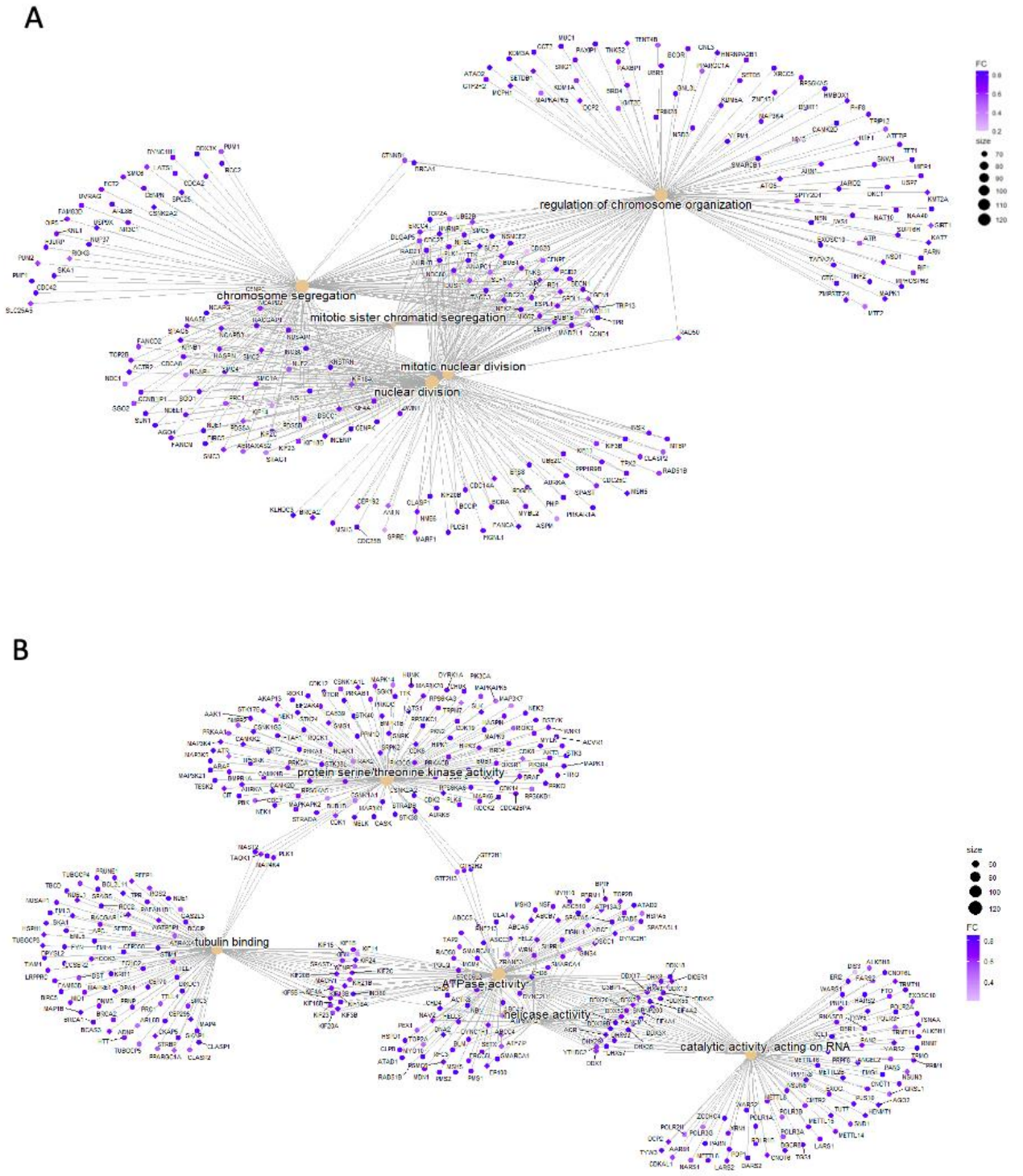

Figure 23. Cnetplot. (ClusterProfiler R package) of the top 5 Biological Process terms **(A)** and GO Molecular Function terms **(B)** under DIS3 silencing.

Finally, to find possible molecular subsets of genes that were coordinately modulated in DIS3-silenced in comparison to control NCI-H929 cells, Gene Set Enrichment Analysis (GSEA) was performed on global annotated PC gene expression profiles (19048 genes)

and most significant gene sets were selected under stringent conditions (nominal p-value < 0.05 and FDR q-value<5%).

Among the most significantly up-regulated gene sets in DIS3-silenced NCI-H929 cells, we evidenced some involved in degradation of extracellular matrix, DNA and histone epigenetic modifications, DNA recombination and repair, whereas cell cycle checkpoint, chromosome organization, RNA processing and degradation as expected due to the role of DIS3; regulation of TP53 activity and numerous cells signaling pathways resulted among the most significant under-expressed gene sets, in DIS3 silenced cells (Figure 24A-F).

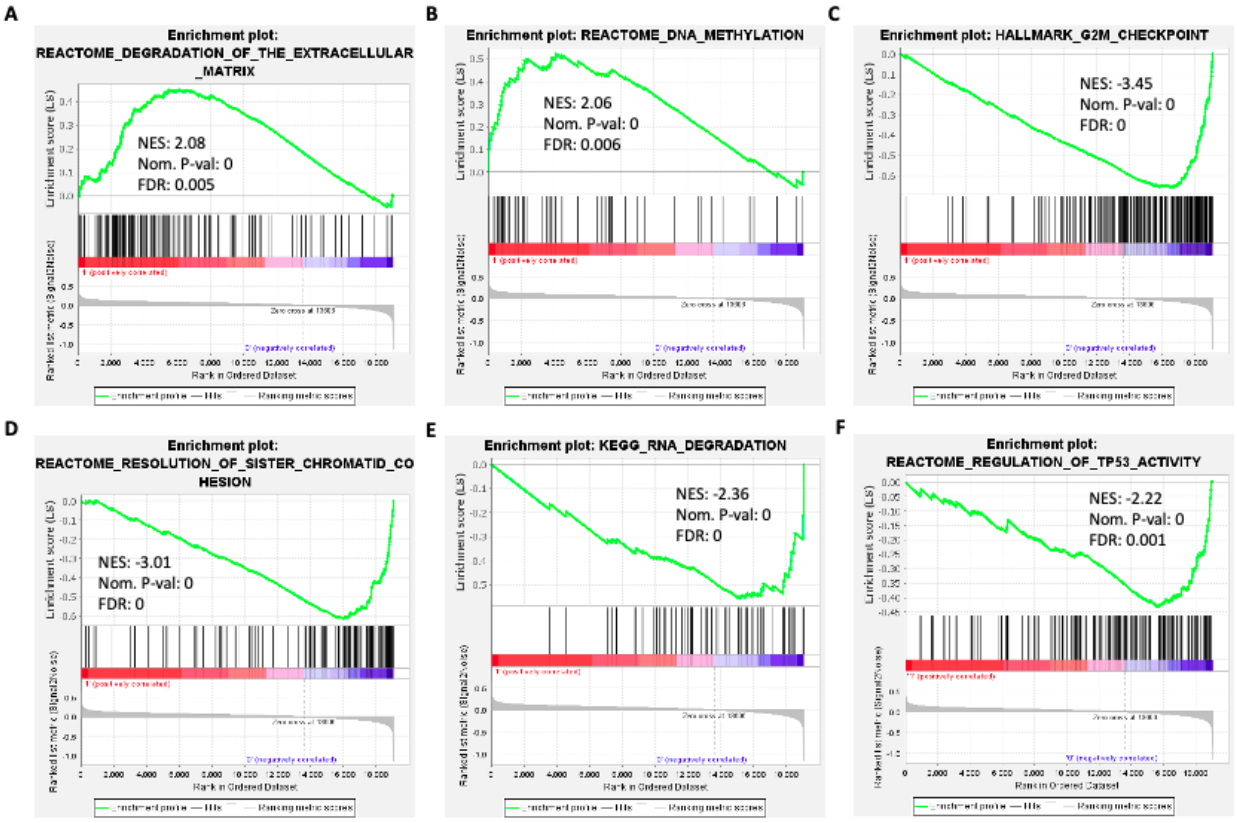

Figure 24. GSEA analysis on NCI-H929 DIS3 silenced cells. A-F A positive enrichment score (ES) indicates gene set enrichment at the top of the ranked list; a negative ES indicates gene set enrichment at the bottom of the ranked list. The analysis demonstrates that (A) Degradation of extracellular matrix and (B) DNA methylation are upmodulated in gDIS3 silenced groups, while (C) G2/M checkpoint (D) Resolution of sister chromatid cohesion (E) RNA degradation and (F) Regulation of TP53 activity are downmodulated in gDIS3 silenced group.

6.4. Validation of gene expression data in DIS3 silenced MM cell lines

Comparing the transcriptional profiles of DIS3-silenced cells to controls, we observed among the genes differentially expressed, most downregulated in DIS3 KD cell line.

Interestingly, we found RAD51B and ARID5B involved in Homologous Recombination (HR) and DNA repair process; CCNB1, CDC20, KIF14, TOP2A and POLR2H, all of them involved in cell cycle process: CCNB1 is essential for the control of the cell cycle at G2/M transition; CDC20 acts as a regulatory protein interacting with the anaphase promoting complex/cyclosome (APC/C); KIF14 a microtubule motor protein with ATPase activity that play an important role in cell division, cytokinesis and also in cell proliferation. TOP2A is a DNA topoisomerase that alters the topologic states of DNA during transcription and POLR2H that is an RNA polymerase, its role is to catalyze the transcription of DNA into RNA.

Based on these results, first we validated genes downregulation by qRT-PCR in AMO-1 and NCI-H929 cell lines treated with gapmeR against DIS3 for five days. Notably, both HMCLs tested showed a downregulation of these gene (Figure 25A).

Analysis of purified primary MM plasma cells treated with gDIS3 at different time point also confirmed the downregulation of these transcripts, excepts for those transcripts (CCNB1 and CDC20) that are involved in cell cycle progression and probably due to the reason that primary *ex vivo* CD138+ not duplicate (Figure 25B).

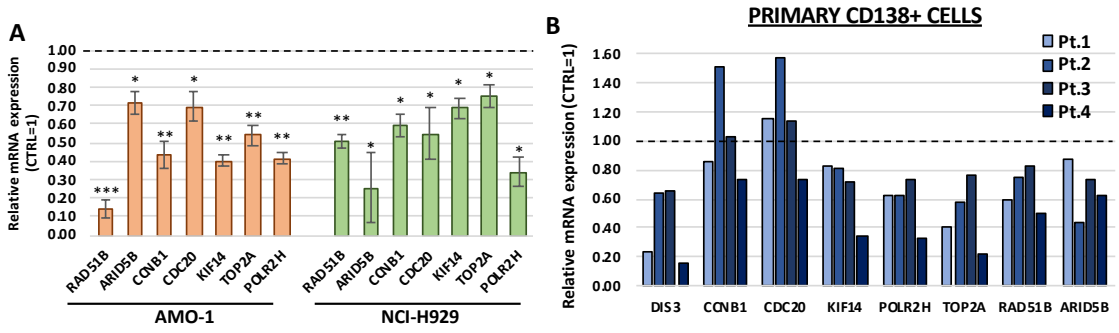

Figure 25. Validation of gene expression data in NCI-H929 and AMO-1 cell lines. A Histogram of genes expression levels (5-day time point) in AMO-1 and NCI-H929 cells after DIS3 KD compared to CTRL (black line) and in primary tumors (**B**). NCI-H929 cell line were synchronized in G0/G1 phase by synchroset protocol. Cell cycle progression was monitored by PI staining and FACS analysis of the DNA content of cell at the time points indicated in CTRL and gDIS3 KD. *p < 0.05, **p < 0.01, ***p < 0.001, Student's t test.

6.5. DIS3 KD leads to a modulation of cell cycle checkpoint proteins

The downregulation of cell cycle checkpoints genes following DIS3 silencing was confirmed by the Gene Set Enrichment Analysis (GSEA) in NCI-H929 cell line.

Focusing on this pathway, we investigated proteins that are reported associated to the different cell cycle checkpoints.

As show in figure 26A-B DIS3 silencing resulted in a reduced levels of the cell cycle proteins valuated. Furthermore, Histone H3 variant CENP-A that plays a fundamental role in defining centromere identity and structure (90) showed a down-modulation (Figure 26A-B).

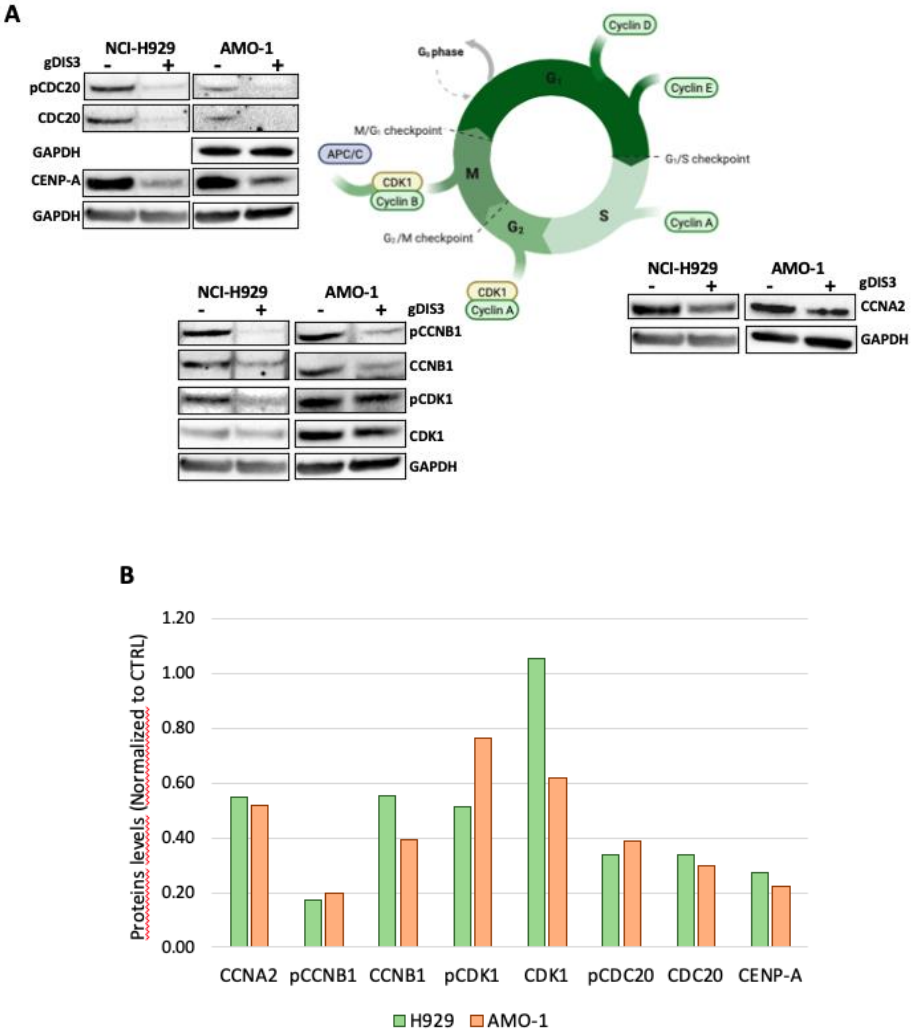

Fugure 26. WB analysis on cell cycle checkpoint protein. A-B WB of cell cycle proteins in AMO-1 and NCI-H929 5 days after delivery of gDIS3 gapmeR (5 μM) with the respective densitometry. The image shows a cell cycle scheme with the proteins evaluated and linked to the different cell cycle checkpoints.

Also, DIS3 protein was investigated, and the downregulation was confirmed (Figure 27). DIS3 appears to be required for the optimal cell cycle development, activation of the spindle checkpoint, and for the fidelity of mitosis process.

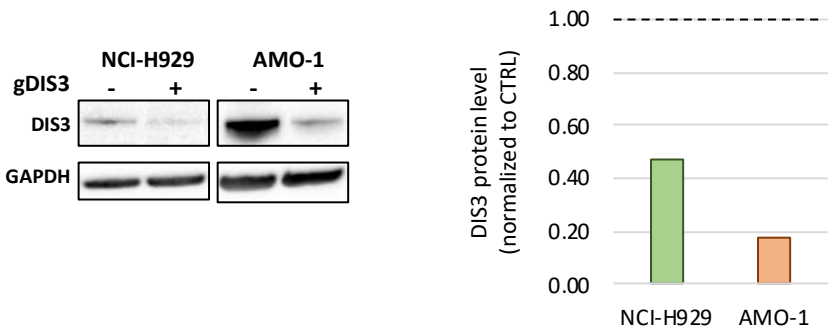

Figure 27. WB on DIS3 protein. WB of DIS3 proteins in AMO-1 and NCI-H929 5 days after delivery of gDIS3 gapmeR (5 μM).

6.6. The impact of DIS3 KD on mitotic spindle

Correct progression through mitosis is essential for cell survival and proper cell division and as we demonstrated above, is carefully monitored by several proteins involved in cell cycle checkpoint. One of the major drivers of the complex genomic landscape in MM is genomic instability which promotes genome alterations during cell division. It is already known, as regard yeast and Drosophila melanogaster model, that RNase activity of DIS3 is required for proper mitotic cell division and correct chromosome condensation (60,91,92).

We analyzed the changes in spindle organization in gDIS3 compared to CTRL condition in MM synchronize cell lines (Figure 28A); notably depletion of DIS3 causes mitotic defect in NCI-H929 and AMO-1 cell lines. In contrast to normal spindle localization and normal bipolar cell division in control cells, DIS3 KD results in a significantly higher presence of multipolar spindles during mitosis (Figure 28B). Spindle alteration observed in DIS3 depleted cells were quantified and plotted as a histogram (Figure 28C). These findings suggest that the spindle assembly checkpoint, a surveillance mechanism that ensures the fidelity of chromosome segregation during mitosis, might be defective in DIS3 depleted AMO-1 and NCI-H929 cells.

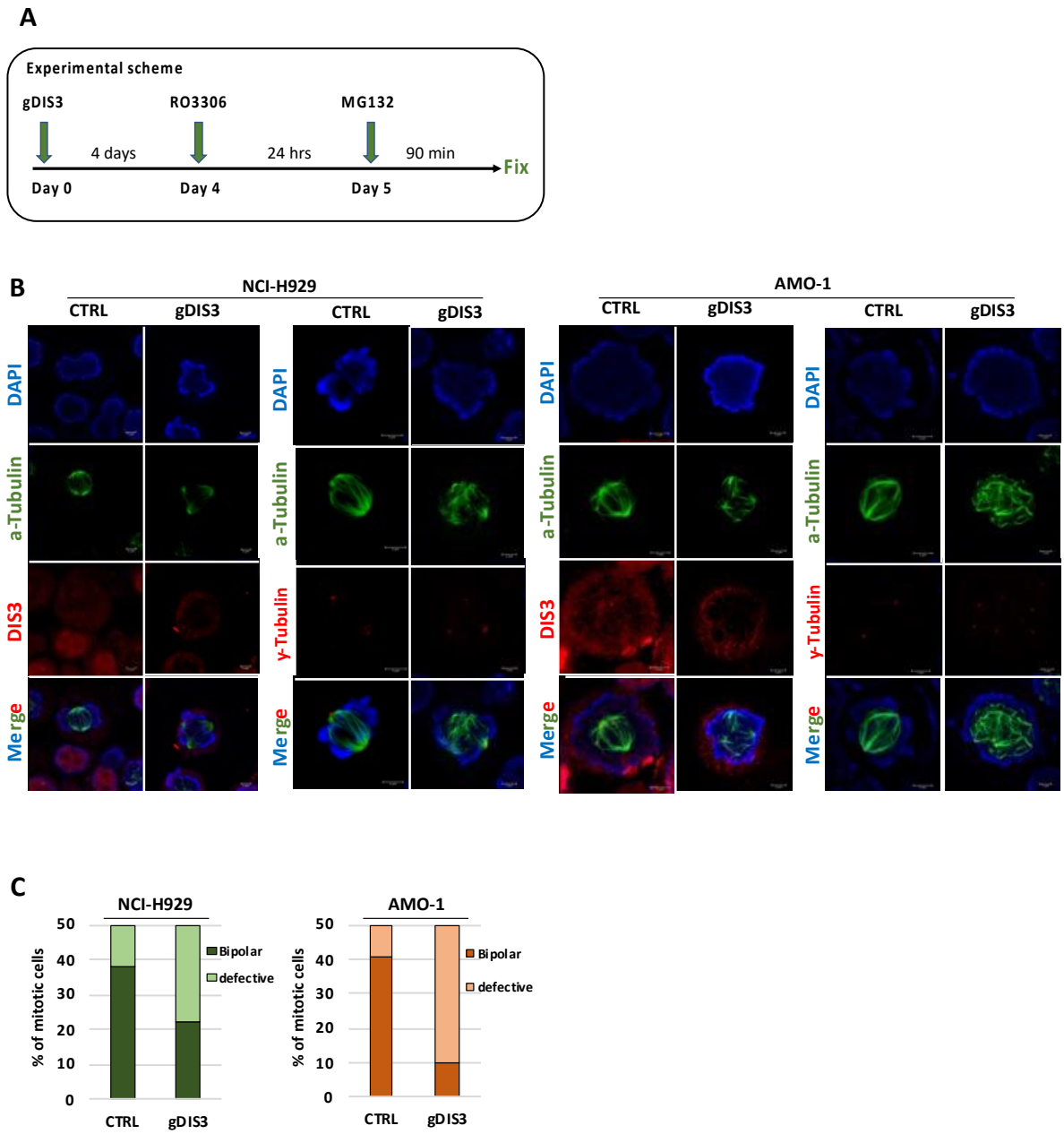

Figure 28. A Schematic representation of the experimental setup utilized to synchronized cell lines. Cells were seeded at day0 and treated with gDIS3 5μM, after 4 days were synchronized with 7,5μM RO-3306 for 24hrs. Cells were then treated with MG-132 for 90 minutes and fixed. **B** Imaging of metaphase spindle in NCI-H929 and AMO-1 cells treated with gDIS3 and control condition (left panel per cell lines). Representative images of multipolar spindles in both cell lines following gDIS3 knockdown (right panel per cell lines). Cells were stained with anti-Tubulin, DIS3 and DAPI. Scale bar, 5μm. **C** Percentage of mitotic cells with defective spindle in NCI-H929 and AMO-1 cells treated with gDIS3 versus CTRL.

6.7. Biological effect obtained by DIS3 KD in combination with ARRY-520 drug

The mitotic defects observed DIS3 silenced cells suggest that the lack of DIS3 could sensitize MM cells with to drugs that act on mitosis and in particular on spindle organization.

For these reasons we try to evaluate the effects of DIS3 silencing in combination with ARRY-520 a drug currently tested for MM treatment (93,94), which causes inhibition of cell proliferation via preclusion of proper mitotic spindle assembly.

The rationale of the experiment is given by the mechanism of action that ARRY520 carries out: cause inhibition of cell proliferation via preclusion of proper mitotic spindle assembly.

To this aim, we treated AMO-1 and NCI-H929 cells with ARRY-520 in presence or not of DIS3 gapmeR and then we evaluated the number of viable cells in each sample at 4 days; as show in Figure 29A, DIS3 KD with ARRY-520 treatment resulted in a marked reduction in cell growth compared to single treatment. Furthermore, the combination revealed a pronounced spindle alteration (Figure 29B).

These results indicate that DIS3 silencing triggers a sensitizing effect to ARRY-520 drugs.

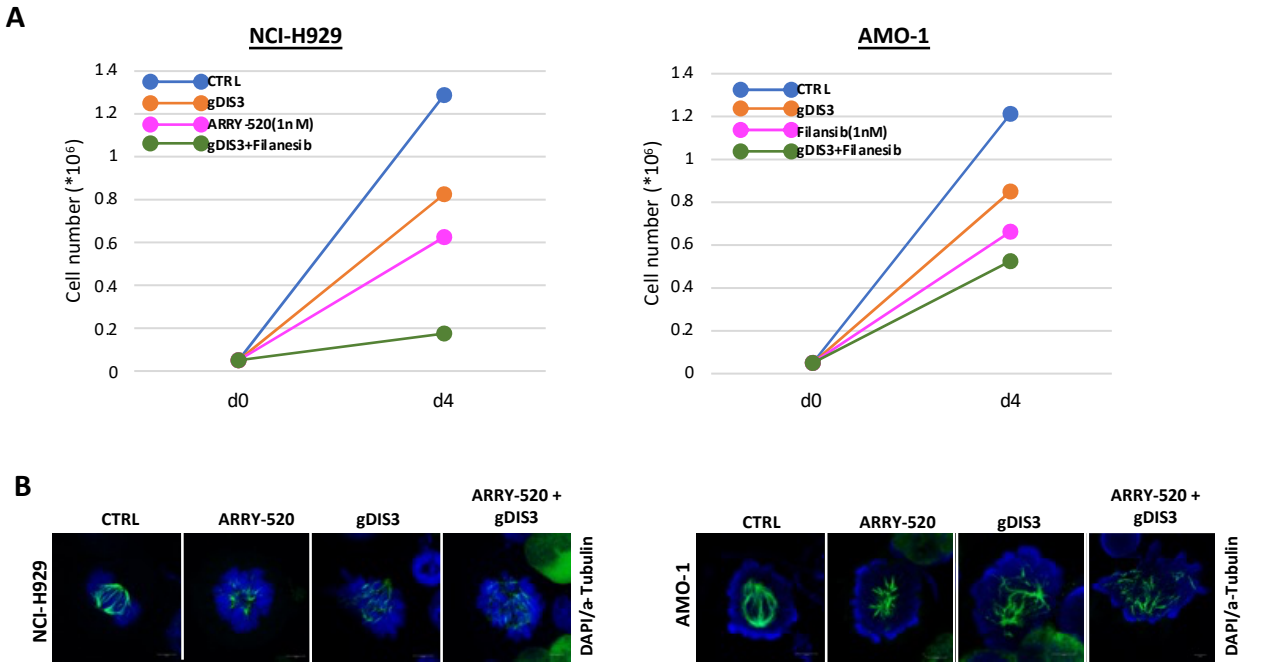

Figure 29. Growth curve and immunofluorescence of DID3 KD in combination with ARRY-520. A Growth curve of NCI-H929 and AMO-1 treated with gDIS3, ARRY-520 and combo, compared to CTRL condition. Cells were treated at d0 with gapmeR gDIS3 5µM (orange), at day1 were added filanesib 1nM (violet) and combo gDIS3 plus filanesib 1nM (green), or DMSO (blue). **B** Imaging of metaphase spindle in NCI-H929 and AMO-1 cells treated with gDIS3, ARRY-520 (1nM), combo and control condition. Representative images of spindles in both cell lines. Cells were stained with anti-Tubulin and DAPI. Scale bar, 5µm.

7. Discussion and Conclusions

To date, MM remains an incurable malignancy characterized by a clonal expansion of bone marrow plasma cells with a heterogeneous and complex genomic landscape. Copy number alterations and structural changes due to genomic instability are characteristic of MM (84).
There are two types of chromosomal instability: numerical and structural. The copy number alterations (CNAs) can be amplifications or deletions of chromosome (20,95). The second type of chromosomal alterations are characterized by structural changes, such as random rearrangements, inversions or translocation, manly involving chromosome 14q32 and a large array of different loci (96). Cells subject to chromosomal instability have an increased probability to acquire mutations, sometimes reaping benefits that lead tumor adaptability (97). This instability is revealed by the malfunction of genes involved in the mitotic network, DNA replication and transcription regulation (98).

There are several genetic events, defined primary and secondary, involving in the transformation and progression of a multistep pathology such as MM.
Within this scenario, an important role is attributed to DIS3, whose mutation is linked to one of the primary genetic events such as the monosomy of chr13/del(13q). DIS3 encodes for an exoribonuclease that acts from the 3' end, and is localized on chromosome 13. Important about 50% of MM patients carry a monoallelic condition as regard chromosome 13.
A study developed by the Intergroupe du Francophone du Myélome demonstrate that the 14q32 (involving the immunoglobulin IgH locus) and 13q chromosomal abnormalities are the most frequent ones and are not randomly distributed, but they are strongly interconnected and associated with clinical status and prognostic presentation (99).
In MM disease, DIS3 mutations were identified in about 13% of patients and the transcriptional signature associated to DIS3 mutations indicate mostly the impairment of the RNA exosome function and the DIS3 ribonucleolytic activity.
As demonstrated in HEK293 cells, DIS3 mutations is associated with theaccumulation of exosome substrates, such as tRNA, rRNA, PROMPTs and RNA polymerase III; causing aberrant RNA metabolism and slower proliferation (56) .

In B cells, DIS3 was found highly expressed during the transition from pro to pre-B cells, where the V(D)J recombination occurs.

DIS3 targets sites of somatic hypermutation (SHM) and class switch recombination (CSR), facilitating AID recruitment. Since PROMPTs and Enhancer RNAs (eRNAs) expressed from active promoters and enhancers are among the most prominent DIS3 substrates, even the slight increase in B- cells mutational rate bearing the mutated DIS3 in the short period of SHM and CSR can significantly impact oncogenesis. Although AID participates in class switch recombination, the MM associated DIS3 variants are clinically predominantly related to pathological translocations rather than point mutations (55). Analysis of mutation signatures in MM patients shows a correlation between DIS3 mutations and lesions associated with DNA stress.

My work was focused to investigate the involvement in genomic complexity and to characterize functional and biological relevance of DIS3 in MM.
At first, I explored the impact of DIS3 mutations and their association with chromosome 13 deletion or the biallelic condition in the transcriptional signature and clinical outcome.
Then, I explored the physiological contribution of DIS3 in MM cell lines, taking advantage of a loss of function approach by performing the gymnotic delivery of the DIS3-specific LNA-gapmeR (gDIS3#13).
Therefore, my work is shared into two parts:

1. The impact of DIS3 mutations in the clinical outcome and their related transcriptional signature.

Using CoMMpass dataset we investigated the type and frequency of DIS3 mutations in MM and their impact on the transcriptional signature and the clinical outcome.
In agreement with previously reported data (15,54,105), we assessed DIS3 mutations frequency in NDMM at 10%, associated with del(13q); the bi-allelic events range is about 72% of the observed cases. Most DIS3 mutations are missense. Indeed, about 100 missense single nucleotide variants have been reported, localized mainly in the two catalytic subunits of the protein.
The lack of truncating mutations, together with their clustering at the level of particular codons, is not typical of a tumor-suppressor gene and may suggest an oncogenic potential for DIS3.
This this consideration and the lack of further evidence do not make it clear what role DIS3 plays in MM, whether it is a tumor-suppressor or oncogene.

From the analysis DIS3 mutations showed a clear pattern of co-occurrence with other molecular alterations, in particular with chromosomal translocations. This phenomenon could be explained through the interaction between the RNA exosome and the protein Activation-Induced Cytidine Deaminase (AID) during the process of class switching and hypermutation of B-cells (61).
Indeed, during germinal center development of B lymphocyte, AID generates different type of mutations through a mechanism still not well understood. AID is currently thought to be the master regulator of the secondary antibody diversification. It is involved in the initiation of three separate immunoglobulin (Ig) diversification processes: somatic hypermutations, class switch recombination and gene conversion. The RNA exosome plays a fundamental role in degrading germline transcripts at repetitive and G-rich switch regions, necessary for class switch recombination during B cell activation (101). As a matter of fact, it is reported in the literature, that the expression of the RNA subunits complex includes DIS3, is increased during V(D)J recombination in bone marrow B cells and regulates germline transcripts normally processed by the RNA surveillance machinery (102). Therefore, through the disruption of an interaction with AID, DIS3 mutations could indirectly cause a targeting error of the somatic hypermutation process leading to chromosomal translocations.

In particular, we observed that DIS3 mutations are associated with patients carrying translocation t(4;14), a molecular lesion associated with a poor prognosis MM subgroup (100). Moreover, our analyses pointed out that t(4;14) significantly occurred in patients with the bi-allelic lesions.
Notably, another oncogenic event frequently co-occurring with DIS3 mutations is 1q gains. This chromosomal aberration results in the positive regulation of mitosis entry and the deactivation of TRAF2 gene associated with the regulation of the NF-κB signaling pathway (54).
These data suggest that mutations in DIS3, along with other oncogenic events, may contribute to greater genomic instability in MM.

Overall, this spectrum of molecular lesions suggests that there is a functional constraint of cooperating oncogenic events in MM. The occurrence of later lesions seems to be restricted by those appearing first in the transformed cell. With regards to this, DIS3 mutations were found to be both clonal in some patients and sub-clonal in others, indicating that they might be both early or late hits (54,103).

This study established that bi-allelic lesions of DIS3 significantly affect PFS, whereas the monoallelic condition predicted worse OS. Notably, these alterations remain valuable independent predictors also when tested in combination with the clinical and poor prognosis molecular variables used to predict the clinical outcome.
The differential impact of the monoallelic or bi-allelic lesions on MM outcome could be explained by our results showing two patterns of DIS3 lesions:

- del(13q) co-existing with non-hotspot DIS3 mutations.
- hotspot DIS3 mutations which rarely show bi-allelic events.

Again, this is a rather intriguing pattern that may suggest either haploinsufficiency for some mutations and not others, or a different function with some mutations showing loss and others showing gain of function. This might also explain the different clinical consequences on PFS and OS observed with the two genetic statuses.
Indeed, previous reports showed how different types of DIS3 mutations could lead to different biological effects either by impairing the exosome function through a reduced/modified DIS3 activity (56), or through a dominant negative effect exerted by mutated DIS3 on the other exosome catalytic subunits, such as EXOSC10 acting in the exosome complex and harboring only endoribonuclease activity (29).

As expected, we showed that DIS3 mutations affected the transcriptome. Interestingly, our analyses showed the up-regulation of several cell signaling pathways, including those associated to the interferon response, TNFα, NFKB or B-cell receptor (104).
Furthermore, we observed in DIS3 mutated samples negatively modulated genes implicated in DNA repair process and chromatin modifying enzymes, whereas genes involved in chromatin organization and the cell cycle check points, particularly those regulating the mitotic spindle checkpoint, were found up-regulated. Overall, these data suggest that DIS3 may have a role in mitotic fidelity as described in yeast, where DIS3 mutations or DIS3 loss are associated with defects in the mitotic spindle formation and excessive chromatin condensation (91,105).
Based on these observations, mutated or deregulated DIS3 gene could help drive or increase genome instability, which is a very common feature in MM.

Our interest has also turned to the non-coding portion of DIS3, which are also known to play a role in genomic instability in MM (106).

DIS3 is a key component of the multisubunit RNA exosome complex in eukaryotic cells involved in the processing, quality control and degradation of virtually all classes of RNA. Our study further supports and extends the notion that DIS3 mutations affect the transcriptome, showing a stronger impact on noncoding RNA species, mainly lncRNA.

In this work, we highlighted 12 lncRNAs, 5 of which are independent predictors of poorer OS and 9 of worse PFS, 2 are independent predictors both OS and PFS: AC015982.2 and AL445228.3. As regards AC015982.2, today nothing is reported in literature, whereases AL445228.3 is associated to poor prognosis in Willms tumor (108).

Moreover, the clinical impact of the 9 lncRNAs predicting lower PFS when expressed at higher levels was independent of the DIS3 genetic status.

The impact of these 12 lncRNAs on the pathobiology of MM disease remains to be fully elucidated; indeed, they all are novel transcripts, none of them currently reported as associated with cancer.

Interestingly, some of them showed a strict correlation in terms of expression levels with the corresponding nearby genes, thus suggesting a cis-regulatory relationship between the paired transcripts. Although these findings need to be further investigated, this could be the case for genes involved in fundamental molecular pathways, such as MGST3, involved in the production of leukotrienes and prostaglandin E, which are important mediators of inflammation (109); ASH1L, histone-lysine N-methyltransferase already known to be involved in cancer (110); and MSTO1, important for mitochondrial fusion and intracellular distribution (111).

Finally, the expression of four of these lncRNAs was validated in NDMM samples by quantitative RT-PCR showing their significant overexpression in DIS3 mutated as compared to unmutated MM cases.

Overall, our assessment considering the clinical and transcriptional consequences of DIS3 mutations or deficit in MM indicates that in both conditions it may play a highly important role in the mechanisms of transformation and progression of MM.

Furthermore, it would be important to characterize lncRNAs associated with DIS3 mutations as they could play a role in different tumor-associated processes, as demonstrated in the literature for other already well characterized lncRNAs (89,112).

These results led us to the publication of an article on Haematologica of which I am co-author (Todoerti K. et al., Haematologica 2022) (113).

2. Molecular and Functional characterization of DIS3 relevance in HMCLs

The results obtained in the first part of the thesis work are mainly focused on the identification of the transcriptional profile and the clinical impact of the mutations linked to DIS3, not only as a single event but also in association with the deletion of chr13 and the biallelic alteration. These data prompted me to investigate the impact of the lack of DIS3 in MM,

Already available literature data have highlighted the role of DIS3 in the regulation of cell cycle progression and in the correct development of mitosis (59,114). Nowadays, with the exception of the observation obtained in Drosophila, which indicates that DIS3 silencing leads to early larval arrest and reduces tissue growth (56,57,115), the DIS3 role in higher eukaryotic model system has not been rigorously studied. In this work, we aimed to clarify how DIS3 regulates the cell cycle progression and the proper kinetochore development and function.

To address this issue, I began to investigate the impact of the lack of the physiological DIS3 activity in MM by silencing DIS3 expression in two MM cell lines: one was wild type for DIS3 and the other carried the deletion of chromosome 13 and therefore only one functioning allele.

I used a loss-of-function approach with the LNA-gapmeR ASO technology which has proved to be an exceptional tool for obtaining strong and long-lasting transcript silencing.

Overall, I have obtained significant results in terms of silencing efficiency and biological effects, such as marked reduction in cell growth, increase in the apoptotic percentage and reduction of the clonogenic potential.

Since the most consistent biological effect obtained is related to a significant reduction in cell growth and, as mentioned above, the involvement of DIS3 in interfering with cell progression is known, I investigated this aspect in MM cells.

At first, cell cycle distribution was investigated in unsynchronized MM cells by flow cytometry after DIS3 silencing and we observed an increase in cell population in the G0/G1 phase of the cell cycle and a reduction in the subsequent phases.

This effect was more pronounced in the NCI-H929 cell line which carries the deletion of chromosome 13 than in the AMO-1 cell line without 13q abnormalities..

Considering this evidence, we aimed to study in a cleaner way the distribution of the cell cycle in DIS3 silenced cells, using synchronization to better studying events that take place in specific phases of the cell cycle.
The results of the synchronization showed a significant percentage of cells arrested in G0/G1 with impairement in the progression to S phase consistent with the effect observed in yeast and drosophila (58,60). Morever, we observed a reduction of the M phase which consistent with mitotic defects associated with the lack of DIS3 in the same models already reported.
The results experiments showed that DIS3 could be involved in regulating cell cycle progression also in MM cell lines.

To understand if DIS3 cell cycle regulation occurred at transcriptional level, we investigated the transcriptional profile of the NCI-H929 cell line after DIS3 silencing.
Transcriptomic analysis on DIS3-silenced NCI-H929 cells highlighted a large amount of differentially expressed genes.
Among the limited number of significantly upregulated genes, many are involved in extracellular matrix degradation, DNA and histone epigenetic modifications, DNA recombination and repair.
However, upn DIS3 silencing, the most genes were significantly downregulated and included genes involved in cell cycle checkpoints (according to the observed biological functions), chromosomal organization, and RNA metabolism. The observed down-regulation of the RNA metabolism pathway is in line with the RNA processing and degradation activity carried out by DIS3, in fact the modulation of this pathway is also a confirmation of the good silencing of DIS3 obtained.

Interestingly, among DIS3-regulated genes we found RAD51B and ARID5B; CCNB1, CDC20, KIF14, TOP2A and POLR2H, all involved in the cell cycle process. In particular, CCNB1 is essential for cell cycle control at the G2/M transition; CDC20 acts as a regulatory protein by interacting with the anaphase/cyclosome (APC/C) promoter complex; KIF14 a microtubule motor protein with ATPase activity that plays an important role in cell division, cytokinesis and also cell proliferation. TOP2A is a DNA topoisomerase which alters the topological states of DNA during transcription and POLR2H which is an RNA polymerase, its role is to catalyze the transcription of DNA into RNA.

What we know from the literature is that the RNA exosome complex is associated with transcription elongation and termination (116,117) and that DIS3 is key factor of this complex required for the proper chromatin formation and for the establishment of the interaction between kinetochore and microtubules; what we have observed is that silencing of DIS3 leads to a reduction of POLR2H which could result in a reduced accessibility of chromatin.

In our study we also highlighted that DIS3 silencing led to significant downregulation of two other genes, ARID5B and RAD51B. In particular, ARID5B is a protein that plays a crucial role in HR, it safeguards genome integrity and gives cells the ability to fend off DNA damage-induced apoptosis (118,119). RAD51 also promotes the progression of the replication fork by blocking its collapse , ensuring cell proliferation.
Furthermore, RAD51 controls cell cycle progression by maintaining the G2/M transition.
Since RAD51 is an essential protein for DNA damage repair systems, we might expect that its downregulation induced by DIS3 silencing could lead to an increased level of cellular DNA damage.
The preservation of genomic integrity relies on the ability of cells to undergo cell cycle arrest after DNA damage repair system.
A transcriptomic change related to DNA damage suggests the possible involvement of DIS3 deficiency in DNA damage, but further assays should be performed to confirm this hypothesis.

The transcripts mentioned above were subsequently validated not only in NCI-H929 and AMO-1 cell lines, but also in malignant plasma cells derived from patients and silenced for DIS3. Unfortunately, with the exception of CCNB1 and CDC20, we could not confirm the involvement of the analysed transcripts in the cell cycle regulation of primary MM cells, possibly due to reduced mitotic activity of malignant plasma cells when cultured in vitro.

Overall, the transcriptional results suggest that DIS3 KD plays a significant role in the regulation of pathways associated with the cell cycle, and this is consistent with what has been reported in the literature, except for myeloma. This prompted us to evaluate not only at the transcriptional level but also at the post-transcriptional level some of the proteins that are part of the cell cycle checkpoints.
Normally, the accumulation of Cyclin A creates a decision window from G0/G1 to enter in S phase and to initiate DNA replication and in this case, we observed a decrease of Cyclin A

protein in DIS3 silenced cells. Subsequently, the accumulation of cyclin A/B-CDK1 complex creates a second decision window (120). At this point the spindle assembly checkpoint (SAC) prevents chromosome mis-segregation and errors by delaying sister chromatid separation until all chromosomes have achieved bipolar kinetochore–microtubule attachment (121). This delay is obtained by inhibiting a complex of specific proteins (anaphase-promoting complex/cyclosome, APC/C) through the activity of spindle checkpoint proteins which are recruited to unattached kinetochores (121). Furthermore, CDC20 is a critical checkpoint effector of mitosis and its overexpression is associated to several cancer type, included MM (122,123).
Interestingly in our experiments, we observed a decrease in CDC20 protein levels and its phosphorylated fraction in DIS3 silenced cell lines. Furthermore, Histone H3 variant CENP-A that plays a fundamental role in defining centromere identity and structure and a critical protein for the proper formation of mitotic spindle (90) showed a down-modulation in AMO-1 and NCI-H929 cell lines.
It should be noted that these results also confirm at the protein level the effect of DIS3 silencing on the cell cycle perturbation.

The reported mitotic cell cycle defects in cells lacking the function of DIS3 led us to examine the role of DIS3 exonuclease activity in mitosis. Literature data in Drosophila reported defects in mitotic spindles attributable to multipolar, disorganized and short microtubules. They also showed evidence of over-condensed chromosomes commonly observed when cells are blocked in mitosis, since chromosomal condensation occurs during the arrest (58). Thus these data suggested that DIS3 exonuclease activity is required for normal mitotic spindle formation.
Consistent with the mitotic defects reported in Drosophila, we observed in MM cells silenced for DIS3 clear mitotic alterations such as multipolar spindles. The mitotic defect index of cells lacking DIS3 exonuclease activity suggest that these may be blocked or delayed in mitosis and that the exonuclease activity of DIS3 is required for mitotic exit.

In order to provide a translational potential to our DIS3 silencing data, we investigated if DIS3 depletion could be synergize with a drug that acts on mitosis, namely ARRY-520, a kinesin spindle protein inhibitor that interferes with proper mitotic spindle formation, which is currently in clinical trials and has demonstrated clinical efficacy in patients with MM (81).

Our data indicate that DIS3-depleted cells, when treated with ARRY-520, showed an increased sensitization in terms of marked reduction in cellular growth with a more altered mitotic spindle than with single treatment.
In conclusion, although the detailed molecular mechanisms through which DIS3 can influence cell cycle control and mitotic progression remain fully to be elucidated, based on the presented data we can hypothesize that DIS3 silencing is associated with a sensitizing effect in combination with ARRY-520, thus making its targeting a promising strategy for novel anti-MM combination therapies.

Significant work is still needed to clarify how DIS3 regulates cell cycle progression. In humans, most multiple myeloma specific DIS3 mutations are clustered in its exonuclease domain and appear to reduce, but not eliminate, DIS3 exonuclease activity (28,53,54,56).
Thus, DIS3 likely mediates its effects on cell division via exonucleolytic degradation or modification of specific RNA species that regulate cell cycle progression.
Clearly, DIS3 could control the cell cycle also by targeting individual mRNAs or miRNAs. In support of this idea, in human myeloma cell lines and mouse NIH3T3 cells, reduction of DIS3 activity appears to decrease let-7 miRNA expression, causing increased expression of let-7 target genes, including RAS and MYC (124).
An alternative, non-mutually exclusive model is that DIS3 might regulate cell division epigenetically. In yeast, DIS3 has been shown to associate with centromeric-repeat DNA, to promote heterochromatin silencing at centromeres, and to inhibit accumulation of noncoding centromeric repeat RNAs (60). Consistently, , small centromeric RNAs have been shown to regulate centromere formation and function in human cells (125).
Further experimental data is needed to support these models with future work focusing on identifying DIS3-bound RNAs and elucidating the function of these RNAs or their encoded products on cell cycle progression.
Finally, the approach shown in this work, based on the use of gapmeR technology to KD DIS3, provides clear experimental evidence that the reduction in DIS3 function has a biological impact on MM cells. We provided for the first time that DIS3 is required for the proliferation of MM cells, cell cycle progression and mitotic fidelity and may represent a new possible future target in MM.

Acknowledgments

I would like to express my deep gratitude to my supervisor, Prof. Antonino Neri, who guided me in this project.

I would like to thank the technical and moral support provided by the research group in which I conducted my doctoral work and which for me was my second family, especially Dr. Elisa Taiana and Dr. Ilaria Silvestris.

I would like to thank my other supervisos, Prof. Raffaella Chiaramonte, for giving me the opportunity to pursue this PhD and for supporting me.

I would like to thank the University of Milan and the PhD in Experimental Medicine for giving me the opportunity to complete my research training and engage in this exciting research project.

I would like to thank my family for all of their love and encouragement and my brilliant group of friends, who I am very lucky to have in my life.

Finally, I cannot begin to express how grateful I am to my partner Sebastiano, without him none of this would have been possible. His support, encouragement, understanding and belief in me during this particular journey has been immeasurable. This was not only one of the biggest challenges of my life, but his too, and I'm sure the terms "mitotic spindle" and "DIS3" will always evoke unique memories.

Bibliography

1. Palumbo A, Anderson K. Multiple Myeloma. N Engl J Med. 2011 Mar 17;364(11):1046–60.
2. SEER Cancer Statistics Review 1975-2007 - Previous Version - SEER Cancer Statistics [Internet]. SEER. [cited 2022 Sep 8]. Available from: https://seer.cancer.gov/archive/csr/1975_2007/index.html
3. Kristinsson SY, Landgren O, Dickman PW, Derolf AR, Björkholm M. Patterns of survival in multiple myeloma: a population-based study of patients diagnosed in Sweden from 1973 to 2003. J Clin Oncol. 2007 May 20;25(15):1993–9.
4. Brenner H, Gondos A, Pulte D. Recent major improvement in long-term survival of younger patients with multiple myeloma. Blood. 2008 Mar 1;111(5):2521–6.
5. Utley A, Lipchick B, Lee KP, Nikiforov MA. Targeting Multiple Myeloma through the Biology of Long-Lived Plasma Cells. Cancers (Basel). 2020 Jul 30;12(8):2117.
6. O'Connor BP, Gleeson MW, Noelle RJ, Erickson LD. The rise and fall of long-lived humoral immunity: terminal differentiation of plasma cells in health and disease. Immunol Rev. 2003 Aug;194:61–76.
7. Kyle RA. Monoclonal gammopathy of undetermined significance. Natural history in 241 cases. Am J Med. 1978 May;64(5):814–26.
8. Dhodapkar MV. MGUS to myeloma: a mysterious gammopathy of underexplored significance. Blood. 2016 Dec 8;128(23):2599–606.
9. Kyle RA, Larson DR, Therneau TM, Dispenzieri A, Kumar S, Cerhan JR, et al. Long-Term Follow-up of Monoclonal Gammopathy of Undetermined Significance. N Engl J Med. 2018 Jan 18;378(3):241–9.
10. Weiss BM, Abadie J, Verma P, Howard RS, Kuehl WM. A monoclonal gammopathy precedes multiple myeloma in most patients. Blood. 2009 May 28;113(22):5418–22.
11. Sirohi B, Powles R. Multiple myeloma. The Lancet. 2004 Mar 13;363(9412):875–87.
12. Usmani SZ, Rodriguez-Otero P, Bhutani M, Mateos MV, Miguel JS. Defining and treating high-risk multiple myeloma. Leukemia. 2015 Nov;29(11):2119–25.
13. Dutta AK, Fink JL, Grady JP, Morgan GJ, Mullighan CG, To LB, et al. Subclonal evolution in disease progression from MGUS/SMM to multiple myeloma is characterised by clonal stability. Leukemia. 2019 Feb;33(2):457–68.
14. Walker BA, Wardell CP, Melchor L, Brioli A, Johnson DC, Kaiser MF, et al. Intraclonal heterogeneity is a critical early event in the development of myeloma and precedes the development of clinical symptoms. Leukemia. 2014 Feb;28(2):384–90.
15. Aksenova AY, Zhuk AS, Lada AG, Zotova IV, Stepchenkova EI, Kostroma II, et al. Genome Instability in Multiple Myeloma: Facts and Factors. Cancers (Basel). 2021 Nov 26;13(23):5949.
16. Manier S, Salem KZ, Park J, Landau DA, Getz G, Ghobrial IM. Genomic complexity of multiple myeloma and its clinical implications. Nat Rev Clin Oncol. 2017 Feb;14(2):100–13.
17. Maura F, Rustad EH, Boyle EM, Morgan GJ. Reconstructing the evolutionary history of multiple myeloma. Best Pract Res Clin Haematol. 2020 Mar;33(1):101145.
18. Bolli N, Genuardi E, Ziccheddu B, Martello M, Oliva S, Terragna C. Next-Generation Sequencing for Clinical Management of Multiple Myeloma: Ready for Prime Time? Front Oncol. 2020;10:189.
19. Keats JJ, Craig DW, Liang W, Venkata Y, Kurdoglu A, Aldrich J, et al. Interim Analysis Of The Mmrf Commpass Trial, a Longitudinal Study In Multiple Myeloma Relating Clinical Outcomes To Genomic and Immunophenotypic Profiles. Blood. 2013 Nov 15;122(21):532.
20. Bakhoum SF, Landau DA. Chromosomal Instability as a Driver of Tumor Heterogeneity and Evolution. Cold Spring Harb Perspect Med. 2017 Jun 1;7(6):a029611.
21. Negrini S, Gorgoulis VG, Halazonetis TD. Genomic instability--an evolving hallmark of cancer. Nat Rev Mol Cell Biol. 2010 Mar;11(3):220–8.
22. Smadja NV, Fruchart C, Isnard F, Louvet C, Dutel JL, Cheron N, et al. Chromosomal analysis in multiple myeloma: cytogenetic evidence of two different diseases. Leukemia. 1998 Jun;12(6):960–

9.
23. Fonseca R, Bergsagel PL, Drach J, Shaughnessy J, Gutierrez N, Stewart AK, et al. International Myeloma Working Group molecular classification of multiple myeloma: spotlight review. Leukemia. 2009 Dec;23(12):2210–21.
24. Kuehl WM, Bergsagel PL. Multiple myeloma: evolving genetic events and host interactions. Nat Rev Cancer. 2002 Mar;2(3):175–87.
25. Pl B, Wm K. Molecular pathogenesis and a consequent classification of multiple myeloma. Journal of clinical oncology : official journal of the American Society of Clinical Oncology [Internet]. 2005 Oct 9 [cited 2022 Sep 9];23(26). Available from: https://pubmed.ncbi.nlm.nih.gov/16155016/
26. Tanay A, Regev A, Shamir R. Conservation and evolvability in regulatory networks: the evolution of ribosomal regulation in yeast. Proc Natl Acad Sci U S A. 2005 May 17;102(20):7203–8.
27. Walker BA, Boyle EM, Wardell CP, Murison A, Begum DB, Dahir NM, et al. Mutational Spectrum, Copy Number Changes, and Outcome: Results of a Sequencing Study of Patients With Newly Diagnosed Myeloma. J Clin Oncol. 2015 Nov 20;33(33):3911–20.
28. Morgan GJ, Walker BA, Davies FE. The genetic architecture of multiple myeloma. Nat Rev Cancer. 2012 Apr 12;12(5):335–48.
29. Chlebowski A, Lubas M, Jensen TH, Dziembowski A. RNA decay machines: the exosome. Biochim Biophys Acta. 2013 Jul;1829(6–7):552–60.
30. Liu Q, Greimann JC, Lima CD. Reconstitution, activities, and structure of the eukaryotic RNA exosome. Cell. 2006 Dec 15;127(6):1223–37.
31. Symmons MF, Jones GH, Luisi BF. A duplicated fold is the structural basis for polynucleotide phosphorylase catalytic activity, processivity, and regulation. Structure. 2000 Nov 15;8(11):1215–26.
32. Januszyk K, Lima CD. The eukaryotic RNA exosome. Curr Opin Struct Biol. 2014 Feb;0:132–40.
33. Schaeffer D, Reis FP, Johnson SJ, Arraiano CM, van Hoof A. The CR3 motif of Rrp44p is important for interaction with the core exosome and exosome function. Nucleic Acids Res. 2012 Oct;40(18):9298–307.
34. Schneider C, Leung E, Brown J, Tollervey D. The N-terminal PIN domain of the exosome subunit Rrp44 harbors endonuclease activity and tethers Rrp44 to the yeast core exosome. Nucleic Acids Res. 2009 Mar;37(4):1127–40.
35. Lorentzen E, Basquin J, Tomecki R, Dziembowski A, Conti E. Structure of the active subunit of the yeast exosome core, Rrp44: diverse modes of substrate recruitment in the RNase II nuclease family. Mol Cell. 2008 Mar 28;29(6):717–28.
36. Tomecki R, Kristiansen MS, Lykke-Andersen S, Chlebowski A, Larsen KM, Szczesny RJ, et al. The human core exosome interacts with differentially localized processive RNases: hDIS3 and hDIS3L. EMBO J. 2010 Jul 21;29(14):2342–57.
37. Staals RHJ, Bronkhorst AW, Schilders G, Slomovic S, Schuster G, Heck AJR, et al. Dis3-like 1: a novel exoribonuclease associated with the human exosome. EMBO J. 2010 Jul 21;29(14):2358–67.
38. Chang HM, Triboulet R, Thornton JE, Gregory RI. A role for the Perlman syndrome exonuclease Dis3l2 in the Lin28-let-7 pathway. Nature. 2013 May 9;497(7448):244–8.
39. Lubas M, Damgaard CK, Tomecki R, Cysewski D, Jensen TH, Dziembowski A. Exonuclease hDIS3L2 specifies an exosome-independent 3'-5' degradation pathway of human cytoplasmic mRNA. EMBO J. 2013 Jul 3;32(13):1855–68.
40. Astuti D, Morris MR, Cooper WN, Staals RHJ, Wake NC, Fews GA, et al. Germline mutations in DIS3L2 cause the Perlman syndrome of overgrowth and Wilms tumor susceptibility. Nat Genet. 2012 Feb 5;44(3):277–84.
41. Zuo Y, Deutscher MP. Exoribonuclease superfamilies: structural analysis and phylogenetic distribution. Nucleic Acids Res. 2001 Mar 1;29(5):1017–26.

42. Briggs MW, Burkard KT, Butler JS. Rrp6p, the yeast homologue of the human PM-Scl 100-kDa autoantigen, is essential for efficient 5.8 S rRNA 3' end formation. J Biol Chem. 1998 May 22;273(21):13255–63.
43. Januszyk K, Liu Q, Lima CD. Activities of human RRP6 and structure of the human RRP6 catalytic domain. RNA. 2011 Aug;17(8):1566–77.
44. Butler JS, Mitchell P. Rrp6, Rrp47 and cofactors of the nuclear exosome. Adv Exp Med Biol. 2010;702:91–104.
45. Schneider C, Tollervey D. Threading the barrel of the RNA exosome. Trends Biochem Sci. 2013 Oct;38(10):485–93.
46. Houseley J, LaCava J, Tollervey D. RNA-quality control by the exosome. Nat Rev Mol Cell Biol. 2006 Jul;7(7):529–39.
47. Kilchert C, Wittmann S, Vasiljeva L. The regulation and functions of the nuclear RNA exosome complex. Nat Rev Mol Cell Biol. 2016 Apr;17(4):227–39.
48. Wyers F, Rougemaille M, Badis G, Rousselle JC, Dufour ME, Boulay J, et al. Cryptic pol II transcripts are degraded by a nuclear quality control pathway involving a new poly(A) polymerase. Cell. 2005 Jun 3;121(5):725–37.
49. Preker P, Nielsen J, Kammler S, Lykke-Andersen S, Christensen MS, Mapendano CK, et al. RNA exosome depletion reveals transcription upstream of active human promoters. Science. 2008 Dec 19;322(5909):1851–4.
50. Schneider C, Kudla G, Wlotzka W, Tuck A, Tollervey D. Transcriptome-wide analysis of exosome targets. Mol Cell. 2012 Nov 9;48(3):422–33.
51. Kadaba S, Krueger A, Trice T, Krecic AM, Hinnebusch AG, Anderson J. Nuclear surveillance and degradation of hypomodified initiator tRNAMet in S. cerevisiae. Genes Dev. 2004 Jun 1;18(11):1227–40.
52. Zinder JC, Lima CD. Targeting RNA for processing or destruction by the eukaryotic RNA exosome and its cofactors. Genes Dev. 2017 Jan 15;31(2):88–100.
53. Chapman MA, Lawrence MS, Keats JJ, Cibulskis K, Sougnez C, Schinzel AC, et al. Initial genome sequencing and analysis of multiple myeloma. Nature. 2011 Mar 24;471(7339):467–72.
54. Lohr JG, Stojanov P, Carter SL, Cruz-Gordillo P, Lawrence MS, Auclair D, et al. Widespread genetic heterogeneity in multiple myeloma: implications for targeted therapy. Cancer Cell. 2014 Jan 13;25(1):91–101.
55. Lionetti M, Barbieri M, Todoerti K, Agnelli L, Fabris S, Tonon G, et al. A compendium of DIS3 mutations and associated transcriptional signatures in plasma cell dyscrasias. Oncotarget. 2015 Sep 22;6(28):26129–41.
56. Tomecki R, Drazkowska K, Kucinski I, Stodus K, Szczesny RJ, Gruchota J, et al. Multiple myeloma-associated hDIS3 mutations cause perturbations in cellular RNA metabolism and suggest hDIS3 PIN domain as a potential drug target. Nucleic Acids Res. 2014 Jan;42(2):1270–90.
57. Hou D, Ruiz M, Andrulis ED. The ribonuclease Dis3 is an essential regulator of the developmental transcriptome. BMC Genomics. 2012 Aug 1;13:359.
58. Snee MJ, Wilson WC, Zhu Y, Chen SY, Wilson BA, Kseib C, et al. Collaborative Control of Cell Cycle Progression by the RNA Exonuclease Dis3 and Ras Is Conserved Across Species. Genetics. 2016 Jun;203(2):749–62.
59. Smith SB, Kiss DL, Turk E, Tartakoff AM, Andrulis ED. Pronounced and extensive microtubule defects in a Saccharomyces cerevisiae DIS3 mutant. Yeast. 2011 Nov;28(11):755–69.
60. Murakami H, Goto DB, Toda T, Chen ES, Grewal SI, Martienssen RA, et al. Ribonuclease activity of Dis3 is required for mitotic progression and provides a possible link between heterochromatin and kinetochore function. PLoS One. 2007 Mar 21;2(3):e317.
61. Pefanis E, Basu U. RNA Exosome Regulates AID DNA Mutator Activity in the B Cell Genome. Adv Immunol. 2015;127:257–308.
62. Rajkumar SV, Dimopoulos MA, Palumbo A, Blade J, Merlini G, Mateos MV, et al. International Myeloma Working Group updated criteria for the diagnosis of multiple myeloma.

Lancet Oncol. 2014 Nov;15(12):e538-548.
63. Cowan AJ, Green DJ, Kwok M, Lee S, Coffey DG, Holmberg LA, et al. Diagnosis and Management of Multiple Myeloma: A Review. JAMA. 2022 Feb 1;327(5):464–77.
64. Durie BGM, Kyle RA, Belch A, Bensinger W, Blade J, Boccadoro M, et al. Myeloma management guidelines: a consensus report from the Scientific Advisors of the International Myeloma Foundation. Hematol J. 2003;4(6):379–98.
65. Durie BGM, Harousseau JL, Miguel JS, Bladé J, Barlogie B, Anderson K, et al. International uniform response criteria for multiple myeloma. Leukemia. 2006 Sep;20(9):1467–73.
66. Paiva B, Vidriales MB, Cerveró J, Mateo G, Pérez JJ, Montalbán MA, et al. Multiparameter flow cytometric remission is the most relevant prognostic factor for multiple myeloma patients who undergo autologous stem cell transplantation. Blood. 2008 Nov 15;112(10):4017–23.
67. Ladetto M, Pagliano G, Ferrero S, Cavallo F, Drandi D, Santo L, et al. Major tumor shrinking and persistent molecular remissions after consolidation with bortezomib, thalidomide, and dexamethasone in patients with autografted myeloma. J Clin Oncol. 2010 Apr 20;28(12):2077–84.
68. Avet-Loiseau H, Soulier J, Fermand JP, Yakoub-Agha I, Attal M, Hulin C, et al. Impact of high-risk cytogenetics and prior therapy on outcomes in patients with advanced relapsed or refractory multiple myeloma treated with lenalidomide plus dexaméthasone. Leukemia. 2010 Mar;24(3):623–8.
69. Sawin KE, Mitchison TJ, Wordeman LG. Evidence for kinesin-related proteins in the mitotic apparatus using peptide antibodies. J Cell Sci. 1992 Feb;101 (Pt 2):303–13.
70. Sawin KE, LeGuellec K, Philippe M, Mitchison TJ. Mitotic spindle organization by a plus-end-directed microtubule motor. Nature. 1992 Oct 8;359(6395):540–3.
71. Blangy A, Lane HA, d'Hérin P, Harper M, Kress M, Nigg EA. Phosphorylation by p34cdc2 regulates spindle association of human Eg5, a kinesin-related motor essential for bipolar spindle formation in vivo. Cell. 1995 Dec 29;83(7):1159–69.
72. Wakana Y, Villeneuve J, van Galen J, Cruz-Garcia D, Tagaya M, Malhotra V. Kinesin-5/Eg5 is important for transport of CARTS from the trans-Golgi network to the cell surface. J Cell Biol. 2013 Jul 22;202(2):241–50.
73. Bartoli KM, Jakovljevic J, Woolford JL, Saunders WS. Kinesin molecular motor Eg5 functions during polypeptide synthesis. Mol Biol Cell. 2011 Sep;22(18):3420–30.
74. Mann BJ, Wadsworth P. Kinesin-5 Regulation and Function in Mitosis. Trends Cell Biol. 2019 Jan;29(1):66–79.
75. Garcia-Saez I, Skoufias DA. Eg5 targeting agents: From new anti-mitotic based inhibitor discovery to cancer therapy and resistance. Biochem Pharmacol. 2021 Feb;184:114364.
76. Hansen GM, Justice MJ. Activation of Hex and mEg5 by retroviral insertion may contribute to mouse B-cell leukemia. Oncogene. 1999 Nov 11;18(47):6531–9.
77. Castillo A, Morse HC, Godfrey VL, Naeem R, Justice MJ. Overexpression of Eg5 causes genomic instability and tumor formation in mice. Cancer Res. 2007 Nov 1;67(21):10138–47.
78. Shah JJ, Kaufman JL, Zonder JA, Cohen AD, Bensinger WI, Hilder BW, et al. A Phase 1 and 2 study of Filanesib alone and in combination with low-dose dexamethasone in relapsed/refractory multiple myeloma. Cancer. 2017 Dec 1;123(23):4617–30.
79. Pan D, Kaufman JL, Htut M, Agrawal M, Mazumder A, Cornell RF, et al. Filanesib plus bortezomib and dexamethasone in relapsed/refractory t(11;14) and 1q21 gain multiple myeloma. Cancer Med. 2022 Jan;11(2):358–70.
80. Owens B. Kinesin inhibitor marches toward first-in-class pivotal trial. Nat Med. 2013 Dec;19(12):1550.
81. Algarín EM, Hernández-García S, Garayoa M, Ocio EM. Filanesib for the treatment of multiple myeloma. Expert Opin Investig Drugs. 2020 Jan;29(1):5–14.
82. Lee HC, Shah JJ, Feng L, Manasanch EE, Lu R, Morphey A, et al. A phase 1 study of filanesib, carfilzomib, and dexamethasone in patients with relapsed and/or refractory multiple myeloma. Blood Cancer J. 2019 Oct 1;9(10):80.

83. Phase 2 Study of Carfilzomib (CFZ) with or without Filanesib (FIL) in Patients with Advanced Multiple Myeloma (MM) - ScienceDirect [Internet]. [cited 2022 Sep 9]. Available from: https://www.sciencedirect.com/science/article/pii/S0006497118477075
84. Neuse CJ, Lomas OC, Schliemann C, Shen YJ, Manier S, Bustoros M, et al. Genome instability in multiple myeloma. Leukemia. 2020 Nov;34(11):2887–97.
85. Walker BA, Mavrommatis K, Wardell CP, Ashby TC, Bauer M, Davies FE, et al. Identification of novel mutational drivers reveals oncogene dependencies in multiple myeloma. Blood. 2018 Aug 9;132(6):587–97.
86. Tusher VG, Tibshirani R, Chu G. Significance analysis of microarrays applied to the ionizing radiation response. Proc Natl Acad Sci U S A. 2001 Apr 24;98(9):5116–21.
87. Divergent transcription of long noncoding RNA/mRNA gene pairs in embryonic stem cells - PubMed [Internet]. [cited 2022 Sep 9]. Available from: https://pubmed.ncbi.nlm.nih.gov/23382218/
88. Tan JY, Smith AAT, Ferreira da Silva M, Matthey-Doret C, Rueedi R, Sönmez R, et al. cis-Acting Complex-Trait-Associated lincRNA Expression Correlates with Modulation of Chromosomal Architecture. Cell Rep. 2017 Feb 28;18(9):2280–8.
89. Taiana E, Favasuli V, Ronchetti D, Todoerti K, Pelizzoni F, Manzoni M, et al. Long non-coding RNA NEAT1 targeting impairs the DNA repair machinery and triggers anti-tumor activity in multiple myeloma. Leukemia. 2020 Jan;34(1):234–44.
90. Pesenti ME, Raisch T, Conti D, Walstein K, Hoffmann I, Vogt D, et al. Structure of the human inner kinetochore CCAN complex and its significance for human centromere organization. Molecular Cell. 2022 Jun 2;82(11):2113-2131.e8.
91. Robinson SR, Oliver AW, Chevassut TJ, Newbury SF. The 3' to 5' Exoribonuclease DIS3: From Structure and Mechanisms to Biological Functions and Role in Human Disease. Biomolecules. 2015 Jul 17;5(3):1515–39.
92. Davidson L, Francis L, Cordiner RA, Eaton JD, Estell C, Macias S, et al. Rapid Depletion of DIS3, EXOSC10, or XRN2 Reveals the Immediate Impact of Exoribonucleolysis on Nuclear RNA Metabolism and Transcriptional Control. Cell Reports. 2019 Mar;26(10):2779-2791.e5.
93. Naymagon L, Abdul-Hay M. Novel agents in the treatment of multiple myeloma: a review about the future. J Hematol Oncol. 2016 Jun 30;9(1):52.
94. Filanesib plus bortezomib and dexamethasone in relapsed/refractory t(11;14) and 1q21 gain multiple myeloma - Pan - 2022 - Cancer Medicine - Wiley Online Library [Internet]. [cited 2022 Sep 9]. Available from: https://onlinelibrary.wiley.com/doi/full/10.1002/cam4.4451
95. Sansregret L, Vanhaesebroeck B, Swanton C. Determinants and clinical implications of chromosomal instability in cancer. Nat Rev Clin Oncol. 2018 Mar;15(3):139–50.
96. Frontiers | Multi-Layered Cancer Chromosomal Instability Phenotype [Internet]. [cited 2022 Sep 12]. Available from: https://www.frontiersin.org/articles/10.3389/fonc.2013.00302/full
97. Thompson LL, Jeusset LMP, Lepage CC, McManus KJ. Evolving Therapeutic Strategies to Exploit Chromosome Instability in Cancer. Cancers (Basel). 2017 Nov 1;9(11):151.
98. Decaux O, Lodé L, Magrangeas F, Charbonnel C, Gouraud W, Jézéquel P, et al. Prediction of Survival in Multiple Myeloma Based on Gene Expression Profiles Reveals Cell Cycle and Chromosomal Instability Signatures in High-Risk Patients and Hyperdiploid Signatures in Low-Risk Patients: A Study of the Intergroupe Francophone du Myélome. JCO. 2008 Oct 10;26(29):4798–805.
99. Avet-Loiseau H, Facon T, Grosbois B, Magrangeas F, Rapp MJ, Harousseau JL, et al. Oncogenesis of multiple myeloma: 14q32 and 13q chromosomal abnormalities are not randomly distributed, but correlate with natural history, immunological features, and clinical presentation. Blood. 2002 Mar 15;99(6):2185–91.
100. Boyle EM, Ashby C, Tytarenko RG, Deshpande S, Wang H, Wang Y, et al. BRAF and DIS3 Mutations Associate with Adverse Outcome in a Long-term Follow-up of Patients with Multiple Myeloma. Clin Cancer Res. 2020 May 15;26(10):2422–32.
101. Bransteitter R, Pham P, Scharff MD, Goodman MF. Activation-induced cytidine deaminase deaminates deoxycytidine on single-stranded DNA but requires the action of RNase. Proceedings of

the National Academy of Sciences. 2003 Apr;100(7):4102–7.
102. Laffleur B, Batista CR, Zhang W, Lim J, Yang B, Rossille D, et al. RNA exosome drives early B cell development via noncoding RNA processing mechanisms. Sci Immunol. 2022 Jun 3;7(72):eabn2738.
103. Weißbach S, Langer C, Puppe B, Nedeva T, Bach E, Kull M, et al. The molecular spectrum and clinical impact of DIS3 mutations in multiple myeloma. Br J Haematol. 2015 Apr;169(1):57–70.
104. Chesi M, Bergsagel PL. Advances in the pathogenesis and diagnosis of multiple myeloma. International Journal of Laboratory Hematology. 2015;37(S1):108–14.
105. Milbury KL, Paul B, Lari A, Fowler C, Montpetit B, Stirling PC. Exonuclease domain mutants of yeast DIS3 display genome instability. Nucleus. 2019 Dec;10(1):21–32.
106. Taiana E, Gallo Cantafio ME, Favasuli VK, Bandini C, Viglietto G, Piva R, et al. Genomic Instability in Multiple Myeloma: A "Non-Coding RNA" Perspective. Cancers. 2021 Jan;13(9):2127.
107. Rothschild G, Zhang W, Lim J, Giri PK, Laffleur B, Chen Y, et al. Noncoding RNA transcription alters chromosomal topology to promote isotype-specific class switch recombination. Sci Immunol. 2020 Feb 7;5(44):eaay5864.
108. Liu H, Zhang M, Shi M, Zhang T, Zhang Z, Cui Q, et al. A Survival-Related Competitive Endogenous RNA Network of Prognostic lncRNAs, miRNAs, and mRNAs in Wilms Tumor. Front Oncol. 2021;11:608433.
109. Higgins LG, Hayes JD. Mechanisms of induction of cytosolic and microsomal glutathione transferase (GST) genes by xenobiotics and pro-inflammatory agents. Drug Metab Rev. 2011 May;43(2):92–137.
110. Xu B, Qin T, Yu J, Giordano TJ, Sartor MA, Koenig RJ. Novel role of ASH1L histone methyltransferase in anaplastic thyroid carcinoma. J Biol Chem. 2020 Jun 26;295(26):8834–45.
111. Chapman J, Ng YS, Nicholls TJ. The Maintenance of Mitochondrial DNA Integrity and Dynamics by Mitochondrial Membranes. Life (Basel). 2020 Aug 26;10(9):E164.
112. N A, Ma S, G J, E M, M F, M M, et al. Drugging the lncRNA MALAT1 via LNA gapmeR ASO inhibits gene expression of proteasome subunits and triggers anti-multiple myeloma activity. Leukemia [Internet]. 2018 Sep [cited 2022 Sep 14];32(9). Available from: https://pubmed.ncbi.nlm.nih.gov/29487387/
113. Todoerti K, Ronchetti D, Favasuli V, Maura F, Morabito F, Bolli N, et al. DIS3 mutations in multiple myeloma impact the transcriptional signature and clinical outcome. Haematologica. 2022 Apr 1;107(4):921–32.
114. Ohkura H, Adachi Y, Kinoshita N, Niwa O, Toda T, Yanagida M. Cold-sensitive and caffeine-supersensitive mutants of the Schizosaccharomyces pombe dis genes implicated in sister chromatid separation during mitosis. EMBO J. 1988 May;7(5):1465–73.
115. Towler BP, Jones CI, Viegas SC, Apura P, Waldron JA, Smalley SK, et al. The 3'-5' exoribonuclease Dis3 regulates the expression of specific microRNAs in Drosophila wing imaginal discs. RNA Biol. 2015;12(7):728–41.
116. Andrulis ED, Werner J, Nazarian A, Erdjument-Bromage H, Tempst P, Lis JT. The RNA processing exosome is linked to elongating RNA polymerase II in Drosophila. Nature. 2002 Dec 19;420(6917):837–41.
117. Lemay JF, Larochelle M, Marguerat S, Atkinson S, Bähler J, Bachand F. The RNA exosome promotes transcription termination of backtracked RNA polymerase II. Nat Struct Mol Biol. 2014 Oct;21(10):919–26.
118. Kujjo LL, Laine T, Pereira RJG, Kagawa W, Kurumizaka H, Yokoyama S, et al. Enhancing survival of mouse oocytes following chemotherapy or aging by targeting Bax and Rad51. PLoS One. 2010 Feb 12;5(2):e9204.
119. Wu L. Wrestling off RAD51: a novel role for RecQ helicases. BioEssays. 2008;30(4):291–5.
120. Matthews HK, Bertoli C, de Bruin RAM. Cell cycle control in cancer. Nat Rev Mol Cell Biol. 2022 Jan;23(1):74–88.
121. Musacchio A, Salmon ED. The spindle-assembly checkpoint in space and time. Nat Rev Mol

Cell Biol. 2007 May;8(5):379–93.
122. Lub S, Maes A, Maes K, De Veirman K, De Bruyne E, Menu E, et al. Inhibiting the anaphase promoting complex/cyclosome induces a metaphase arrest and cell death in multiple myeloma cells. Oncotarget. 2015 Dec 26;7(4):4062–76.
123. Bruno S, Rorà AGL di, Napolitano R, Soverini S, Martinelli G, Simonetti G. CDC20 in and out of mitosis: a prognostic factor and therapeutic target in hematological malignancies. Journal of Experimental & Clinical Cancer Research [Internet]. 2022 Apr 30 [cited 2022 Sep 9];41(1). Available from: https://moh-it.pure.elsevier.com/en/publications/cdc20-in-and-out-of-mitosis-a-prognostic-factor-and-therapeutic-t
124. Segalla S, Pivetti S, Todoerti K, Chudzik MA, Giuliani EC, Lazzaro F, et al. The ribonuclease DIS3 promotes let-7 miRNA maturation by degrading the pluripotency factor LIN28B mRNA. Nucleic Acids Res. 2015 May 26;43(10):5182–93.
125. Wong LH, Brettingham-Moore KH, Chan L, Quach JM, Anderson MA, Northrop EL, et al. Centromere RNA is a key component for the assembly of nucleoproteins at the nucleolus and centromere. Genome Res. 2007 Aug;17(8):1146–60.

List of figures and tables

Dissemination of results

During my PhD, I disseminated my findings relating to DIS3 role in MM through an open access publication in an international journal.
In fact, I am a co-author of the original paper published in 2022 titled "DIS3 mutations in multiple myeloma impact the transcriptional signature and clinical outcome" which was accepted for publication in the Haematologica jurnal.

To further disseminate the results, during the PhD, I discussed my results in the presence of experts in the sector, participating at national and international conferences:

- Favasuli et al., Depletion of DIS33 in multiple myeloma leads to perturbation in RNA metabolism, cell cycle progression and mitotic checkpoint. EHA, European Haematolgy Association, Vienna, Austria, June 9-12, 2022.
- Favasuli et al., Depletion of DIS3 in multiple myeloma causes extensive perturbation in RNA metabolism, cell cycle progression and mitotic checkpoint: implications for the pathogenetic role in the disease. XVII national congress SIES 2022, Rome, Italy (31March - 1-2April)
- Favasuli et al., DIS3 mutations in multiple myeloma impact the transcriptional signature and clinical outcome, 48th national congress SIE, Società Italiana di Ematologia, Milan, Italy, October 24-27 2021 (Abstract n. 255, poster P019). haematologica | 2021; 106 (s3)

Appendix

Published paper entitled “DIS3 mutations in multiple myeloma impact the transcriptional signature and clinical outcome”.